

See discussions, stats, and author profiles for this publication at: <https://www.researchgate.net/publication/51827441>

Nano-Gold Catalysis in Fine Chemical Synthesis

ARTICLE *in* CHEMICAL REVIEWS · NOVEMBER 2011

Impact Factor: 46.57 · DOI: 10.1021/cr200260m · Source: PubMed

CITATIONS

249

READS

193

4 AUTHORS, INCLUDING:



Feng Shi

Chinese Academy of Sciences

73 PUBLICATIONS 2,997 CITATIONS

SEE PROFILE

Nano-Gold Catalysis in Fine Chemical Synthesis

Yan Zhang,[†] Xinjiang Cui,^{†,‡} Feng Shi,^{*,†} and Youquan Deng[†]

[†]Centre for Green Chemistry and Catalysis, Lanzhou Institute of Chemical Physics, Chinese Academy of Sciences, Lanzhou, 730000, China

[‡]Graduate School of the Chinese Academy of Sciences, Beijing, 100049, China

CONTENTS

1. Introduction	A	3.8.5. Arabinose Oxidation	Y
2. Selective Hydrogenation Reactions	B	4. Other Reactions	Y
2.1. 1,3-Butadiene Hydrogenation	B	4.1. Hydrochlorination of Alkynes	Y
2.2. α,β -Unsaturated Aldehyde Hydrogenation	C	4.2. Carbon–Carbon Bond Formation Reactions	Z
2.2.1. Crotonaldehyde Hydrogenation	C	4.2.1. Coupling Reactions	Z
2.2.2. Acrolein Hydrogenation	D	4.2.2. Sequential Oxidation–Addition Reactions	AA
2.2.3. Other α,β -Unsaturated Aldehydes	E	4.2.3. Benzylolation by Benzyl Alcohol	AB
2.3. Nitro Group Hydrogenation	E	4.2.4. Synthesis of Substituted Phenols	AB
2.3.1. Synthesis of Anilines	E	4.3. C–N Bond Formation	AB
2.3.2. To Other Compounds	G	4.3.1. Amination Reactions	AB
2.3.3. Other Reducing Agents	G	4.3.2. Nucleophilic Addition	AC
2.4. Anhydride Hydrogenation	G	4.4. Carbonylation Reactions	AD
2.5. Aromatic Ring Hydrogenation	G	4.4.1. Carbamates Synthesis	AD
2.6. Other Reduction Reactions	G	4.4.2. Carbonates Synthesis	AD
3. Selective Oxidation Reactions	H	4.4.3. Hydroformylation	AE
3.1. Selective Oxidation of Alkanes	H	4.5. Three-Component Coupling Reactions	AE
3.1.1. Benzylic and Allylic C–H Bonds Oxidation	H	4.6. Cyclization Reactions	AE
3.1.2. Cyclohexane Oxidation	H	4.7. Epoxide Isomerization to Allylic Alcohol	AF
3.2. Epoxidation Reactions	I	5. Conclusions and Outlook	AF
3.2.1. Propylene Epoxidation with H ₂ /O ₂	I	Author Information	AG
3.2.2. Propylene Epoxidation with O ₂ or O ₂ /H ₂ O	K	Biographies	AG
3.2.3. Kinetic and Mechanism Study	K	Acknowledgment	AG
3.2.4. Other Epoxidation Reactions	L	References	AH
3.3. Alcohols Oxidation	M		
3.3.1. Monoalcohol Oxidation	M		
3.3.2. Mechanism Exploration	P		
3.4. Selective Oxidation of Polyols	Q		
3.4.1. Ethylene Glycol Oxidation	Q		
3.4.2. 1,4-Diols Oxidation	R		
3.5. Aldehydes Oxidation	R		
3.6. Selective Oxidation of Amines	S		
3.6.1. Imine Synthesis	S		
3.6.2. N-Formylation of Amines	T		
3.6.3. To Other Compounds	U		
3.7. Silanes Oxidation and Hydrosilylation Reactions	U		
3.8. Biomass Transformation to Fine Chemicals	V		
3.8.1. Glucose Oxidation	V		
3.8.2. Glycerol Oxidation	W		
3.8.3. Cellobiose Oxidation	Y		
3.8.4. 5-Hydroxymethyl-2-furfural Oxidation	Y		

1. INTRODUCTION

Gold has been used for coinage, jewelry, and other arts for thousands of years due to its stability in air. Catalytic researchers were long misled by this common sense until the exciting discovery that gold possessed unique catalytic activity in the oxidative elimination of carbon monoxide^{1,2} and ethyne hydrochlorination,³ although some research with gold catalysis had been shown before.^{4–6} These studies opened the era of gold catalysis. Interest in gold catalysis can be quantitatively ascertained by the exponential growth in the number of publications, Figure 1. Today the “yellow metal” is considered as the catalyst of choice for many reactions such as oxidation of alcohols and aldehydes, epoxidation of propylene, hydrochlorination of ethyne, carbon–carbon bond formation, and so on. In particular, in recent years, many books and reviews have appeared on this

Received: July 12, 2011

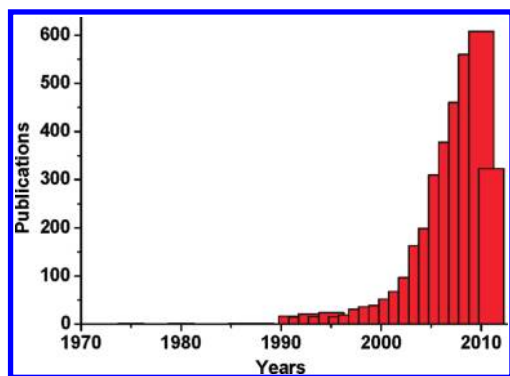
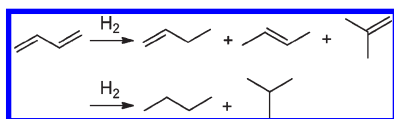


Figure 1. Publications on “gold catalysis” from 1970 to June 12th, 2011 by the ISI web of science.

Scheme 1. Possible Compounds Produced in the 1,3-Butadiene Hydrogenation Reaction



topic. These articles concentrated on the study of gold in various fields.^{7–50} However, regarding the application of gold in catalysis, normally homogeneous $\text{Au}^+/\text{Au}^{3+}$ complexes in organic synthesis were touched. The last review articles concerning nano-gold catalysis in fine chemical synthesis extensively were presented by Huntchings et al. in 2006²² and Corma et al. in 2008.¹⁶ Large numbers of results appeared, and about 60% of the publications covering nano-gold-catalyzed fine chemical synthesis have been published since 2008. In the above reviews, the preparation and characterization of nano-gold catalysts have been summarized in detail. Thus, the current review concentrates on the use of nano-gold catalysts in fine chemical synthesis, which covers literature published between the end of 1999 and June 2011. The review is organized into several sections for reaction types with discussion in the sequence of catalytic results and mechanism study.

2. SELECTIVE HYDROGENATION REACTIONS

Catalytic hydrogenation is one of the most important reactions extensively employed in industry. Traditionally, selective hydrogenation was catalyzed by VIII–X group metals such as Ni, Pd, Ru, and Pt.^{51–54} In comparison to these metals, gold metal has been classified as a poor catalyst due to its super resistance to oxidation reaction, although early studies showed that supported gold exhibited some activity in the hydrogenation reactions.^{22,27} At the end of the 1980s catalyst researchers were awakened suddenly that gold metal was an active catalyst when its particle size was minimized into nanoscale and immobilized onto different supports with proper methodology. Thus, gold has been tested again in hydrogenation reactions. It acts as a very promising catalyst, especially in selective hydrogenation reactions.

2.1. 1,3-Butadiene Hydrogenation

Selective hydrogenation of 1,3-butadiene to butene has been studied with gold catalyst since the 1970s.^{5,55–57} Usually selective hydrogenation of 1,3-butadiene (C_4H_6) produced three isomers of butene (C_4H_8), i.e., 1-butene, *cis*-2-butene, and *trans*-2-butene, Scheme 1.

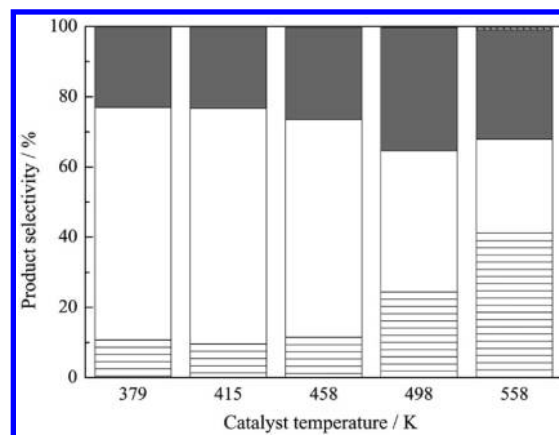


Figure 2. Product selectivity in 1,3-butadiene hydrogenation over the DP-Au/ Al_2O_3 catalyst: (□) 1-butene, (shaded light gray) *trans*-2-butene, and (shaded dark gray) *cis*-2-butene. Reprinted with permission from ref 58. Copyright 2002 Elsevier.

Okumura et al. prepared a series of alumina-immobilized nano-gold catalysts with different methods and tested their activity in 1,3-butadiene hydrogenation.⁵⁸ Among all the catalysts $\text{Au}/\text{Al}_2\text{O}_3$ prepared with the deposition–precipitation method (DP) exhibited the best performance. Conversion of 1,3-butadiene was $\sim 100\%$, and good selectivity to 1-butene was obtained, Figure 2, which was normally $>60\%$. The results suggested that hydrogenation of 1,3-butadiene over Au catalysts was somewhat insensitive to the Au particle size and composition of metal oxide support.

Piccolo et al.⁵⁹ reported that gold as an additive can promote the catalytic efficiency of Pd in the selective hydrogenation of 1,3-butadiene. For comparison, several catalysts including $\text{Au}(111)$, $\text{Pd}-\text{Au}(111)$, $\text{Pd}-\text{Au}(110)$, and $\text{Pd}(111)$ were prepared. All catalysts were characterized by LEED, AES, and LEIS. The study revealed that the bimetallic catalyst could improve the selectivity to butenes effectively, which reached $\sim 100\%$ on the $\text{Pd}_{70}\text{Au}_{30}$ (111) lattice plane. Gold may favor butene desorption from catalyst surface.

The presence of small amounts of alkadienes in light alkenes results in catalyst poisoning in the polymerization process. Catalytic conversion of alkadienes into alkenes is a good choice to solve this problem. Thus, Delannoy et al. studied the selective hydrogenation of 1,3-butadiene in the presence of a large excess of propene using nano-gold catalysts.⁶⁰ The model system was composed with 0.3% butadiene, 30% propene, 20% hydrogen, and balanced with 49.7% helium. It was shown that supported nano-gold catalysts prepared with the deposition–precipitation (DP) method exhibited better catalytic performance. The effect of supports, including TiO_2 , CeO_2 , Al_2O_3 , and ZrO_2 , on the catalytic activity was studied, but there is no significant difference. Under the optimized reaction conditions, at 170°C , 100% conversion of 1,3-butadiene with 1-butene as the main product was obtained. The total amount of alkanes was ~ 100 ppm. Further incorporation of Pd as the second metal promoted the activity remarkably.⁶¹ The temperature of the total conversion of 1,3-butadiene decreased to $\sim 90^\circ\text{C}$ with $<1\%$ propene conversion using $\text{Au}-\text{Pd}/\text{Al}_2\text{O}_3$ ($\text{Au}:\text{Pd} = 20$). In the stability measurement, the reaction progressed smoothly for >900 min.

Meanwhile, Xu et al. reported a simple method for preparing zirconia-supported nano-gold catalyst with low gold loading

(<0.1%).^{62,63} This Au/ZrO₂ catalyst possessed high activity for selective hydrogenation of 1,3-butadiene without any butane byproduct formation. The catalyst was well characterized with TPR and XPS, and the results demonstrated that the most active sites for the selective hydrogenation reaction were isolated Au³⁺ ions at the zirconia surface. Recently, they further reported that the gold oxidation state and hydroxyl groups on the support oxide surface played vital roles.⁶⁴ If the hydroxyl groups were removed by treating ZrO₂ at elevated temperature, the catalyst became inactive while an active catalyst was obtained again if it was subjected to a simple water treatment. The coinvolvement of Au⁰ and Au³⁺ on hydroxyl-rich ZrO₂ was the structural feature of active sites for H₂ activation, Figure 3.

In order to understand why gold can inhibit the deep hydrogenation of the gas-phase butene to butane, Liu et al.⁶⁵ studied the 1,3-butadiene hydrogenation using density functional theory (DFT) calculations. They found that Au⁺ on ZrO₂ is the catalytically active species, which is produced from Au³⁺ by in-situ reduction, Figure 4. The oxides not only stabilized Au monomers as the solution does in homogeneous catalysis but can also act as catalysts that provide additional reaction sites. Moreover, they proved that the deep hydrogenation of gas-phase butene to butane becomes kinetically unlikely due to the high kinetic energy barrier.

2.2. α,β -Unsaturated Aldehyde Hydrogenation

Unsaturated alcohols are important chemical intermediates. As a challenging topic in chemistry, selective hydrogenation of α,β -unsaturated aldehydes (R₁R₂C=CH–CH=O) to unsaturated alcohols (R₁R₂C=CH–CH₂OH) has been investigated for a long time,^{66,67} Scheme 2. However, normally, it was found that the major products are saturated aldehydes or saturated alcohols when conventional hydrogenation catalysts were used. This result is reasonable because hydrogenation of the C=C bond of R₁R₂C=CH–CH=O is thermodynamically more favorable over hydrogenation of the C=O bond.⁶⁶ Moreover, the C=C bond is more reactive than the C=O group due to kinetic reasons.

2.2.1. Crotonaldehyde Hydrogenation. Early research about nano-gold-catalyzed gas-phase hydrogenation of crotonaldehyde was reported by Hutching et al., and nano-gold catalysts including Au/ZnO, Au/ZrO₂, and Au/SiO₂ were checked.⁶⁸ In this work, an interesting phenomenon was discovered, i.e., addition of a catalytic amount of thiophene into the reaction flow could improve the selectivity to crotyl alcohol. FT-IR study provided evidence for direct modification of the Au surface by thiophene or products of thiophene. The selectivity to crotyl alcohol was influenced slightly by the supports.⁶⁹ Hydrogenation of crotonaldehyde over Au/ZnO catalysts gave >80% crotyl alcohol selectivity with 7.7% crotonaldehyde conversion.⁷⁰ As discussed above, the selectivity to crotyl alcohol was improved with modification of a suitable amount of thiophene, but conversion of crotonaldehyde decreased.

Touroude et al. presented the Au/TiO₂-catalyzed liquid-phase hydrogenation of crotonaldehyde.⁷¹ The catalysts were prepared by the deposition–precipitation (DP) method with urea and pre-treated under hydrogen or air flow before use. The results showed that the catalytic activity was strongly affected by the size of the nano-Au particle, Figure 5. Peak activity was obtained when its size was ~2 nm, which was 10-fold higher than that with the 4 nm Au particle. Importantly, the selectivity to crotyl alcohol was maintained (60–70%) with up to 50% crotonaldehyde conversion.

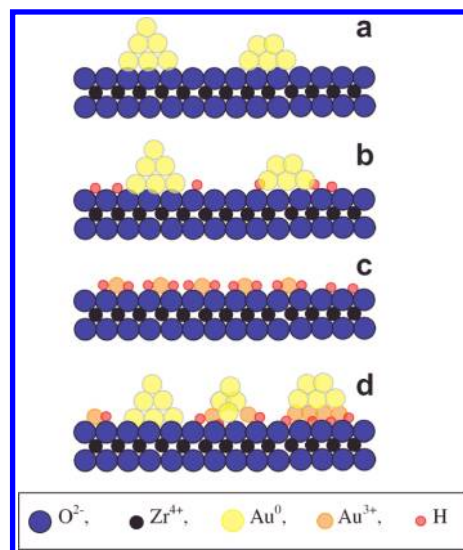


Figure 3. Proposed structure models for Au/ZrO₂ catalysts: (a) metallic Au⁰ particles deposited on OH-free ZrO₂-CP-1073 or ZrO₂-AN-1073; (b) metallic Au⁰ particles deposited on OH-carrying ZrO₂; (c) immobilized isolated Au³⁺ species on ZrO₂; (d) dispersed Au⁰ particles and Au³⁺ species on ZrO₂ with varying OH concentrations. Reprinted with permission from ref 64. Copyright 2011 Elsevier.

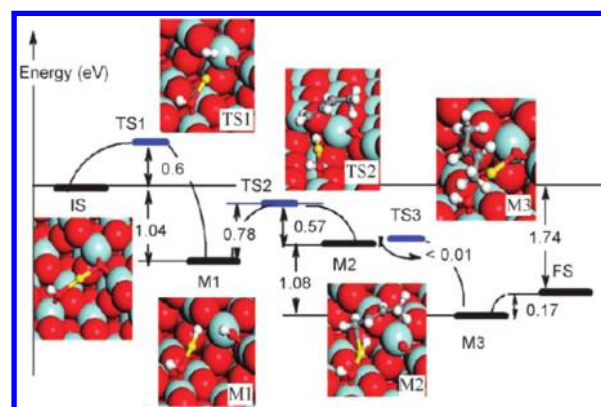
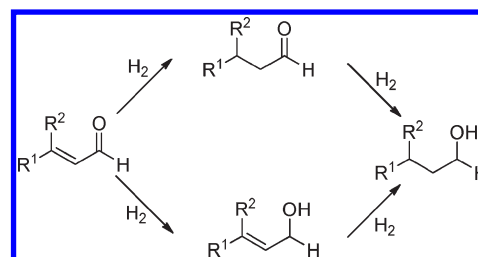


Figure 4. Overall energy profile and reaction snapshots for 1,3-butadiene hydrogenation (formation of butane) on the AuOH/t-ZrO₂-f surface. IS = initial state, FS = final state, M = intermediate state, and TS = transition state. Reprinted with permission from ref 65. Copyright 2006 Wiley-VCH.

Scheme 2. Reduction of α,β -Unsaturated Aldehydes



Then, the gas-phase hydrogenation reaction was tested with Au/HSA-CeO₂ (high surface area CeO₂, 240 m²/g) by Volpe et al.⁷² The catalysts were prepared by the DP method with

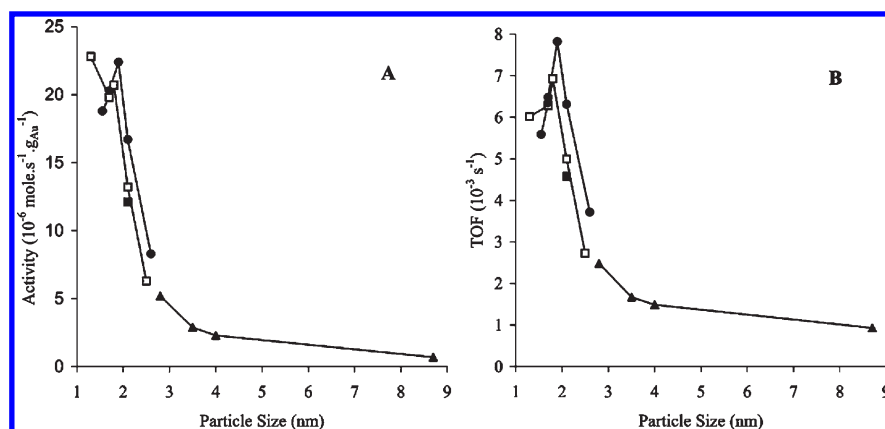


Figure 5. Activity (A) and TOF (B) versus the average particle size of DP Urea 16 h pretreated under H_2 (●), DP Urea 2 h pretreated under H_2 (■), DP Urea 2 h and DP Urea 1 h pretreated under air (◆), and DP NaOH 2 h pretreated under H_2 (□). Reprinted with permission from ref 71. Copyright 2004 Elsevier.

sodium carbonate and pretreated with H_2 or air before activity measurement. The calcination treatment before reduction was crucial to get high selectivity. After improvement, it was found that the selectivity to unsaturated alcohol was maintained >70% with ~8% conversion under the steady-stage regime in the flow reaction at 120 °C. If CeO_2 supports with low or medium surface areas (80 and 150 m^2/g) were employed, the selectivity to crotyl alcohol dropped to 20–30%.⁷³ However, the promoting effect of high surface area CeO_2 disappeared if the reaction was performed in the liquid phase.⁷⁴ The selectivity to crotyl alcohol decreased to 29% with the same high surface area CeO_2 -supported nano-gold as catalyst.⁷²

Chen et al. supported nano-gold particles onto Mg_2AlO hydrotalcite for the liquid-phase crotonaldehyde hydrogenation.⁷⁵ In comparison with nano-gold supported on FeOOH , Fe_2O_3 , CeO_2 , TiO_2 , and Al_2O_3 , this $\text{Au}/\text{Mg}_2\text{AlO}$ catalyst exhibited much higher catalytic activity. Conversion was >20% using $\text{Au}/\text{Mg}_2\text{AlO}$ but <5% with other catalysts. Meanwhile, the selectivities to crotyl alcohol were all 50–60%.

The combination of Au and In on γ -aminopropyltrimethoxysilane (APTMS) modified SBA-15, i.e., $\text{Au-In/APTMS-SBA-15}$, produced an excellent catalyst for liquid-phase hydrogenation of crotonaldehyde.⁷⁶ Incorporation of In species remarkably improved the catalytic activity with a highest yield of 71% to crotyl alcohol. Recently, from the same group, a novel nano-Au catalyst was prepared by heteroepitaxial growth of gold on flowerlike hematite materials for the liquid-phase crotonaldehyde hydrogenation to crotyl alcohol.⁷⁷ HRTEM characterization confirmed the heteroepitaxial growth of the AuNPs on the underlying magnetite. These flowerlike magnetite-supported gold catalysts exhibited good catalytic performance, and >75% crotyl alcohol yield is achieved. It was magnetically separated and reused 6 times without deactivation.

Although many studies have been performed in the nano-gold-catalyzed selective hydrogenation of crotonaldehyde to crotyl alcohol, the origin of the catalytic activity of nano-gold catalysts was still ambiguous. Volpe et al. extensively studied the activity–structure relationship in $\text{Au}/\text{Fe}_2\text{O}_3\text{--Al}_2\text{O}_3$ -catalyzed selective hydrogenation of crotonaldehyde and cinnamaldehyde.⁷⁸ Under the optimized reaction conditions the selectivity to crotyl alcohol is >50% with 20–30% crotonaldehyde conversion. TEM, TPR, and XANES characterization revealed that the high selectivity would not be related to the redox properties of the iron and

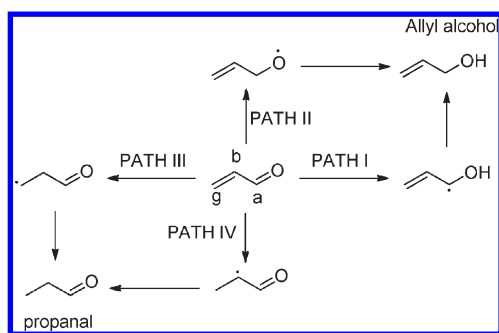
charged gold particle. Noteworthy, a controversial aspect concerning the hydrogenation of α,β -unsaturated compound with nano-gold catalysts is discussed, i.e., what is the suitable size of gold particle. In the work they suggested that the morphology but not the particle size of gold has a great influence on the selectivity.

2.2.2. Acrolein Hydrogenation. Claus et al. studied the effect of the electronic and structural properties of Au/TiO_2 and Au/ZrO_2 catalysts on the catalytic hydrogenation of acrolein.⁷⁹ Three Au/TiO_2 catalysts were prepared by DP, impregnation (I), and sol–gel (SG) methods. The Au/ZrO_2 catalyst was prepared by the coprecipitation (CP) method and DP method. The results showed that the activity and selectivity to the desired allyl alcohol increased with increasing gold particle size in the range of 1.1–3.8 nm. Possibly this is caused by the favorable adsorption of the carbonyl group of the α,β -unsaturated aldehyde so that the increased fraction of dense (111) planes of the larger gold particles offers more opportunity for allyl alcohol formation. By TEM/HRTEM and in-depth characterization with EPR it was shown that the origin of the antipathetic structure sensitivity of the hydrogenation of the $\text{C}=\text{O}$ vs $\text{C}=\text{C}$ group may be attributed to quantum size effects which alter the electronic properties of sufficiently small gold particles. By applying Au/TiO_2 -DP as catalyst, the selectivity to allyl alcohol reached 43% with <10% acrolein conversion.

Then, the influence of the structure of gold catalysts on the reaction was studied in more detail.⁸⁰ Almost all aspects, such as support effects, support–particle interactions, gold particle sizes, and the real structure of Au (shape, degree of rounding), that affected the catalytic activity were explored. A series of well-structured nano-gold catalysts was prepared and tested. The results suggested that a higher number of multiply twinned particles (MTPs) resulted in a lowering of selectivity to the desired product as well as a lowering of the turnover frequency. The higher activity of a gold catalyst supported on TiO_2 compared to ZrO_2 is attributed to a higher degree of rounding.

Later, identification the active site in the partial hydrogenation of acrolein was attempted by addition of indium to Au/ZnO .⁸¹ Addition of indium in an appropriate quantity can result in a selective decoration of the faces of gold particles and just poisons undesired active sites, while the active sites necessary to hydrogenate the $\text{C}=\text{O}$ functional group remain unchanged. The results showed that $\text{Au}(111)$ and (100) faces are active for preferential production of propionaldehyde, and the edges or

Scheme 3. Possible Reaction Routes for the Hydrogenation of Acrolein^a



^a Reprinted with permission from ref 82. Copyright 2009 Elsevier.

corners of nano-gold particle are responsible for formation of allyl alcohol.

Liu et al. reported a prediction of the catalytic performance of oxide-supported single gold catalysts for selective hydrogenation of acrolein with DFT periodic calculations.⁸² It was shown that Au^{3+} cations can be stable on the support, although it is reduced to Au^+ in the presence of hydrogen and activation of hydrogen molecule occurred on $(\text{AuOH})/\text{m-ZrO}_2$ (212), which determines the hydrogenation of acrolein to allyl alcohol. According to the hydrogenation process, four different pathways can be distinguished according to the position of acrolein where the first H attaches, as shown in Scheme 3. The calculations show that the lowest energy barrier to allyl alcohol is 0.46 eV, whereas that to propanal is 0.82 eV. It is thus expected from kinetics that good selectivity to allyl alcohol was achieved. The strong electrostatic interaction between the negative “O” end of acrolein and the proton on the “ O_{latt} ” facilitated the first hydrogenation step. Once the “O” of acrolein is protonated, the next hydrogenation is again facile between the positively charged α -C and the hydride.

It cannot be concluded definitely what controls the effectiveness in the nano-Au-catalyzed selective hydrogenation reaction of α,β -unsaturated compounds. Possibly, all factors such as Au particle size, support property and structure, and the interaction between nano-Au species and supports are important.

2.2.3. Other α,β -Unsaturated Aldehydes. Galvagno et al. explored the catalytic behavior of $\text{Au}/\text{Fe}_2\text{O}_3$ in the selective hydrogenation of citral to nerol and geraniol.⁸³ After improvement, conversion of citral reached 90% and the selectivity is higher than 95%. Reusability test showed 20% activity loss, but the selectivity remained unchanged. Selective hydrogenation of citral over Au/TiO_2 thin film in a capillary microreactor was studied, and similar results were obtained, i.e., >95% conversion and ~80% selectivity.⁸⁴

Xu et al. prepared a series of silica-gel-supported nano-gold catalysts from PVA-stabilized colloidal nano-Au solution with a controllable Au particle size of 3, 5, and 10 nm.⁸⁵ The nano-Au particle of size ~5 nm exhibited excellent activity for hydrogenation of the C=C bonds of cinnamaldehyde with up to 100% conversion and selectivity. Nano-gold colloid immobilized on ZrO_2 exhibited much lower activity and selectivity.

The $\text{Au}/\text{Mg}_2\text{AlO}$ hydrotalcite was active in cinnamaldehyde hydrogenation too.⁸⁶ Under the optimized reaction conditions the yield to cinnamyl alcohol was >80%. If the hydrogenation reaction of cinnamaldehyde was carried out in ethanol using

Au/TiO_2 as the catalyst,⁸⁷ cinnamyl ethyl ether was achieved with 33% selectivity and 50% cinnamaldehyde conversion.

Selective hydrogenation of benzalacetone, 4-methyl-1,3-penten-2-one, and 3-penten-2-one to the corresponding unsaturated alcohols was realized using $\text{Au}/\text{Fe}_2\text{O}_3$ catalyst.⁸⁸ For hydrogenation of benzalacetone and 4-methyl-1,3-penten-2-one, >50% selectivity was achieved with ~90% conversion. However, if 3-penten-2-one was employed as starting material, the selectivity was only 16.2%. Then, the role of different iron oxides, including goethite, maghemite, and hematite, as supports in nano-gold-catalyzed α,β -unsaturated aldehyde hydrogenation was explored using the liquid-phase reduction of *trans*-4-phenyl-3-buten-2-one or benzalacetone as the model system.⁸⁹ The results suggested that the selectivity toward hydrogenation of the conjugated C=O bond of benzalacetone is strongly influenced by the support. By applying goethite-immobilized nano-gold as the catalyst, the selectivity to unsaturated alcohol was 64% with >90% conversion. However, under the same conditions, the selectivity was only 6% when $\alpha\text{-Fe}_2\text{O}_3$ was used as the support.

De Vos et al. tested the polymer-stabilized nanometal clusters in the selective hydrogenation of α,β -unsaturated aldehyde/ketones.⁹⁰ The nanometal clusters were prepared in *N,N*-dimethylformamide (DMF) using polyvinylpyrrolidone (PVP) as a stabilizer. Among all the nanometal clusters tested, Au and Ag exhibited the best selectivity to the α,β -unsaturated alcohols. In their scope screening, 24 α,β -unsaturated aldehydes/ketones with various structures were transformed into the corresponding alcohol with up to 88% yields. This represents the most general catalytic system for selective hydrogenation of α,β -unsaturated aldehyde/ketones ever reported.

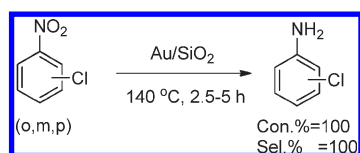
Jin et al. reported that quasi-homogeneous $\text{Au}_{25}(\text{SR})_{18}$ was active in the selective hydrogenation of α,β -unsaturated aldehydes.⁹¹ The results suggested this thiolate-stabilized gold nanoparticles exhibited excellent selectivity to produce unsaturated alcohols. By applying benzalacetone, crotonaldehyde, and acrolein as starting materials, the selectivities to the desired products were 91–100% with 19–50% conversions.

2.3. Nitro Group Hydrogenation

Aromatic amines are extensively found in biologically active natural products, pharmaceuticals, dyes, and ligands for transition-metal-catalyzed reactions. In industry, nevertheless, the catalytic hydrogenation of nitroarene to aniline serves as the key technology.⁹² Development of an effective catalyst for hydrogenation of functional nitrobenzenes is highly desirable.

2.3.1. Synthesis of Anilines. **2.3.1.1. Chloronitrobenzenes Hydrogenation.** Catalytic hydrogenation of chloronitrobenzenes has been studied extensively,^{93–95} but the hydrodechlorination reaction significantly limits the selectivity to chloroanilines. Nano-gold catalysis provides a new choice to solve this problem. One of the pioneering works of nano-gold-catalyzed selective reduction of chloronitrobenzenes was reported by Chen et al. using Au/SiO_2 catalyst.⁹⁶ Under the optimized reaction conditions, the conversion of *o*-, *m*-, or *p*-chloronitrobenzene and the selectivity to the corresponding chloroaniline were all close to 100% at 140 °C, 4.0 MPa H_2 , and 2.5–5 h, Scheme 4. This catalyst was active for hydrogenation of other nitrobenzenes with different functional groups.

Au nanoparticles on ZrO_2 were shown to be highly efficient catalysts for selective hydrogenation of chloronitrobenzenes without any dechlorination.⁹⁷ Hydrogenation of *p*-chloronitrobenzene occurred with >99% conversion and selectivity.

Scheme 4. Selective Hydrogenation of Chloronitrobenzenes over Au/SiO₂

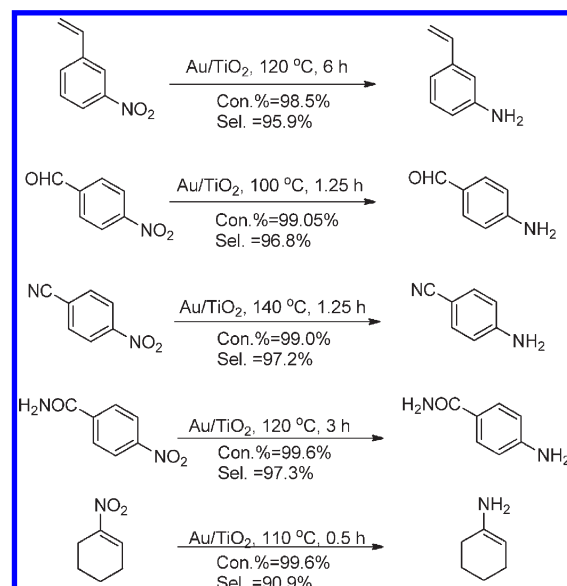
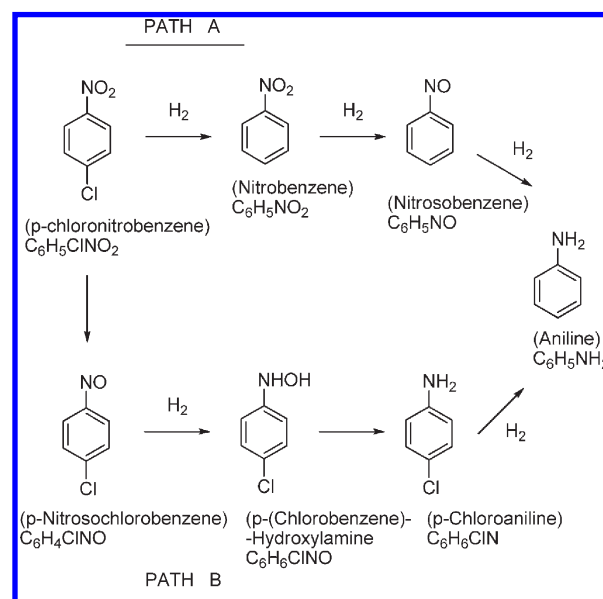
Relatively lower conversions, i.e., 81% and 85%, were observed for hydrogenation of *o*-chloronitrobenzene and 2,5-dichloronitrobenzene.

Keane et al. reported the gas-phase hydrogenation of *p*-chloronitrobenzene over Au supported on alumina⁹⁸ or titania.⁹⁹ They found that the conversion of *p*-chloronitrobenzene was appreciably lower than that with supported Pd, which generated nitrobenzene and aniline (nonselective hydrogenation) as the principal products with a significant temporal loss of activity.⁹⁹

2.3.1.2. Other Nitrobenzenes Hydrogenation. A general method about nano-gold-catalyzed selective hydrogenation of nitrobenzenes with excellent functional group tolerance was reported by Corma et al., Scheme 5.¹⁰⁰ Under the optimized reaction conditions, nitro compounds with olefin, aldehyde, nitrile, and amide groups were selectively hydrogenated into the corresponding amines with >99% conversion and >90% selectivity. Good activity and selectivity were obtained by means of polyaryl ether trisacetic acid ammonium chloride dendrons stabilized Au–Pt bimetallic nanoparticles.¹⁰¹ For reduction of 4-nitrophenol and 2-methoxynitrobenzene, the conversion and selectivity reached 100% but only a moderate yield was obtained with other nitrobenzenes.

In previous works it has been reported that relatively small Au clusters show a quantum confinement effect and exhibit distinct energy gaps in their electronic structure, which are responsible for the extraordinary catalytic performance.^{102,103} On the basis of this philosophy, the concept of ferric hydroxide-supported gold subnanoclusters or quantum dots catalysts were presented by Deng et al. for highly active nitrobenzene hydrogenation.¹⁰⁴ The key step for preparation of this quantum dot catalyst was based on control of the temperature; preparation should proceed under low temperature, i.e., $\leq 200\text{ }^{\circ}\text{C}$. In the traditional nano-gold preparation method, the calcination temperature was $\sim 400\text{ }^{\circ}\text{C}$. The chemoselective hydrogenation of aromatic nitro compounds containing carbonyl, halogen, olefin, and ester as well as nitrile groups was realized with 99% selectivity and 96–99% conversion. HR-TEM characterization showed that there is no observable gold particle for the sample calcined/dried at $200\text{ }^{\circ}\text{C}$, but 3–5 nm nano-gold particles formed after being calcined at $400\text{ }^{\circ}\text{C}$.

2.3.1.3. CO/H₂O as Reducing Agent. Catalytic reduction of nitro compounds with CO and H₂O as the hydrogen source is facile and cost effective. Research about nano-gold-catalyzed selective reduction of nitrobenzenes in the presence of CO and H₂O was reported by Deng et al.¹⁰⁵ By using 1.5 wt % Au/Fe(OH)x as catalyst, >95% conversions and selectivities were obtained for reduction of nitrobenzenes with different functional groups. Moreover, CO₂ was identified to be formed, while no H₂ was detectable in the hydrogenation reactions. Thus, the H species originated from H₂O during the water–gas shift (WGS) reaction might participate in the hydrogenation of aromatic nitro compounds immediately without release of molecular H₂. Subsequently, Cao et al. presented an Au/TiO₂ catalytic system for this process.¹⁰⁶ In comparison with the ferric hydroxide-supported nano-gold catalytic system, the Au/TiO₂ catalyst was more active and can work under milder conditions, i.e., $25\text{ }^{\circ}\text{C}$ and 1 atm of CO.

Scheme 5. Selective Hydrogenation of Nitro Compounds**Scheme 6. Reaction Pathways Associated with the Hydrogen-Mediated Conversion of *p*-Chloronitrobenzene^a**

^a Reprinted with permission from ref 110. Copyright 2009 Elsevier.

2.3.1.4. Kinetic and Mechanism Study. Commonly, two possible reaction pathways are associated with hydrogenation of *p*-chloronitrobenzene, Scheme 6. Both mechanisms have been reported for gas- and liquid-phase catalytic operation over supported metals.^{107–109} Bimetallic Pd–Au/Al₂O₃ catalysts were designed and prepared by the deposition–precipitation (DP) and impregnation (IPM) methods with Au/Pd mol/mol = 8, 20, and 88 in order to combine the high catalytic activity of palladium with the high selectivity of gold catalyst.¹¹⁰ Delightfully, these catalysts really directed the reaction along Path B without formation of aniline in continuous flow operation. Inclusion of Pd (at Au/Pd ≥ 20 , IMP and DP) resulted in 3-fold higher activity while retaining exclusivity to *p*-chloroaniline.

Corma et al. built a kinetic model for the chemoselective hydrogenation of nitroaromatic compounds on Au/TiO₂ by combining the Hougen–Watson formalism and isotopic studies.¹¹¹ The results suggested that the controlling step in the reaction is dissociation of the hydrogen molecule on the gold atoms and incorporation of platinum,^{112,113} which is highly efficient for hydrogen molecule dissociation, can improve the catalytic activity significantly, but high chemoselectivity is maintained. In order to explain the high catalytic activity and chemoselectivity of the bimetallic catalyst system, the reaction process was illustrated in Figure 6. The hydrogen molecule was dissociated on platinum, and the activated “H” species moved to the nitrobenzene compound, which was activated on the interface of nano-gold and titanium.

2.3.2. To Other Compounds. Several other works concern the reduction of nitrobenzenes to products with specific structure. Au/ZrO₂ was an effective catalyst for the transfer–hydrogenative photocatalytic reduction of nitrobenzenes to azobenzenes.¹¹⁴ Normally, azo benzenes with different functional groups were synthesized in >80% yield. Gas-phase hydrogenation of *m*-dinitrobenzene over Au/TiO₂ catalysts was reported.¹¹⁵ Formation of *m*-nitroaniline and *m*-phenylenediamine was observed during the reaction. In this reaction the catalytic activity is sensitive to the particle size, i.e., higher catalytic activity was achieved with smaller Au particles. The support composition (anatase:rutile ratio) did not influence the catalytic activity on nitro-group reduction, and *m*-nitroaniline formation was favored over Au particles < 5 nm. If nickel was added, the catalytic activity was modified and more *m*-phenylenediamine was produced.¹¹⁶

2.3.3. Other Reducing Agents. Several nano-gold catalysts were employed in the reduction of 4-nitrophenol with NaBH₄.^{117,118} Au/TiO₂ was shown to be active in the selective reduction of nitrobenzenes using ammonium formate (HCOONH₄) as the reductant.¹¹⁹ Although HCOONH₄ could not be applied in the large-scale production of anilines, it might have interest in laboratory-scale synthesis. This Au/TiO₂ catalyst possessed good functional group tolerance, and nitrobenzenes with different functional groups were selectively reduced to the corresponding amines. If more HCOONH₄ was added, further N-formylation of the anilines occurred and good yields were obtained.

2.4. Anhydride Hydrogenation

γ -Butyrolactone and pyrrolidone are important solvents or fine chemical intermediates in industry. The γ -butyrolactone and pyrrolidone synthesis via succinic anhydride hydrogenation or amination–hydrogenation catalyzed by Au/TiO₂ catalyst was reported, Scheme 7.¹²⁰ The selectivities to γ -butyrolactone were >99% at 80% conversion and 97% at >97% conversion. With addition of a small amount of Pt, the catalytic efficiency was further improved without selectivity decreasing. Au/TiO₂ catalyzed the one-pot synthesis of pyrrolidone and pyrrolidone derivatives from succinic anhydride and amine with >80% conversion. If phthalic anhydride was used as the starting material, phthalide was selectively synthesized (>90% conversion).¹²¹

2.5. Aromatic Ring Hydrogenation

Due to the high stability of aromatic rings, Pt, Pd, and Rh are the ideal choices to fabricate active catalyst.^{122–124} Unfortunately, the Pt, Pd, and Rh catalysts are easily poisoned even by few ppm of sulfur. Recent studies showed that nano-gold was active and stable in the elimination of N-, S-, or Cl-containing compounds,^{125–127} which inspired the researchers that incorporation of gold may be a possible solution to improve the sulfur resistibility of Pt, Pd, and Rh catalysts. That was confirmed by

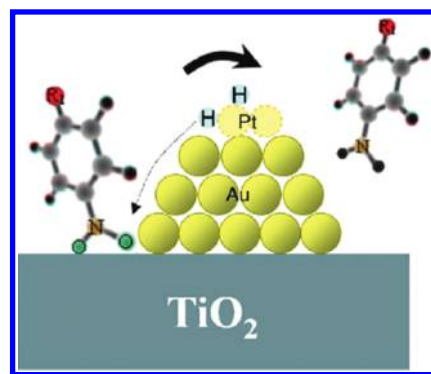
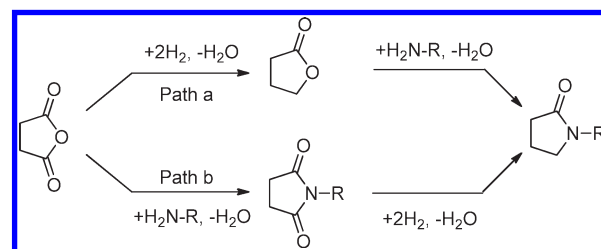


Figure 6. Plausible reaction pathway for the Au–Pt/TiO₂ catalyst exhibited high activity and chemoselectivity. Reprinted with permission from ref 112. Copyright 2009 Elsevier.

Scheme 7. Successive Hydrogenation and Dehydration of Succinic Anhydride^a



^a Reprinted with permission from ref 120. Copyright 2008 Elsevier.

Venezia et al. in a study on the hydrodesulfurization of dibenzothiophene (DBT) and thiophene over SiO₂-supported Au–Pd catalyst.^{128,129} They studied the role of alumina-supported Au–Pd alloy in selective hydrogenation of an aromatic ring with a mixture of DBT, naphthalene (NP), and toluene dissolved in hexadecane as a model system.¹³⁰ The presence of gold is found to improve the sulfur tolerance. Under the optimized reaction condition, the selectivity to tetralin is 90.7% with a weight hourly space velocity (WHSV) of 41.2 h^{–1}. Better performance was achieved with an improved AuPtPd/ASA (amorphous silica–alumina) catalyst.¹³¹ The DBT in the reaction mixture was totally hydrogenated, and conversion of naphthalene reached 100% with >90% tetraline selectivity. Formation of Au–Pd alloy, which possibly optimizes the surface acidity, and the presence of Au⁰ species, which increases the exposure of the Pt/Pd surface and weakens the adsorption of aromatic compounds, might be the reason for good sulfur tolerance.

The catalytic activity of Fe-, Ce-, or Ti-modified mesoporous silica-immobilized nano-gold catalysts in the selective hydrogenation of biphenyl to bicyclohexyl was tested.¹³² Generally, catalysts with different supports possessed a similar nano-gold particle size distribution, i.e., 3.2–6.5 nm. The iron-modified mesoporous silica-supported nano-gold catalyst exhibited the highest catalytic activity and best selectivity. It is possible that incorporation of iron produces a more active Au species, i.e., Au^{δ+}.

2.6. Other Reduction Reactions

Researchers have paid much attention to the selective epoxidation of olefins (see the discussions below). Recently, the reverse reaction, i.e., the nano-gold-catalyzed deoxygenation of epoxide, was reported.¹³³ During the reaction alcohols such as

2-propanol, benzyl alcohol, and 1-phenylethanol were added as the reducing agent with Au/hydrotalcite (HA) catalyst. Epoxides with different structures were deoxygenated to the corresponding olefins with 72–99% yields. The reaction progressed well using molecular hydrogen as the reducing agent too.¹³⁴ This system exhibited good generality, and the yields were >80%. Moreover, the particle size of nano-gold had a dramatic effect on the catalytic efficiency. Both the conversion and the selectivity decreased when the nano-gold particle size was bigger than 5.8 nm. A carbon monoxide/water mixture was used as the reductant too.¹³⁵

Nano-gold catalysts such as Au/TiO₂ were active in the transfer hydrogenative reduction of aldehydes using isopropanol as the reducing agent.¹³⁶ Benzylic, allylic, and aliphatic aldehydes and ketones were reduced into the corresponding alcohols with up to 99% yield. Similar reactions were realized if HCOOK was used as the reductant instead of isopropanol over Au/*meso*-CeO₂.¹³⁷ However, only aldehydes were reduced. Dumesic et al. reported the reduction of benzene in aqueous solution of polyoxometalates in the presence of nano-gold and CO/H₂O under electrochemical conditions.¹³⁸

3. SELECTIVE OXIDATION REACTIONS

Selective oxidation reactions constitute industrial core technologies for converting bulk chemicals to useful products of a higher oxidation state.^{139,140} Development of green oxidation systems is an important goal in catalysis. Due to the specific activity in selective oxidation reactions, nano-gold catalysts might offer a good choice to build clean and economic selective oxidation methods.

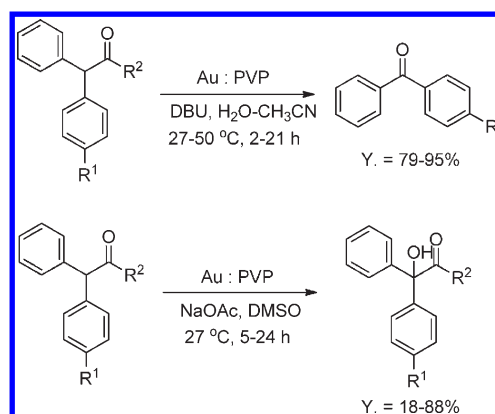
3.1. Selective Oxidation of Alkanes

3.1.1. Benzylic and Allylic C–H Bonds Oxidation. Selective oxidation of benzylic and allylic C–H bonds was initially carried out by Hutchings et al. with Au/C or Bi–Au/C.¹⁴¹ Selective oxidation of cyclohexene was investigated first. The solvent has a great effect on the catalytic oxidation reaction. No reaction occurred in polar solvents such as water, methanol, and THF. Different products were obtained via solvent variation with addition of 5% *tert*-butyl hydroperoxide (TBHP). In 1,3,5-trimethylbenzene, the major product was cyclohex-2-enone with 78.1% selectivity and 8% conversion. When 1,4-dimethylbenzene was used as the solvent, the major product that resulted was cyclohexane-1,2-dione with 43.5% selectivity and 53.5% conversion. Cyclohexene oxide was obtained with 50.2% selectivity and 29.7% conversion if the reaction was performed in 1,2,3,5-tetramethylbenzene. If cyclooctene was used as the starting material, the conversion was quite low, i.e., 7.9%, and the main product was cyclooctene oxide with ~80% selectivity. Recently, pyrrolidon-modified SBA-15 or manganese oxide octahedral molecular sieve supported nano-gold catalyst was used in the selective oxidation of cyclohexene, and similar results were obtained.^{142,143}

Under ambient conditions, selective oxidation of benzylic ketones was realized with good selectivity using the Au:PVP catalyst system, Scheme 8.¹⁴⁴ In the H₂O–CH₃CN system, 79–95% C–C bond oxidative cleavage products were obtained. When applying the reaction in DMSO, hydroxylation was the major reaction with 18–88% yields.

Au/SiO₂ was shown to be an active catalyst for the oxidative dehydrogenation of 1-butene to 1,3-butadiene if it was admixed with SiC to improve the temperature control.¹⁴⁵ Under the

Scheme 8. Oxidative C–C Bond Cleavage or Hydroxylation of Benzylic Ketones



optimized reaction conditions, conversion of 1-butene was 58% with 82% 1,3-butadiene selectivity. The oxidative dehydrogenation of ethylbenzene to styrene was checked in the presence of nano-gold catalysts with different metal oxides as supports.¹⁴⁶ Finally, it was found that Au/CeO₂ was an active and stable catalyst at 450 °C.

Oyama et al. tried to produce propylene oxide (PO) through selective oxidation of propane.¹⁴⁷ Au/TiO₂ and Au/TS-1 were chosen as catalysts. With these two catalysts a two-catalyst bed was built, i.e., dehydrogenation occurred on Au/TiO₂ and the epoxidation reaction progressed on Au/TS-1 sequentially in the presence of O₂/H₂. Under optimized reaction conditions, overall propane conversion was 2% and the selectivities to propylene and PO were 57% and 8%, respectively. Although the result was not good enough in comparison with the PO synthesis from propylene, it offered a new choice for PO synthesis.

Darapurkar et al. tested the Au/TiO₂-catalyzed selective oxidation of primary C–H bond in benzylic compounds at 1 atm O₂.¹⁴⁸ For the selective oxidation reactions of different benzylic compounds, 85–100% selectivities to the corresponding ketones were obtained with 12–65% conversions. Recently, the solvent-free oxidation of primary carbon–hydrogen bonds in toluene and its derivatives was realized using Au–Pd alloy nanoparticles immobilized on carbon or TiO₂.¹⁴⁹ The major product was benzyl benzoate with >80% selectivity, Figure 7.

The byproducts were benzaldehyde and benzoic acid. Moreover, it was found that Au/C was more active than Au/TiO₂. Characterization results suggested that the most important difference was the morphology of the Au–Pd particles. For Au–Pd/TiO₂, the Au–Pd species were highly faceted and primarily cube-octahedral or singly twinned in character, which preferentially exposed distinct {111}- and {100}-type facets. In contrast, the Au–Pd particles on carbon were more rounded with icosahedral and decahedral (5-fold twinned).

3.1.2. Cyclohexane Oxidation. Selective oxidation of cyclohexane to KA oil, i.e., mixture of cyclohexanol and cyclohexanone, is still a challenge in chemical industry.¹⁵⁰ Pioneering work on nano-gold-catalyzed cyclohexane oxidation was reported by Suo et al. with Au/ZSM and Au/MCM-41 catalysts.^{151–153} Under optimized reaction conditions 92% selectivity to KA oil was obtained with up to 16% conversion using Au/ZSM-5 catalyst. If MCM-41 was employed as the support conversion reached 12% with 97% selectivity and 11 214 h^{–1} turnover numbers. An extremely good result was reported by Richards et al.¹⁵⁴ In their work, the SBA-15

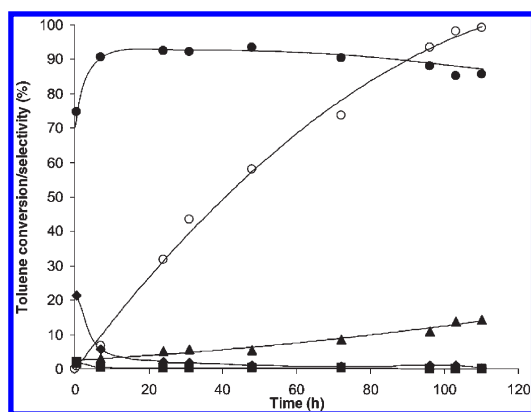


Figure 7. Toluene conversion and selectivity to benzyl alcohol, benzaldehyde, benzoic acid, and benzyl benzoate: reaction temperature, 160 °C (433 K); 0.1 MPa partial pressure of oxygen (P_{O_2}); 20 mL of toluene; 0.8 g of catalyst [1 wt % (wt %) Au–Pd/C prepared by sol immobilization with a 1:1.85 Au/Pd ratio]; toluene/metal molar ratio of 3250; and reaction time 110 h. Open circles indicate conversion, squares indicate selectivity to benzyl alcohol, diamonds indicate selectivity to benzaldehyde, triangles indicate selectivity to benzoic acid, and solid circles indicate selectivity to benzyl benzoate. Reprinted with permission from ref 149. Copyright 2011 AAAS.

support was modified by chlorine and then treated with 1-methylimidazole. The modified SBA-15 was used to immobilize nano-gold species with the deposition–precipitation method (DP). By applying this catalyst under optimized reaction conditions 28% conversion of cyclohexane and 94% selectivity were achieved!

Later, Hutchings et al. explored the activity of Au/C with *tert*-butyl hydroperoxide as an additive.¹⁵⁵ Then, Zhu et al. prepared several nano-Au catalysts with Al_2O_3 , TiO_2 , and $SiO_2-Al_2O_3$ supports.^{156–158} The best catalyst performance in cyclohexane oxidation to date was obtained with the Au/ SiO_2 catalyst. The turnover numbers reached $113\,201\ h^{-1}$. Ji et al. performed cyclohexane oxidation in a continuously stirred tank reactor with an air-like O_2/N_2 mixture, and good results were obtained with Au/SBA-15 catalyst.¹⁵⁹ Immobilization of manganese tetraphenylporphyrin on Au/ SiO_2 resulted in an effective catalyst for cyclohexane oxidation,¹⁶⁰ and 5.39% conversion was obtained with 88.74% selectivity to KA oil.

Selective oxidation of cyclohexane was extensively explored using different nano-gold catalysts, i.e., Au/ Al_2O_3 , Au/ TiO_2 , and Au/SBA-15,¹⁶¹ and Au/SBA-15 exhibited the best performance. The selectivity to KA oil was 71% with 4% conversion. Combining Au/SBA-15 with Co^{2+} increased the selectivity to KA oil to 75%. Meanwhile, the lowest amount of peroxide byproduct was detected in the presence of Au/SBA-15.

Tsukuda et al. prepared series of hydroxyapatite (HAP) supported nano-gold catalysts, i.e., Au/HAP.¹⁶² The nano-gold clusters contained 10, 18, 25, 39, and 85 gold atoms. Utilization of these catalysts in cyclohexane oxidation gave interesting results. Initially, the turnover frequency increased with increasing Au particle size, and the peak activity was obtained when the Au atom number was 39 (turnover number $18\,500\ h^{-1}$), Figure 8. Then, its activity decreased dramatically. By applying the best catalyst, conversion of cyclohexane reached 10%, maintaining ~99% selectivity.

Photocatalytic oxidation of cyclohexane with Au/Hombikat UV100 TiO_2 and selective oxidation of the primary C–H bonds in propene and acrolein on Au(111) were explored.^{163,164} By

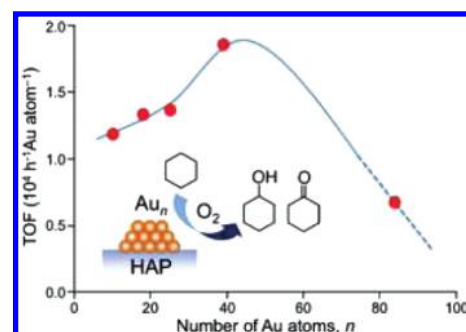
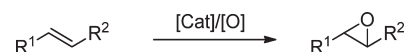


Figure 8. Selective oxidation of cyclohexane catalyzed by Au/HAP. Reprinted with permission from ref 162. Copyright 2011 American Chemical Society.

Scheme 9. Epoxidation Reaction of Olefin



applying Au/ TiO_2 as the catalyst and *tert*-butyl hydroperoxide as the oxidant, selective oxidation of α -pinene was realized.¹⁶⁵

3.2. Epoxidation Reactions

Selective epoxidation of olefins possesses peculiarly important status in chemical industry because epoxide is the starting material in the production of large numbers of bulk, fine, and pharmaceutical-grade chemicals, Scheme 9.¹⁶⁶ Research of the selective epoxidation of olefin with air, oxygen, or H_2/O_2 using nano-gold catalysts is one of the most prominent achievements in gold catalysis.

3.2.1. Propylene Epoxidation with H_2/O_2 . Haruta et al. presented the application of titania-immobilized nano-gold catalyst in the selective oxidation of propylene to PO with a mixture of H_2 and O_2 .¹⁶⁷ From this study, Ti is normally used in order to achieve catalytically active nano-gold catalyst for epoxidation reactions.^{168–170} Pd/ TiO_2 , Pt/ TiO_2 , Cu/ TiO_2 , and Ag/ TiO_2 were prepared for comparison, and the results suggested that both Au and TiO_2 are indispensable for selective formation of PO. After optimization, the selectivity to PO reached 90% and conversion of propylene was 1–2% with carbon dioxide as the major byproduct. Moreover, according to TEM characterization it was shown that the particle size of nano-gold on titania is the crucial factor affecting the catalytic activity. Hydrogenation of propylene becomes the major reaction when the particle size of nano-gold is smaller than 2 nm. It was supposed that the active oxygen species are produced by reductive activation of molecular oxygen with molecular hydrogen at the perimeter boundary between the Au particles and the TiO_2 support. Nano-gold immobilized on TS-1 or other titanium-containing supports catalyzed propylene epoxidation was reported.¹⁷¹ All catalysts were prepared by the deposition–precipitation method (DP). Similar to the above system, the yield of PO was 1–2%.

Then, a new catalyst Au/Ti-HMM (hybrid mesoporous silsesquioxane material) was prepared by the deposition–precipitation method (DP).¹⁷² Incorporation of Ti-HMM improved the efficiency remarkably. Up to 3.9% propylene conversion with 97.1% selectivity to PO was obtained. The efficiency was further improved with the use of MCM-48 as the support after carefully tuning the catalyst structure via preparation procedure variation.¹⁷³ Series of factors possibly affecting the catalytic activity,

such as the Si/Ti ratio (30, 50, 75, and 100), bases (LiOH, NaOH, KOH, RbOH, and CsOH), pH value (6–8), Au loading (20–25 wt % in solution), and calcination temperatures (150–500 °C), were screened extensively. After optimization, it was found that Si/Ti mole ratio = 50, NaOH as the precipitating agent, 0.3 wt % Au loading, 7.0 ± 0.1 pH value of solution, and 300 °C calcination temperature offered the best catalyst performance, i.e., 5.6% conversion and 92% selectivity. Later, Qi et al. found that addition of CsNO₃ could promote conversion of propylene with slightly lower propylene selectivity.¹⁷⁴ If KBr was used as promoter, propionaldehyde was formed as the major product with <0.1% propylene conversion.

The low capture efficiency of gold species is one of the major disadvantages in nano-gold catalyst preparation with the deposition–precipitation method (DP). In order to enhance the gold capture efficiency, an improved technology for Au/TS-1 preparation was employed.¹⁷⁵ The key step to prepare this Au/TS-1 catalyst was to modify the TS-1 support with NH₄NO₃ solution before immobilization of nano-gold species. Clearly, modification of TS-1 with NH₄NO₃ resulted in a 4-fold increase in gold capture efficiency, which reached 4–70%. Moreover, by applying NC_0.058_1.73 (NH₄NO₃-treated TS-1 with 0.058 wt % Au loading and 1.73 wt % Ti loading) as catalyst, 5% propylene conversion with 83% selectivity was obtained at 200 °C and the TOF to PO was 76 g PO h^{−1} kg_{cat}^{−1}, which is equal to 0.1 molecule of PO production per Au atom per second. Kinetic analysis of propylene epoxidation over Au/TS-1 catalysts suggested that a minimum of two active sites must work in conjunction in order to realize the epoxidation reaction.

An excellent catalytic performance was obtained by preparing the Au/TS-1 catalyst with *Cacumen platycladi* extract as the reducing agent and stabilizer through the sol preparation–immobilization (SI) or adsorption–reduction (AR) method.¹⁷⁶ With a feed gas composition of C₃H₆/O₂/H₂/N₂ = 10/10/10/70 (vol %) and space velocity of 4000 mL g_{cat}^{−1} h^{−1}, 12.6% propylene conversion with 70% PO selectivity was obtained at 573 K. Meanwhile, the hydrogen efficiency reached 48.9%.

Continuing the above works, recently, Qi and Haruta et al. extensively studied the relationship between the catalytic activity, the nano-Au particle size, and the presence of alkalis, Figure 9.¹⁷⁷ They revealed that hydrogenation of propylene to propane happened mainly when the nano-Au particle size is smaller than 2 nm or larger than 5 nm. Epoxidation became the major reaction when the nano-Au particle size is in the range of 2–5 nm in the presence of alkalis. Interestingly, addition of a small amount of oxygen can promote hydrogenation of propylene over both Au particles larger than 5.0 nm and clusters smaller than 2.0 nm.

Second metals such as Pt, Pd, Cu, Ge, and Co were added to improve the catalytic performance of nano-gold catalysts. The results suggested that addition of Pd resulted in hydrogenation of propylene to propane and hydrogen oxidation to water.¹⁷⁸ If using Pt as a modifier, the hydrogen and oxygen efficiency was improved.¹⁷⁸ By combining Au and Cu, an Au–Cu alloy bimetallic catalyst formed and high catalytic activity was exhibited.¹⁷⁹ The calcination temperature is essential to build the active catalyst with specific activity. As shown in Figure 10, an alloy catalyst with a suitable interaction between Au–Cu species and TiO₂ support was obtained after calcination at 673 K. The Au–Cu alloy structure possessed a particle size of ~5–6 nm and exhibited a 0.25 mol of PO g_M^{−1} h^{−1} TOF value at 573 K. Incorporation of Ge into catalyst Au/TS-1 could improve the catalytic activity and selectivity in propylene epoxidation reaction, too.¹⁸⁰ The Ge

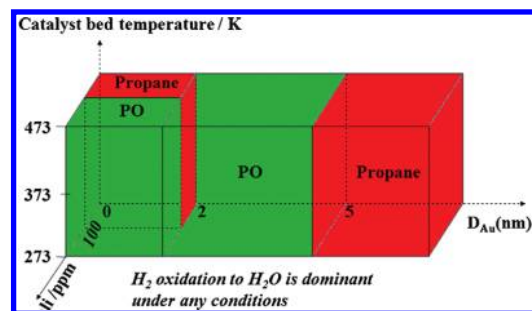


Figure 9. Schematic representation for hydrogenation and epoxidation of propene over Au/Ti-based oxides in the presence of H₂ and O₂. Reprinted with permission from ref 177. Copyright 2011 Elsevier.

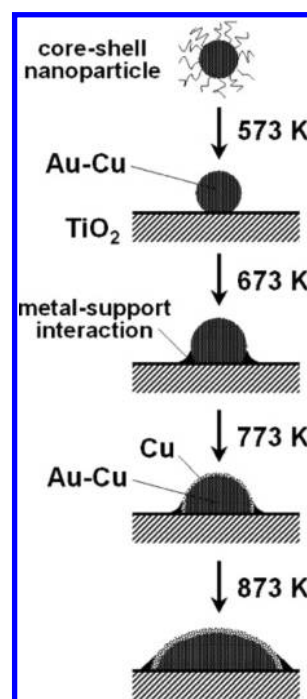


Figure 10. Effect of calcination temperature on the structure of Au–Cu alloy nanoparticles in catalyst Au₃Cu₃/TiO₂ (1.2%). Initially, Au–Cu alloy nanoparticles are capped with an organic envelop. After deposition on TiO₂ and calcination at 573 K the organic envelop is removed but the Au–Cu alloy structure is preserved. At 673 K the size of nanoparticles increases and a strong interaction between nanoparticles and TiO₂ occurs. At 773 K there is a slight enrichment of Cu on the surface, which is more pronounced at 873 K. At this temperature the size of nanoparticles increases strongly. Reprinted with permission from ref 179. Copyright 2008 Elsevier.

precursor was involved during TS-1 preparation and the Au/Ge-TS-1 was prepared with the deposition–precipitation method. By applying Au/Ge-TS-1 catalyst, 4% conversion and 91% selectivity to PO was obtained, while conversion was only 1.6% with 87% selectivity using Au/TS-1. Density functional theory (DFT) calculations indicated that the involvement of Ge decreased the activation energy of the epoxidation reaction. Cobalt was an effective promoter in the Au/TS-1-catalyzed propylene epoxidation reaction.¹⁸¹ As a typical catalyst, 10Au0.4Co/TS-1, in which the Au loading was 10 wt % with 0.4 wt % Co on TS-1, could maintain activity within 7 h at 125 °C with >2% propylene conversion and ~80% PO selectivity.

The improvement of the reactor should be another choice to achieve a fine epoxidation reaction system with O_2/H_2 .¹⁸² Zhou et al. tried to offer a safe propylene epoxidation technology using a microreactor. Classical Au/TiO_2 was packed in a stainless steel tube with a 4 mm internal diameter for catalytic activity evaluation. Deactivation of Au/TiO_2 was observed after ~ 30 min, but $\sim 0.5\%$ propylene conversion was maintained. Oyama et al. developed a packed-bed catalytic membrane reactor for epoxidation of propylene.¹⁸³ Using this specific reactor, the O_2/H_2 mixture gas was safely used in the explosive regime. In this way, the production rate of PO was remarkably improved, i.e., 10% propylene conversion and 80% PO selectivity were obtained with a space–time yield of $150 \text{ g of PO kg}_{\text{cat}}^{-1} \text{ h}^{-1}$ at 180°C .

3.2.2. Propylene Epoxidation with O_2 or $\text{O}_2/\text{H}_2\text{O}$. Approximately 10 years since the oxidants for propylene epoxidation were changed to a O_2/H_2 mixture from organic alkyl hydroperoxide and hydrogen peroxide, Haruta et al. gave the example of the epoxidation of propylene with oxygen as oxidant solely.¹⁸⁴ This represented big progress in nano-gold-catalyzed propylene epoxidation, although conversion of propylene was $<1\%$ with $\sim 50\%$ selectivity. The nano-gold particles were deposited on alkaline-treated titanosilicalite-1 (TS-1) by solid grinding (SG) with dimethyl gold(III) acetylacetonate. The particle size of this new nano-gold catalyst was smaller than 2 nm; only the catalyst with gold particles smaller than 2 nm was a selective catalyst for the epoxidation reaction. Otherwise, propylene was totally oxidized into carbon dioxide. The additional water is very important for selective formation of PO, Figure 11. Clearly, in the absence of H_2O conversion of propylene was only 0.1% without observable PO. With addition of H_2O , conversion of propylene was remarkably increased to $\sim 0.5\%$ with $\sim 47\%$ PO selectivity. In addition, this ultrafine nano-gold catalyst is active for the epoxidation reaction with O_2/H_2 mixture, which showed 8.8% conversion and 82% selectivity.

Almost at the same time a wonderful result was reported by Molina, i.e., Au_{6-10} cluster on irreducible alumina was an active catalyst for epoxidation of propylene using O_2 or $\text{O}_2/\text{H}_2\text{O}$ as oxidant.¹⁸⁵ Moreover, this was the first successful employment of Ti-free nano-gold catalyst in a propylene epoxidation reaction. Ti is considered to be essential for production of $\cdot\text{OH}/\cdot\text{OOH}$ radicals for the partial oxidation step. The subnano- $\{\text{Au}_{6-10}\}^+$ ions were selected by a mass spectrometer quadrupole deflector assembly and deposited onto rough and amorphous alumina on naturally oxidized silicon wafers. This specific catalyst exhibited perfect catalytic activity for epoxidation of propylene using $\text{O}_2/\text{H}_2\text{O}$ as oxidant. Under the improved reaction conditions, the TOF value was $0.1\text{--}0.4 \text{ molecules (site)}^{-1} \text{ s}^{-1}$. Using O_2 as oxidant, the activity dropped dramatically with the progress of the reaction. As shown above,¹⁸⁴ involvement of H_2 or H_2O could improve the reaction significantly and epoxidation of propylene could progress steadily.

Ab initio DFT calculations were performed to determine the origin of the catalytic activity of $\text{Au}_n/\text{Al}_2\text{O}_3$. It was revealed that $\text{C}_3\text{H}_6\text{O}$ metallacycle intermediates could form directly after adsorption of propylene on $\text{Au}_n/\text{Al}_2\text{O}_3$ catalyst surface due to replacement of hydrogen by water. However, when Au/TiO_2 was used, dissociation of hydrogen at the gold nanoparticle is essential to form a surface hydroxyl group, promote oxygen adsorption, and then generate active peroxo COOH radicals for metallacycle intermediates production. Thus, different reaction mechanisms take place for alumina and titanium dioxide supported nano-gold catalysts.

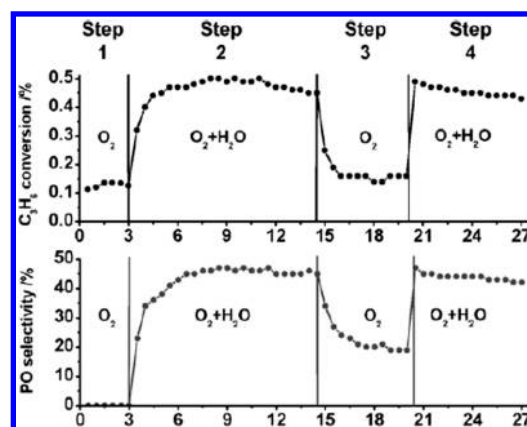


Figure 11. Enhancing effect of H_2O on propene epoxidation with O_2 over 0.10 wt % $\text{Au}/\text{TS-1-K1}$. Reaction conditions: catalyst 0.30 g; reaction temperature 473 K; feed gas $\text{C}_3\text{H}_6/\text{O}_2/\text{Ar} = 10/10/80$ or $\text{C}_3\text{H}_6/\text{O}_2/\text{H}_2\text{O}/\text{Ar} = 10/10/2/78$; space velocity $4000 \text{ mL g}_{\text{cat}}^{-1} \text{ h}^{-1}$. Step 1, without H_2O ; Step 2, H_2O was added to the feed gas; Step 3, addition of H_2O was stopped; Step 4, H_2O was added to the feed gas again. Reprinted with permission from ref 184. Copyright 2009 Wiley-VCH.

3.2.3. Kinetic and Mechanism Study. A series of studies was performed on the kinetic and mechanistic study of nano-gold-catalyzed propylene epoxidation reactions with H_2/O_2 .^{186,187} Interactions of propylene, hydrogen, oxygen, and PO with fresh and deactivated catalysts were characterized by FT-IR. The results suggested that deactivation of the Au/TiO_2 catalyst was due to irreversible adsorption of propoxy species on the active Ti site. Deactivation of the nano-gold catalysts was further explored by in-situ diffuse reflectance infrared Fourier transformed (DRIFT). After exposure of the catalyst to several reaction cycles, an increase in the amount of adsorbed bidentate propoxy species on the surface of the catalyst and a reduction of propene oxide in the gas phase was observed. Adsorption of bidentate propoxy species is irreversible and responsible for deactivation of the Au/TiO_2 catalyst likely. Moreover, formation of carboxylates and carbonates through decomposition of propoxy groups is less possible.

In-situ FT-IR characterization and kinetic study of Au/TiO_2 -catalyzed propylene epoxidation was further employed to explore the role of gold in the reaction, and clearer results were obtained.^{188–190} The results suggested that gold merely provides a peroxide species to epoxidize propene on the titania sites. Moreover, the gold particles catalyze a consecutive oxidation of the bidentate propoxy species to form carbonate/carboxylate species, which is possibly the cause of catalyst deactivation. The bidentate propoxy species is assumed as a reaction intermediate in the epoxidation of propene because the presence of H_2 and O_2 can desorb the propoxy species, Figure 12. A similar conclusion was drawn by modeling the kinetics and exploring the deactivation in the direct oxidation reaction of propene.¹⁹¹

In-situ XANES spectra measurement with inert Au/SiO_2 catalyst suggested adsorption of propylene on gold with π bonding.¹⁹² Utilization of $\text{Au}/\text{Ti-SBA-15}$ ^{193,194} in the propene epoxidation reaction was studied with the steady-state isotopic transient kinetic analysis (SSITKA) technique using $^{16}\text{O}_2/^{18}\text{O}_2$ and $\text{C}^{16}\text{O}_2/\text{C}^{18}\text{O}_2$. Although it is not conclusive, the study assumed that the lattice oxygen inside titania plays an important role in the mechanism cycle because P^{16}O is steadily produced

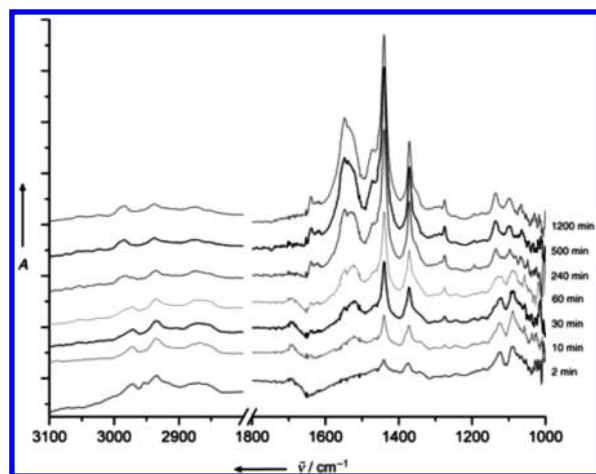


Figure 12. Spectra that demonstrate the gradual oxidation of a bidentate propoxy species on the gold–titania catalyst. Spectra were recorded from 2 to 1200 min after exposure of the catalyst to propene for 2 min (323 K; 10 spectra averaged). Reprinted with permission from ref 188. Copyright 2005 Wiley-VCH.

when the flow was switched from $^{16}\text{O}_2$ to $^{18}\text{O}_2$, Figure 13. Partial oxidation of propylene on Au(111) was explored by DFT study.¹⁹⁵ The results revealed that the key step for propylene oxidation is adsorption of allyl onto Au(111) and formation of OH radicals.

Delgass et al. studied the nano-gold-catalyzed propylene epoxidation extensively from the structure of catalyst and kinetic analysis.^{196,197} Among all the catalysts checked, Au/TiO₂–SiO₂, in which SiO₂ was modified by TiO₂ before immobilization of nano-gold, and Au–TiO₂/SiO₂, in which Au–TiO₂ nanocluster was supported on SiO₂, exhibited better performance than others. The major discovery in this work is that they revealed formation of ethanal and CO₂ as cracking products and PO oligomerization reaction. Generally, Au–TiO₂/SiO₂ possessed higher selectivity to PO due to the presence of isolated Ti atoms. Kinetic isotope effect exploration suggested that a hydroperoxy intermediate is involved in the rate-limiting step for PO formation. Subsequently, they tried to find out the real catalytically active nano-gold sites.¹⁹⁸ By applying TS-1 with different particle size, i.e., ~170 and ~519 nm, two Au/TS-1 catalysts, i.e., I and II, were prepared with the deposition–precipitation method. These catalysts have different surface-to-volume site ratios of Au–Ti. The surface-to-volume site ratio of catalyst I is 0.021 but 0.0068 in catalyst II. After careful TEM characterization and kinetic study it was found that the observable gold particles decorating the TS-1 particles do not account for the total gold content of the catalyst. Some “invisible” Au–Ti sites maintained in the Au/TS-1 catalysts and the active Au–Ti sites are very limited in number.

Kinetic study of propylene epoxidation with H₂/O₂ over a gold/mesoporous titanasilicate (Au/Ti-TUD) was performed.¹⁹⁹ There are three possible mechanisms, Figure 14. Different from the mechanism assumed by Delgass et al., Figure 14b, decoupling of the cycles was suggested, i.e., the hydrogen peroxide produced on the Au could migrate to the Ti sites to carry out the epoxidation reaction, and could separately decompose, Figure 14c. The catalytic effectiveness of the extended gold surface on the epoxidation reaction was studied by means of DFT calculations on Au(111) lattice.

Oyama et al. further investigated the effect of the gold oxidation state on the epoxidation reaction by treating the catalyst Au/TS-1

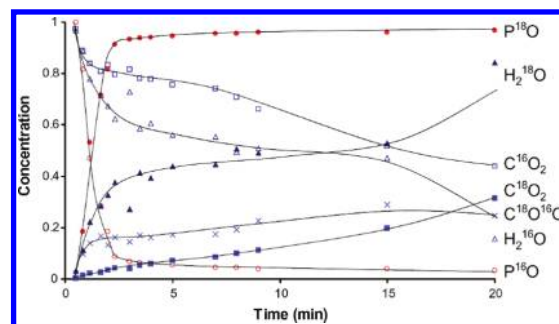


Figure 13. SSITKA transients for switch from $^{16}\text{O}_2$ to $^{18}\text{O}_2$ (at $t = 0$) after running the propene epoxidation over a 0.3 g of 1 wt % Au/Ti-SBA-15 catalyst at 423 K for 40 min (50 N mL/min total flow rate, 10 vol % of H₂, O₂ and propene in Ar/Ne). Reprinted with permission from ref 193. Copyright 2009 Elsevier.

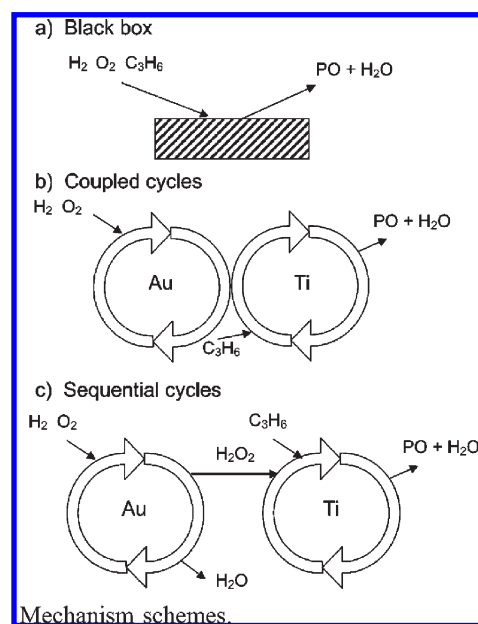


Figure 14. Mechanism schemes. Reprinted with permission from ref 199. Copyright 2007 American Chemical Society.

with NaCN solutions at different concentrations.²⁰⁰ By varying the NaCN concentration, small gold particles were removed at low cyanide concentration and gold (+3) cyanide formed at high concentration. The results suggested that the metallic nano-Au was active for propylene epoxidation and hydrogenation and combustion of H₂. If the particle size of nano-gold was >4.5 nm it was less active for all reactions. In the case where the catalyst was treated with strong solutions, reprecipitation of AuCN happened and nanoscale AuCN formed on TS-1, which was very active for hydrogenation, and no propylene oxidation was observed.

3.2.4. Other Epoxidation Reactions. Epoxidation reactions of styrene and other olefins using nano-gold catalyst were studied. Friend et al. tested the oxidation reaction of styrene and styrene oxide on Au(111) lattice with adsorbed oxygen.²⁰¹ The products of styrene oxidation on oxygen-occupied Au(111) are styrene oxide (parent ion, $m/z = 120$) at 280 K, benzoic acid (parent ion, $m/z = 122$) at 360 K, benzeneacetic acid (parent ion, $m/z = 136$), and combustion products (H₂O and CO₂) at 420 K. If the reaction was performed at higher temperature, i.e., 435 or

470 K, formation of phenylketene and acetophenone was observed. Adsorption of styrene oxide on clean Au(111) lattice showed the ring opening of styrene oxide to styrene at 410 K, along with phenylketene and phenylacetaldehyde formation (440–460 K), which suggested, to some extent, that the epoxidation process is reversible. According to the discussions above, the styrene epoxidation reaction on Au(111) should be performed at low temperature to achieve high selectivity.

Other oxidants such as NO_x , *tert*-butyl hydroperoxide, 3-chloroperoxybenzoic acid, and hydrocarbon/AIBN (azobis-isobutyronitrile) were applied in the olefin epoxidation reactions with nano-gold catalysts.^{202–211} Epoxidation of ethylene with nano-Au catalyst was studied using O_2 as oxidant.²¹²

3.3. Alcohols Oxidation

Aldehydes and ketones are particularly useful in the production of flavors, fragrances, and biologically active compounds. Traditionally, these carbonyl derivatives are produced through selective oxidation of alcohols with a stoichiometric amount of chromium salts, oxalyl chloride, or hypervalent iodines.²¹³ Recently, supported gold nanoparticles have been found to be extremely active catalysts for aerobic oxidation of alcohols.

3.3.1. Monoalcohol Oxidation. Inorganic support immobilized nano-gold-catalyzed aerobic alcohol oxidation should be discussed first due to its specific position in nano-gold catalysts. In early work, it was reported that gold on iron oxide was an effective catalyst for selective oxidation of *o*-hydroxybenzylalcohol to *o*-hydroxybenzaldehyde but the conversion and selectivity were not very high.²¹⁴ Then, employment of nanoceria-supported nano-gold in the selective oxidation of allylic alcohols to the corresponding α,β -unsaturated carbonyl compounds was explored.^{215,216} This nano-gold catalyst exhibited better performance than the Pd-apatite, Au–Pd/ TiO_2 , and Au–Pd– CeO_2 catalysts. Normally, >90% conversion and selectivity were obtained with Au/ CeO_2 , but the selectivities were <60% with other catalysts.

A series of nano-gold catalysts immobilized by different inorganic supports were used in the benzyl alcohol oxidation to benzaldehyde under solvent-free conditions.^{217–219} However, the yield is normally $\sim 50\%$ due to low benzyl alcohol conversion or formation of benzyl benzoate. Yang et al. prepared a series of SBA-16-supported nano-gold catalysts and tested their activity in benzyl alcohol oxidation.²²⁰ Although conversion was normally <20%, it exhibited >99% selectivity and >2000 h^{-1} TOF numbers. Nano-gold supported on $\beta\text{-MnO}_2$ was an effective catalyst for aerobic oxidation of alcohols to aldehydes.²²¹ As a typical result, the selectivity to benzaldehyde was 97% with 55% benzyl alcohol conversion. The presence of positive gold species and more surface oxygen vacancy sites might be the reason for its high activity. From the same research group, Au/ $\gamma\text{-Ga}_2\text{O}_3$ was prepared and excellent results obtained in the alcohol oxidation to aldehyde.²²² For oxidation of benzylic alcohols, normally both the conversion and the selectivity were >95%. Noteworthy, 99% selectivity was achieved with 45% conversion if using 1-octanol as starting material. Baiker et al. investigated the effect of nano-gold particle size on the catalytic activity of Au/ CeO_2 or Au/ TiO_2 in the aerobic oxidation of benzyl alcohol to benzaldehyde.²²³ The results assumed a suitable particle size of 6.9 nm, whereas smaller and bigger particles resulted in inferior activity.

Addition of inorganic base could improve the catalytic efficiency of benzyl alcohol to benzaldehyde using Au/C catalyst.²²⁴ Under base-free conditions, the conversion and selectivity were

$\sim 10\%$. Under the same reaction conditions, with addition of 1 mol % NaOH as cocatalyst, the conversion and selectivity reached $\sim 90\%$. The role of alkali in the reaction was ascribed to formation of $\text{Au}-\text{OH}^-$ sites, which were helpful to promote alcohol oxidation. The promoting effect of base was observed when basic hydrozincite or bismuth carbonate was used as support.²²⁵ Except for using base as promoter for alcohol oxidation, it was reported that addition of a catalytic amount of water could improve the catalytic activity of Au/ TiO_2 .²²⁶ Conversion of benzyl alcohol is 7 times higher in water/*p*-xylene mixture (7:1, mol/mol) than that in the absence of water. Conversion of benzyl alcohol was >80% with 93% benzaldehyde selectivity. Possibly, the presence of water helps form unique droplets in a multiphase reaction system and facilitates O_2 adsorption and activation.

Au/HT (hydrotalcite) was shown to be highly effective in the selective oxidation of alcohols.²²⁷ The effect of solvents, including toluene, heptane, ethyl acetate, *tert*-butyl alcohol, acetonitrile, and water, etc., on the reaction was tested. The results suggested that toluene was the best choice for selective oxidation of 1-phenylethanol. Acetophenone was produced quantitatively in 6 h under atmospheric O_2 at room temperature with 200 000 TON value. Catalyst was recovered and easily reused without obvious deactivation after several runs. Moreover, this Au/HT catalyst was easily applied to selective oxidation of various alcohols. Except primary aliphatic alcohol, alcohols with different structures, i.e., primary and secondary benzylic alcohols, aliphatic secondary alcohols, cycloalcohols, and allyl alcohols, were oxidized into the corresponding aldehydes or ketones with up to 99% yield. Incorporation of basic supports hydrotalcite might be the main reason to obtain the highly active catalyst in which the basicity is helpful to prevent aggregation of nano-gold particle and promote the oxidation reaction of alcohol.

A magnetically separable nano-gold catalyst was prepared and used in the selective oxidation of alcohols.²²⁸ The preparation route of the magnetic support immobilized nano-gold catalyst was shown in Figure 15. This Au/ $\text{SiO}_2\text{-Fe}_3\text{O}_4$ catalyst showed very high activity in the selective oxidation of benzyl alcohol and 1-phenylethanol with 100% conversion to yield the corresponding aldehyde/ketone or ester. Involvement of magnetite as the core of the catalyst makes it easily separable and reusable, and leaching of gold species during reaction is negligible.

Apart from the progress discussed above, some special nano-gold catalytic systems were developed. Kawanami et al. explored the effect of supercritical carbon dioxide on the nano-gold-catalyzed alcohol oxidation to aldehydes.²²⁹ Under weak basic conditions, benzylic alcohols were smoothly oxidized into the corresponding aldehydes with >90% yields. Karimi et al. reported an in-situ-formed Au/ Cs_2CO_3 catalyst for aerobic alcohol oxidation.²³⁰ NaAuCl_4 and Cs_2CO_3 were directly added into the reaction mixture, and the oxidation reaction started in the presence of oxygen. For example, with addition of 0.2% NaAuCl_4 and 3 equiv of Cs_2CO_3 , benzyl alcohol was oxidized into benzaldehyde with >99% yield. This catalyst is effective for oxidation of benzylic alcohols and cyclic alcohols. The gas-phase selective oxidation of benzyl alcohol to benzaldehyde with molecular oxygen was investigated using nanoporous gold.²³¹ Conversion of benzyl alcohol was 61% with 95% selectivity at 240 °C. The catalytic activity was improved remarkably by treating the catalyst with NaOH before reaction.

Au/ TiO_2 was a good catalyst for the synthesis of acetic acid via ethanol oxidation with high efficiency.²³² The nano-gold particle

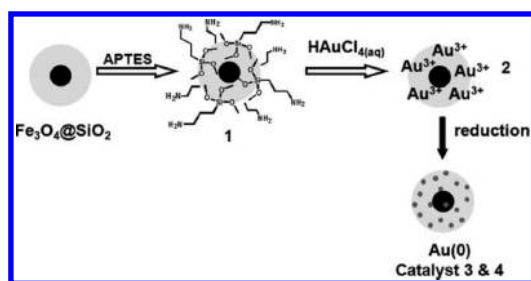


Figure 15. Step-by-step preparation of magnetically recoverable AuNPs. Reprinted with permission from ref 228. Copyright 2010 Royal Society of Chemistry.

has a very narrow size distribution range, and the yield to acetic acid was higher than 80%, Figure 16. The increasing ethanol concentration rendered ethyl acetate as the major product.

Xu et al. reported the application of Au/SiO₂ in the oxidation of ethanol to acetic acid.²³³ The results suggested that the particle size of the nano-gold has a great effect on the catalytic activity, and the highest activity was obtained when the average gold particle size was ~5 nm. Under the optimized reaction conditions the selectivity to acetic acid was >90%.

Oxidative esterification of alcohol is an important reaction in fine chemical synthesis. Addition of base is commonly crucial to gain high activity. Christensen et al. tried the oxidative esterification of various alcohols to the corresponding methyl esters with Au/TiO₂ as the catalyst and NaOCH₃ as the additive.²³⁴ Conversion of the alcohols and the selectivity to the corresponding methyl esters was 88–99%, Scheme 10.

Addition of K₂CO₃, Na₂CO₃, and NaOH, etc., could improve the catalytic efficiency of Au/TiO₂.²³⁵ For example, >99% selectivity was obtained with 30–60% conversion when ethanol, 1-propanol, and 1-butanol were used as starting materials to yield the corresponding esters. Potassium titanate nanowire-supported nano-Au catalyst was the active catalyst for oxidation of benzyl alcohol to methyl benzoate.²³⁶ Addition of KOH as an additive can promote the reaction significantly, and the yield was raised to ~90% from ~10%. Meanwhile, it was shown that methyl propionate was obtained from *n*-propyl alcohol oxidation in methanol with up to 99% selectivity and 63% conversion using Au/TiO₂ as catalyst and NaHCO₃ as additive.²³⁷ Au/SiO₂ catalyst was prepared via deposition of preformed nano-gold particles onto amino-functionalized silica gel in toluene for the one-step oxidative esterification of benzyl alcohol, allyl alcohol, 1-propanol, 1-butanol, and 1-pentanol.²³⁸ Methyl esters with different structures were synthesized with up to 100% selectivity.

A series of nano-gold catalysts supported on Fe-, Ti-, and Ce-modified hexagonal mesoporous silica (Au/M-HMS) was prepared for aerobic oxidative esterification of benzyl alcohol to methyl benzoate.²³⁹ The results showed that the modification with Ti can significantly improve the catalytic activity in oxidative esterification of benzyl alcohol. The turnover frequencies reached ca. 1000 h⁻¹ with up to 95% selectivity.

Hydrogen peroxide and *tert*-butyl hydroperoxide were used as oxidants in the selective oxidation of alcohols using nano-gold catalysts on inorganic supports.^{240–246} It was a good system for selective oxidation of primary aliphatic alcohol to acid and secondary alcohol to ketone, but no good selectivity was obtained for oxidation of a primary aromatic alcohol.

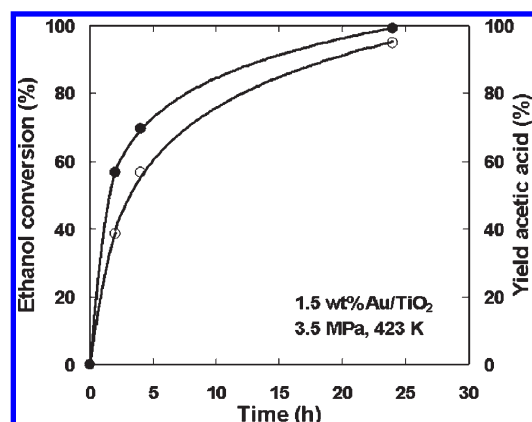
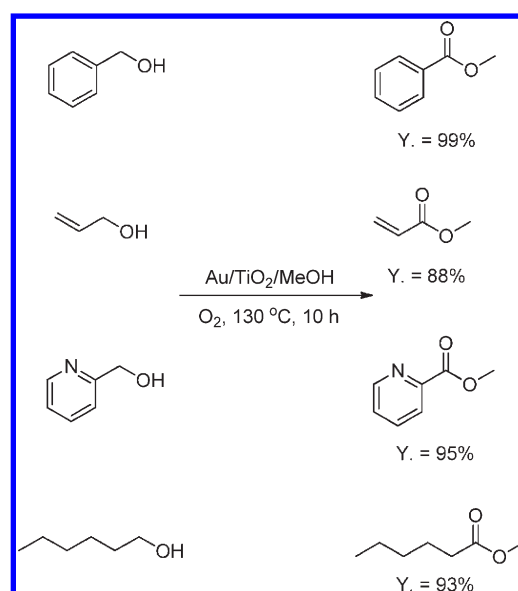


Figure 16. Yield of acetic acid (●) and conversion of ethanol (○) as a function of time. Reprinted with permission from ref 232. Copyright 2007 Elsevier.

Scheme 10. Oxidative Esterification of Alcohols in Methanol



Polymers with different structures were used to immobilize nano-gold catalyst, and nice performance was obtained in the selective oxidation of alcohols. Moderately cross-linked copolymers of *N,N*-dimethylacrylamide (DMAA), 2-(methylthio)ethyl methacrylate (MTEMA), and *N,N*-dimethylenebisacrylamide were prepared and used as supports for Pd and Au nanoclusters via extraction of Pd^{II} and Au^{III} from aqueous solution and subsequent reduction with NaBH₄.²⁴⁷ These catalysts exhibited good activity in the oxidation of 1-butanol to 1-butanaldehyde. The selectivity to butanaldehyde reached 40–70% with 20–40% 1-butanol conversion. Poly(*N*-vinyl-2-pyrrolidone) (PVP) stabilized nano-gold cluster exhibited excellent activity in the selective oxidation of alcohols to the corresponding carboxylic acid with up to 99% yield.²⁴⁸

Tsukuda et al. reported the size-controllable preparation of polymer-stabilized gold nanoclusters for aerobic alcohol oxidation in water.²⁴⁹ Nano-gold samples with gold particle sizes of 1.3 and 9.5 nm were successfully prepared with NaBH₄ or Na₂SO₃ as reductant. For comparison, nanopalladium samples with 1.5 and 2.2 nm were produced with the same procedure.

By applying Au:PVP-1 in the selective oxidation of benzyl alcohol and hydroxyl benzyl alcohol, interesting results were obtained. For the selective oxidation of benzyl alcohol, benzoic acid was the major product with 85% yield.²⁴⁹ The position of the hydroxyl group on the phenyl ring has a remarkable effect on the oxidation reaction. In the oxidation of *o*-hydroxyl benzyl alcohol, the main product was aldehyde. In the oxidation of *m*-hydroxyl benzyl alcohol, a mixture of aldehyde and acid was obtained. If applying *p*-hydroxyl benzyl alcohol as the starting material, only aldehyde was produced with 91%. Kinetic study showed that smaller (1.3 nm) Au nanoclusters exhibit higher catalytic activity than the larger (9.5 nm) nanoclusters and are more active than the Pd nanoclusters. The rate-determining step of the Au:PVP-1-catalyzed reaction may involve H-atom abstraction by a super-oxo-like molecular oxygen species adsorbed on Au:PVP-1. The size-dependent catalytic activity of Au:PVP-1 might be explained by highly efficient activation of O₂ on smaller gold nanoclusters.

Kobayashi et al. developed a polymer-incarcerated, carbon-stabilized nano-gold catalyst, i.e., PI/CB-Au, and its catalytic activity in the selective oxidation of alcohols was tested.²⁵⁰ The polystyrene-based matrix is bifunctional, i.e., stabilizing the gold nanoclusters and preventing the leaching of nano-gold clusters during reaction. This goal was actualized according to the results. Secondary alcohols with different structures were oxidized into the corresponding ketones with high efficiency. Moreover, the catalyst was used 5 runs without deactivation.

Oxidative esterification of alcohols was performed effectively using polymer-supported or modified nano-gold catalysts.²⁵¹ Direct deposition of Au clusters onto porous coordination polymers (PCPs) was realized by solid grinding with a volatile organo-gold complex. The best performance was achieved using Au/MOF-5 ([Zn₄O(bdc)₃]_n (bdc = benzene-1,4-dicarboxylate) as catalyst, which gave 91% yield to methyl benzoate. A general methodology was developed for oxidative esterification of benzylic and allylic alcohols applying polymer-incarcerated nano-gold catalyst by Kobayashi et al. For the preparation of this catalyst, the nano-gold particles were directly deposited onto the polymer but not using polymer to modify the carbon-immobilized nano-gold. The yields to the methyl esters with benzylic and allylic alcohols as starting materials were in the range of 60–99%, and the catalyst was reused 11 runs without deactivation.

Applying Au–M bimetallic nanocatalyst in the selective oxidation of alcohols promotes its catalytic efficiency remarkably. Hutchings et al. reported the supported nano–Au–Pd-catalyzed selective oxidation of alcohol using O₂/H₂ as oxidant.^{252,253} In comparison with those using Au or Pd catalyst solely, both the conversion and the selectivity were improved remarkably, Figure 17. Oxidation of benzyl alcohol was finished in 12 h with >90% selectivity to benzaldehyde with Au–Pd bimetallic catalyst. Conversion of benzyl alcohol was only ~55% using Pd itself as catalyst after 22 h. The Au–Pd/TiO₂ catalyst was used in the selective oxidation of other primary and secondary alcohols with high efficiency with up to 270 000 turnovers per hour. This might be the highest value in the selective oxidation of alcohols. After careful characterization, the structure of the Au–Pd bimetallic nanoparticle was shown to have an Au-rich core surrounded with a Pd-rich shell on titania.

Prati et al. studied the catalytic activity of Au–Pd and Au–Pt bimetallic catalyst systems in the alcohol oxidation reaction to aldehyde.^{254,255} The bimetallic catalysts were prepared by dipping premade Au/AC in Na₂PdCl₄ or K₂PtCl₄ solution containing PVA (polyvinylalcohol). Au–Pd and Au–Pt bimetallic

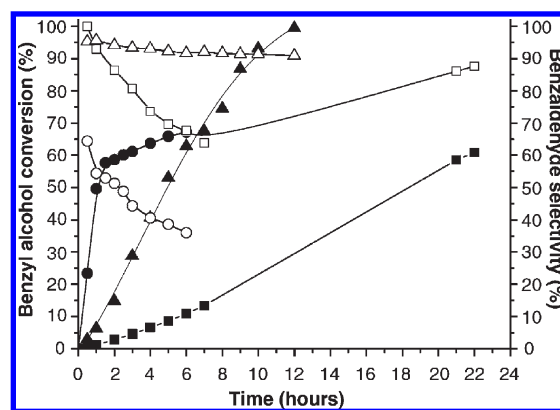


Figure 17. Benzyl alcohol conversion and selectivity in benzaldehyde with the reaction time at 373 K and 0.1 MPa pO₂: squares, Au/TiO₂; circles, Pd/TiO₂; and triangles, Au–Pd/TiO₂. Solid symbols indicate conversion, and open symbols indicate selectivity. Reprinted with permission from ref 252. Copyright 2006 AAAS.

catalysts have a similar particle size distribution and microstructure. Three typical alcohols, i.e., cinnamyl alcohol, benzyl alcohol, and 1-octanol, were used to test the activity of these catalysts using toluene or water as solvent. Better catalytic oxidation performance was achieved in water with 0.73% Au–0.27% Pd/AC (activated carbon). Characterization suggested that the Au–Pd and Au–Pt bimetallic catalysts were single-phase catalysts and presented only alloyed phases of a single composition. The presence of a synergistic effect between the two metals was found in most of the catalytic tests, being positive with Pd and negative with Pt in most cases. The SBA-16-immobilized Au–Pd bimetallic catalyst was active for selective oxidation of benzylic alcohols to the corresponding aldehydes.²⁵⁶ The yields were >90% when cinnamyl alcohol or 1-phenylethanol was employed as starting material.

Although Prati et al. reported Au–Pd possessed better catalytic behavior than Au–Pt in the selective oxidation of alcohol, continued works by Kobayashi et al. reported that an excellent Au–Pt bimetallic catalyst was produced using cross-linked polystyrene derivative as support (PI Au/Pt).²⁵⁷ This PI Au/Pt catalyst showed good catalytic activity for selective oxidation of secondary and cyclic alcohols to the corresponding ketones with 67–99% yields. It was recovered and easily reused without any deactivation after 6 runs. De Vos reported that addition of base into the inorganic support could effectively promote the catalytic activity of the Au–Pd bimetallic catalyst in alcohol oxidation reactions.²⁵⁸ By applying Au⁰–Pd⁰/HSA–BaAl₂O₄ as catalyst, benzylic and allylic alcohols were successfully oxidized into the corresponding ketones or aldehydes with up to 58 020 h^{–1} TOF number and 99% selectivity.

Copper was a fine additive to build the Au–M bimetallic catalyst. Au–Cu/SiO₂ was prepared with the codeposition–precipitation method and used in the gas-phase oxidation of benzyl alcohol.²⁵⁹ Combination of Au and Cu resulted in >98% yield of benzaldehyde under the optimized catalyst composition, i.e., Cu:Au = 1:4 (mol/mol). The yields were 74% and 40% when Au and Cu were used separately.

Au/Cu-fiber catalyst was prepared simply by dipping the Cu-fiber into a HAuCl₄ aqueous solution.²⁶⁰ Typically inactive alcohols such as cyclopropylmethanol, cyclohexanol, 1-octanol, crotyl alcohol, and 3-methylbut-2-enol were oxidized into the

corresponding aldehydes/ketones with 57–91% conversion and 88–99% selectivity. Characterization of the Au/Cu-fiber catalyst sample suggested formation of AuCu(alloy)–Cu₂O composition was responsible for the catalytic activity in the selective oxidation of alcohols.

Dai et al. prepared a series of Au–Ag/TiO₂ catalysts for oxidation of benzyl alcohol to sodium benzoate under solvent-free conditions.²⁶¹ Under optimized reaction conditions, >75% yield to the corresponding product was obtained and the catalyst was reused easily without obvious deactivation.

A poly(vinylpyrrolidone) (PVP)-stabilized Au–Pd core–shell nanocatalyst was prepared for selective aerobic oxidation of crotyl alcohol to crotonaldehyde.²⁶² Different PVP-stabilized Au–Pd core–shell catalysts were prepared using Au nanoparticle as seed, sequential reduction of Au and Pd precursors, and coreduction of Au and Pd precursors. The particle size of the resulting sample was in the range of 3–5 nm. The results suggested that the sequentially reduced nanoparticles possessed Pd-rich surfaces and were excellent catalysts for the room-temperature aerobic oxidation of crotyl alcohol with 88% selectivity and 306 h^{−1} turnover numbers. Under the same reaction conditions, the TOFs using coreduced Au–Pd sample were only 40 h^{−1}. Mechanism exploration suggested a redox cycle of Pd(II) and Pd(0), but the β -H elimination pathway could not be ruled out completely.

Kobayashi et al. designed a microchannel flow reactor by immobilizing nano-gold particles inside the polysiloxane capillary column.²⁶³ By applying an experimental setup as shown in Figure 18, benzylic alcohols with different structures were oxidized into the corresponding aldehydes/ketones with 89–99% yield at 50–70 °C. Under some cases, if the catalytic activity of the nano-gold-decorated capillary column nanoreactor was not high enough, bimetallic Au–Pd was used instead of Au.

Benzaldehyde was obtained via oxidation of styrene catalyzed by nano-gold catalysts using oxygen or NO₂ as oxidants, but the activity was not very high.^{142,264,265}

3.3.2. Mechanism Exploration. The reaction mechanism of the nano-Au-catalyzed selective oxidation of alcohol has been studied extensively with various technologies. Mullins et al. revealed the origin of active oxygen via in-situ observation of the evolution of acetaldehyde and water by impinging ethanol onto oxygen preoccupied Au(111) surface, Figure 19.²⁶⁶ Results from isotopic experiments showed that ethanol initially underwent O–H bond cleavage (producing ethoxide) followed by selective β -C-bond (α to the oxygen) activation to form acetaldehyde and water. These results help us understand the reaction mechanism of alcohol oxidation on high-surface-area-supported Au catalysts (e.g., active sites, elementary steps involving activated oxygen species). Esterification of methanol on the Au(111) surface was traced by temperature-programmed reaction with vibrational (HREEL) spectroscopy. The results suggested that low-temperature formation of methyl formate proceeds by reaction of formaldehyde with the methoxy moiety.²⁶⁷

Baiker et al. tried to determine the active sites of nano-gold catalyst by adding various amounts of thiols to modify the catalyst surface with inorganic supports. Activity variation was tested by benzyl alcohol oxidation and ketopantolactone hydrogenation.²⁶⁸ The supported Au catalysts and the nature of thiol adsorption were investigated by attenuated total reflection infrared (ATR-IR) spectroscopy, TEM, thermogravimetric desorption, and DFT calculations. The results suggested that the oxidation

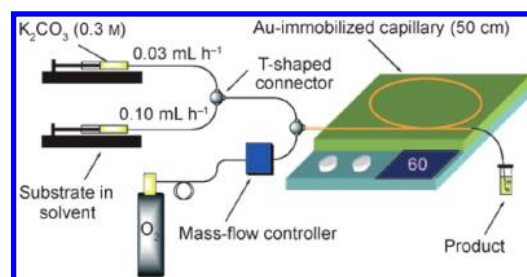


Figure 18. Experimental setup of the gold-catalyzed oxidation reactions. Reprinted with permission from ref 263. Copyright 2009 Wiley-VCH.

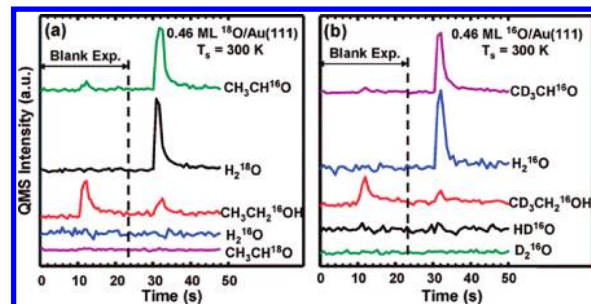


Figure 19. Evolution of acetaldehyde and water from (a) C₂H₅OH impingement on ¹⁸O_a precovered Au(111) at 300 K ($t = 30\text{--}32$ s) and (b) CD₃CH₂OH impingement on ¹⁶O_a precovered Au(111) at 300 K ($t = 30\text{--}32$ s). Atomic oxygen is deposited on Au(111) at 77 K with a coverage of ~ 0.46 ML. A blank experiment is shown from $t \approx 10\text{--}12$ s where an ethanol beam is impinged on an inert-stainless-steel flag placed in front of the Au(111) surface. The sample is heated to 300 K prior to impinging a continuous ethanol beam on the surface. Reprinted with permission from ref 266. Copyright 2008 American Chemical Society.

reaction might be favored on extended active sites on larger Au clusters, but the hydrogenation reaction occurs preferentially at low coordination sites such as corners and edges on smaller Au particles.

Corma et al. further explored the mechanism of the selective oxidation of alcohol to aldehyde on gold catalyst with DFT calculations.²⁶⁹ A series of nano-gold catalyst models including perfect and stepped single-crystal Au surfaces as well as an isolated Au₃₈ nanoparticle were built and studied. The extended surfaces were modeled by (2 × 2) super cell slabs containing a material thickness of ~ 8 Å and a vacuum region of ~ 12 Å. The calculated energy profile given in Figure 20 showed that the activity increased with decreasing Au coordination number. However, the E_{ads} value obtained on the Au-rod model is considerably larger than on the stepped Au(511) surface, which indicated that the coordination number is not the only factor determining energies. This observation was confirmed by the kinetic study of benzyl alcohol oxidation on a series of Au/MgO catalysts having different particle diameter and therefore different concentration of low coordinated Au sites.

Recently, DFT calculations combined with the periodic continuum solvation model were utilized to investigate the role of the nano-Au particle for O₂ activation with selective oxidation of phenylethanol as a model reaction.²⁷⁰ It was shown that the key step for O₂ activation is to produce OOH via O₂ adsorption and hydrogenation. Subsequently, OOH was further hydrogenated to H₂O₂. Water as solvent or additive plays an important role in

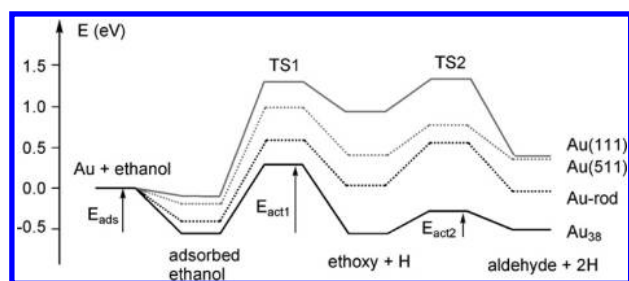


Figure 20. Calculated energy profile for the dehydrogenation of ethanol on different gold catalyst models. Reprinted with permission from ref 269. Copyright 2011 Elsevier.

O₂ activation, which can increase the residence time of O₂ on the surface and reduce the barrier of O₂ hydrogenation. With regard to the active position of the nano-Au particle, the edge site of the Au particle but not the (111) surface is favorable. In the whole pathway for alcohol oxidation, the surface H derived from α -C–H bond breaking on the close-packed (111) surface can be removed by O₂ and OOH via a H₂O₂ pathway without involving atomic O, Figure 21.

Koper et al. studied the reaction mechanism of the electrocatalytic oxidation of alcohols on gold in alkaline media, and interesting results were obtained.²⁷¹ In this work, they tried to build the relationship between the reactivity of alcohol oxidation and its pK_a. Due to the observation of much enhanced activity of alcohol oxidation at higher pH values, i.e., >12, it was assumed that the lower pK_a of an alcohol leads to a higher reactivity. On the basis of careful study it was revealed that oxidation of the alcohol to an aldehyde in alkaline solution involves the transfer of two protons and two electrons. The first deprotonation is base catalyzed, and the second deprotonation is fast but gold catalyzed, in which it primarily acts as an electron acceptor. Moreover, OH[−] in solution but not the hydroxyl group on the Au surface might be more important for alcohol activation because no obvious alcohol oxidation occurred in acidic solution despite formation of a hydroxyl group rich Au surface.

The mechanism of the aerobic oxidation of alcohol catalyzed by organic molecule stabilized nano-gold clusters was discussed as follows. Tsukuda et al. studied the aerobic oxidation of alcohols using poly(*N*-vinyl-2-pyrrolidone)-stabilized nano-gold clusters as catalyst.^{49,272} After careful characterization it was revealed that the nano-Au clusters were negatively charged by electron donation from PVP, and the catalytic activity was enhanced with the increasing electron density on the Au core. Subsequently, the catalytically active superoxo- or peroxo-like species were generated through electron transfer from the anionic Au cores into LUMO (π^*) of O₂, Figure 22.

By applying electron paramagnetic resonance (EPR) spectroscopy and spin-trapping methods the catalytic mechanism was explored with three typical catalysts, i.e., Au/CeO₂, polymer-incarcerated nano-gold clusters, and PPh₃-protected nano-gold clusters.²⁷³ Interestingly, a common mechanism to these catalysts was obtained. The rate-determining step of the overall reaction is a C–H bond cleavage by the gold surface through hydride or hydrogen-atom transfer. Following C–H bond cleavage, the ketone was formed and the Au–H-covered catalyst surface reactivated by oxidation with oxygen, Scheme 11.

On the basis of the above discussions, two general points about the mechanism of nano-gold-catalyzed aerobic alcohol oxidation are summarized here: (1) adsorption of the alcohol molecule on

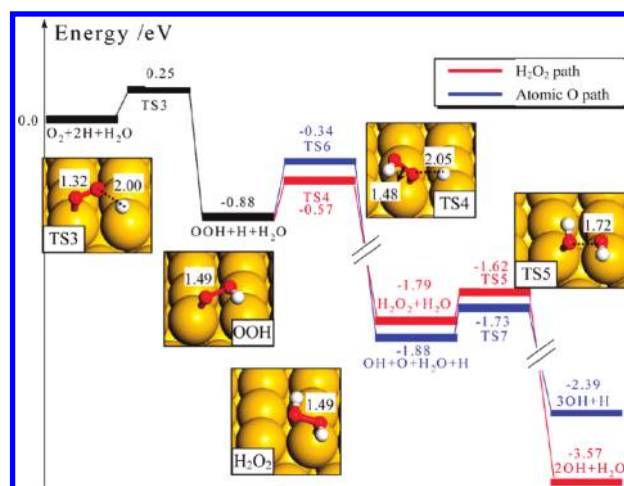


Figure 21. Potential energy diagram (ZPE-corrected) of O₂ reduction by surface H. The energy zero is defined as the individual adsorption state of O₂, H, and H₂O. The key reaction intermediates and the TS's are also shown. The key distances (Angstroms) are indicated. Reprinted with permission from ref 270. Copyright 2011 American Chemical Society.

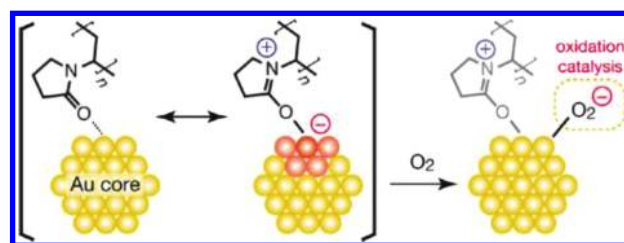


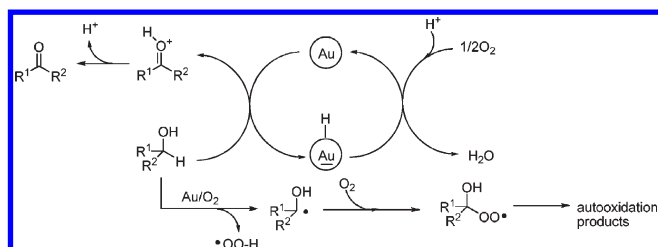
Figure 22. Mechanism for the activation of molecular oxygen by Au: PVP. Reprinted with permission from ref 272. Copyright 2011 American Chemical Society.

the nano-gold surface resulted in active intermediate alkoxide and followed by selective C–H bond (α to the oxygen) activation to form acetaldehyde and water. This was the commonly acceptable mechanism using nano-Au on inorganic supports as catalysts; (2) reversely, in consideration of DFT and EPR study together, C–H bond breaking might be an important step during alcohol oxidation no matter polymer/metal oxide-supported nano-gold or organic molecule-stabilized nano-Au-cluster employed. The Au–H-covered catalyst surface might be reactivated by O₂ and OOH via a H₂O₂ pathway without involving atomic O.

3.4. Selective Oxidation of Polyols

One of the major differences for the oxidation of polyols was the need for a stoichiometric or an excess amount of additional base. Thus, selective oxidation of polyols is discussed separately here.

3.4.1. Ethylene Glycol Oxidation. The early work in this area was the selective oxidation of ethylene glycol to sodium ethylene glycolate with carbon- or alumina-supported nano-gold catalyst.^{274,275} The carbon-immobilized nano-gold catalysts were prepared via dipping activated carbon in the prefabricated nano-gold colloid together with different protecting agents such as poly(oxyethylene(23)lauryl ether) (C₁₂E₂₃), poly{bis(2-chloroethyl)ether-*alt*-1,3-bis[3-(dimethylamino)propyl]urea} (PEG), the poly quaternary salt obtained by reaction of a

Scheme 11. Proposed Mechanism for the Au-Catalyzed Aerobic Oxidation of Alcohols^a

^a Reprinted with permission from ref 273. Copyright 2009 American Chemical Society.

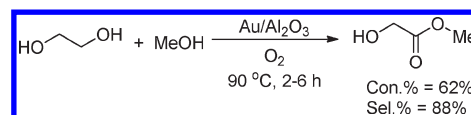
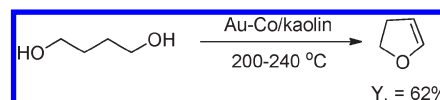
polyethyleneglycole with the bisphenol A diglycidyl ether (PEU), and polysaccharide (dextrin). After optimization, it was found that carbon-supported nano-gold from Au(0)/C₁₂E₂₃ and Au(0)/dextrin systems exhibited better performance. Conversion of ethylene glycol was ~80%. The roles of the stabilizers such as polyvinylalcohol (PVA), tetrakis(hydroxypropyl)phosphonium chloride (THPC), and citrate on the catalytic activity of nano-gold catalyst in glycerol oxidation were studied.²⁷⁶ The results showed that citrate might be the best stabilizer, and ~70% yield to glyceric acid/sodium glycerate was obtained using citrate-stabilized gold colloid as catalyst. In the Au/Al₂O₃-catalyzed ethylene glycol oxidation to glycolic acid²⁷⁵ it was revealed that oxygen adsorption on Au/Al₂O₃ catalysts was well correlated with the activity.

Methyl glycolate was synthesized via ethylene glycol oxidation in methanol using inorganic oxide-supported nano-gold catalysts, Scheme 12.²⁷⁷ The Au/Al₂O₃ catalyst exhibited high selectivity for the synthesis of methyl glycolate. After optimization, 88% selectivity and 62% conversion were obtained. If applying supported Pd or Ru catalysts in the ethylene glycol oxidation, the yield to methyl glycolate was lower than 30%.

By applying Au/C in the selective oxidation of phenylethane-1,2-diol, 83% mandelic acid yield was obtained under optimized reaction conditions.²⁷⁸

3.4.2. 1,4-Diols Oxidation. In the absence of oxygen, cyclodehydration of 1,4-butanediol to 2,3-dihydrofuran was the major reaction with >60% yield using Au–Co/kaolin catalyst, Scheme 13.²⁷⁹ By applying oxygen as oxidant, 1,4-butanediols is transformed to lactones. γ -Butyrolactone was produced quantitatively via Au/TiO₂-catalyzed selective oxidation of 1,4-butanediol using air as oxidant at 140 °C.²⁸⁰ The catalyst was reused for 3 runs without deactivation.

Moreover, if using iron oxide supported nano-gold as catalyst, the calcination temperature of the support has a strong effect on its catalytic activity.²⁸¹ The iron oxides were prepared by a hydrothermal method with altered crystal phase and morphology. The iron oxide supported nano-gold catalysts were prepared by the DP method. Clearly, the as-prepared FeOx supported gold catalysts showed much higher activity, i.e., TOF = 624 h^{−1}, than that supported on commercial γ -Fe₂O₃, i.e., TOF = 63 h^{−1}, in the oxidative dehydrogenation of 1,4-butanediol. Catalyst characterization showed that the high catalytic activity might be attributed to the strong gold–support interaction and negatively charged gold formation on γ -Fe₂O₃-supported gold catalysts. Subsequently, the same group tested the support phase effect on the activity of Au/iron oxide catalysts with commercially available iron oxide with different phase and morphology but similar

Scheme 12. Selective Oxidation of Ethylene Glycol in Methanol to Methyl Glycolate**Scheme 13. 1,4-Butanediol Dehydration and Oxidation Reactions**

physicochemical properties.²⁸² The results showed that selective oxidation of 1,4-butanediol to γ -butyrolactone is highly sensitive toward both the microcrystalline structure and the oxidation state of the iron oxide. The TOF value in the initial period follows the order Au/Fe₃O₄ > Au/ α -Fe₂O₃ > Au/ γ -Fe₂O₃.

A general methodology for selective oxidation of diols was developed when using Au/HT (hydrotalcite) as catalyst.²⁸³ Both 1,4-diols and 1,5-diols with different substituents were converted into the corresponding lactones with up to 99% yield. This Au/HT catalyst was reused several runs without deactivation.

3.5. Aldehydes Oxidation

Apart from the traditional systems using NaOCl, H₂O₂, O₃, or peracids as oxidants,^{284,285} aerobic oxidation of aldehyde has been studied extensively with homogeneous transition metal catalysts or supported Pd or Pt nanocatalysts.^{286,287} Nano-gold catalysts possess good catalytic activity in the aerobic oxidation of aldehyde.

Prati et al. reported their results about Au/C-catalyzed aldehyde aerobic oxidation to carboxylic acid in CCl₄.²⁸⁸ For the oxidation of benzylic and primary aliphatic aldehydes, the yields to the corresponding carboxylic acid were 80–99%. Corma et al. further studied the aldehyde oxidation with Au/CeO₂ and compared its catalytic activity with traditional homogeneous transition metal systems, Figure 23.²⁸⁹ Clearly, Au/CeO₂ exhibited better catalytic performance than the Co, Mn, and Ni homogeneous catalysts.

Christensen et al. studied the Au/TiO₂-catalyzed oxidative esterification of benzaldehyde in different alcohols including methanol, ethanol, 1-propanol, 1-butanol, and benzyl alcohol, and the yields to the corresponding esters were >80% except the reaction performed in 1-butanol, which was ~60%.²⁹⁰ The yield of methyl acrylate was >80% if the oxidative esterification of acrolein was carried out in methanol using Au/ZnO as catalyst. Subsequently, mechanistic investigation of the gold-catalyzed aerobic oxidation of aldehydes was performed.²⁹¹ A significant kinetic isotope effect, i.e., $k_H/k_D = 2.8$ – 2.9 , was found, which indicated that C–H bond cleavage is the rate-determining step. In addition, O¹⁸ labeling of oxygen or methanol showed that the additional oxygen functionality presented in the product ester originated from methanol rather than dioxygen.

Recently, size-selective esterification of benzaldehyde and 3,5-di-*tert*-butyl benzaldehyde in methanol was studied with a well-designed catalyst, i.e., zeolite-encapsulated gold nanoparticles.²⁹² An illustration for the preparation of zeolite-encapsulated nano-gold catalyst was given in Figure 24. The results for oxidative

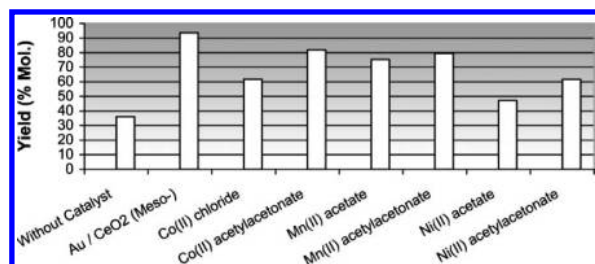


Figure 23. Comparative catalytic activity (yield of carboxylic acid, mol %) of Au/CeO₂ and different metallic homogeneous catalysts for air oxidation of *n*-heptanal at 50 °C during 3.5 h. Reprinted with permission from ref 289. Copyright 2005 Royal Society of Chemistry.

esterification of benzaldehyde and 3,5-di-*tert*-butyl benzaldehyde in methanol confirmed the hypothesis. The yield of methyl benzoate was ~75% but only ~5% of methyl 3,5-di-*tert*-butyl benzoate. For comparison, if catalyst Au/TiO₂ was used, similar yields of methyl benzoate and methyl 3,5-di-*tert*-butyl benzoate were obtained, i.e., ~70%. Thus, possibly, this zeolite-encapsulated nano-gold is a good size-selective catalyst in the oxidation reaction.

Reaction of methanol and formaldehyde, acetaldehyde, benzaldehyde, and benzeneacetaldehyde to methyl esters on oxygen-covered Au(111) was explored through mass spectrometric studies.²⁹³ The results suggested that formation of methoxy intermediate on the Au(111) surface was the key step for ester synthesis, Figure 25. The ester was obtained in high selectivity by nucleophilic attack of methoxy to aldehydes. In another pathway, the combustion reaction occurred via attack of both methanol and the aldehyde by oxygen.

The catalytic behavior of gold nanoparticles in the aerobic oxidation of 4-(dimethylamino)benzaldehyde to 4-(dimethylamino)-benzoic acid was studied by UV–vis.²⁹⁴

3.6. Selective Oxidation of Amines

3.6.1. Imine Synthesis. Imines are ubiquitous and useful intermediates as electrophilic participants in alkylation, condensation, Diels–Alder reaction, and other cycloadditions.^{295,296} The classical methodology for imine synthesis is through addition of amines and carbonyl compounds. Catalytic oxidation of *N*-alkyl amine or oxidative imination of alcohol should be one of the choices to develop a green and economic method to yield the corresponding imine, Scheme 14.

Angelici et al. tried the oxidative dehydrogenation of secondary amines in the presence of Au powders.²⁹⁷ Au loading is quite high in comparison with the common nano-gold catalyst system. Normally, 1 g of Au powders was used for oxidation of 0.2 mmol of secondary amine, and up to 93% yield was obtained under optimized reaction conditions. An Au/Al₂O₃ catalyst was prepared and used for oxidative dehydrogenation of secondary amines, and up to 98% yield was obtained.²⁹⁸

An interesting result was shown using Au(OAc)₃ as catalyst or catalyst precursor for oxidation of dibenzylamine to the corresponding imine (76–97% yield).²⁹⁹ TEM characterization suggested in-situ formation of nano-gold particles during reaction. High catalytic activity was achieved when Au(OAc)₃ was immobilized onto CeO₂ by adding CeO₂ to Au(OAc)₃ solution under vigorous stirring. Despite the simplicity of the method, the activity of the catalysts was comparable to other known catalysts for oxidative dehydrogenation of amines. Catalyst efficiency was improved remarkably if Au(PPh₃)Cl was used as the nano-gold

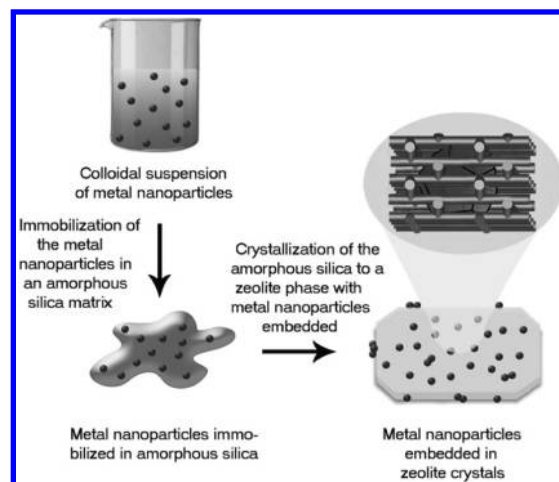


Figure 24. Schematic illustration of the encapsulation of gold nanoparticles in zeolite crystals. Reprinted with permission from ref 292. Copyright 2010 Wiley-VCH.

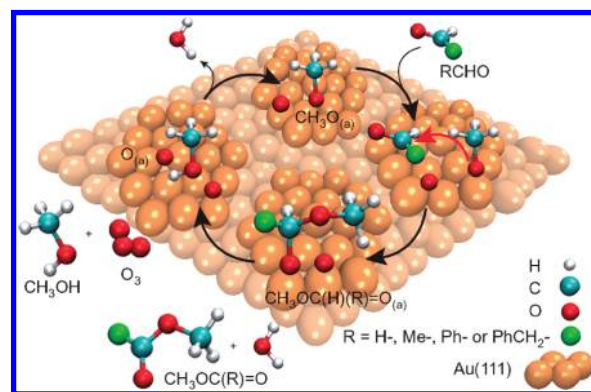
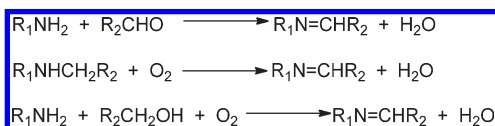


Figure 25. Schematic mechanism for coupling of methanol and aldehydes on oxygen-covered gold particles. Starting from the left-hand side, the reaction steps depicted in the figure are as follows: first, O₃ and CH₃OH are introduced sequentially onto the Au(111) surface to form atomic oxygen (O_(a)) and methoxy (CH₃O_(a)); next, the aldehyde (RCHO) is introduced, after which nucleophilic attack of methoxy to the aldehydic carbon forms the surface intermediate CH₃OC(H)(R)=O_(a) (red arrow represents the nucleophilic attack); and last, further β-H elimination of CH₃OC(H)(R)=O_(a) forms the ester (CH₃OC(R)=O). Reprinted with permission from ref 293. Copyright 2010 Nature Publishing Group.

Scheme 14. Imine Synthesis with Different Methods



precursor and CeO₂ was pretreated at 200 °C.³⁰⁰ The TOF value was 5-fold higher than that using Au(OAc)₃ as nano-gold precursor. A magnetically separable nano-gold catalyst for aerobic oxidation of amines was obtained through deposition of nano-gold particle onto the ceria-embedded iron oxide, Figure 26.³⁰¹ The catalyst showed good activity and high selectivity with up to 87% imine yield and was easily recycled taking advantage of the magnetic property. Che et al. reported

that graphite-supported nano-gold, i.e., AuNPs/C, was a good catalyst for oxidative dehydrogenation of secondary amine to imine.³⁰² Secondary benzylic amines with different substituting groups were successfully oxidized into the corresponding imines with 81–99% yields. Oxidative coupling of benzylic primary amine to imine was realized under the same reaction conditions.

Corma et al. studied the oxidative dehydrogenation of secondary benzylamines extensively with nano-gold catalysts, which involved different supports and supported nano-gold of varied particle sizes.³⁰³ The average particle size of nano-Au catalyst had a significant effect on the catalytic efficiency, Figure 27. No conversion of benzyl amine was observed with Au/TiO₂ of 25 nm nano-gold particle size, but 70 h⁻¹ TOF was obtained with 3.5 nm particle size Au/TiO₂. By applying 0.8 wt % Au/C, which was more active than Au/TiO₂, benzylamine was quantitatively converted into *N*-benzylidene phenylamine. Pd and Pt nanoparticles supported on TiO₂ were active in promoting oxidation of benzylamines, but their activity is lower than gold. Oxidative imination of aniline derivatives with benzylamine derivatives was realized with >99% yields. Tribenzylamine was oxidized into *N*-benzylidene phenylamine and benzaldehyde with >50% conversion and selectivity. Moreover, this nano-gold catalyst was easily applied in the oxidation of heterocyclic amines, i.e., pyridin-2-ylmethanamine and thiophen-2-ylmethanamine, with almost full conversion. The highly efficient transformation of thiophen-2-ylmethanamine is very interesting because the sulfur compounds can act as poisons of the other noble metal catalysts.

Different from the results above, recently, Kobayashi et al. reported that gold catalysts containing relatively larger clusters exhibited better activity when applying polymer-incarcerated nano-Au clusters (PI–Au) as catalysts.³⁰⁴ As a model reaction, >90% of dibenzyl amine was oxidized into imine catalyzed by PI–Au with 6.6–8.5 nm Au particle size. However, only 40% yield was obtained when PI–Au with 3.0 nm Au particle size was employed. Thus, except the Au particle size, the reactivity of nano-Au catalyst is dependent on the choice of support too.

Au/hydroxyapatite (HAP) was an effective catalyst for oxidative coupling of various amines and alcohols to produce the corresponding imine with >90% yield.³⁰⁵ If applying hydroxyl amine as the nitrogen source, oximes were selectively synthesized from benzylic or allylic alcohols. Recently, it was shown that *N*-benzylidene-1-phenylmethanamine was obtained with ~60% yield through the oxidative coupling of benzylamine or the oxidative dehydrogenation of dibenzylamine catalyzed by steel fiber matrix-supported Au–Pd bimetallic catalyst.³⁰⁶ The reaction could occur at ambient temperature using Au/TiO₂ as catalyst, but conversions were normally <60%.³⁰⁷

3.6.2. N-Formylation of Amines. Ishida et al. explored the catalytic activity of Au catalysts such as Au/TiO₂, Au/Al₂O₃, and Au/NiO in the oxidative N-formylation of amines in MeOH.³⁰⁸ Under optimized reaction conditions, by applying benzylamine as starting material, >99% conversion and 90% selectivity to the N-formylation product was obtained. For the other amines including morpholine and aniline, 66% and 72% yields to the N-formylation products were observed. If cyclohexylamine was employed as starting material, the products was tuned by altering the catalysts. In the presence of Au/NiO, the major product was the *N*-cyclohexylformamide with 99% yield. Cyclohexanone oxime was the major product with 37% yield when Au/TiO₂ was used as the catalyst. In this reaction, it was assumed that formation of methyl formate but not hemiaminal was the crucial

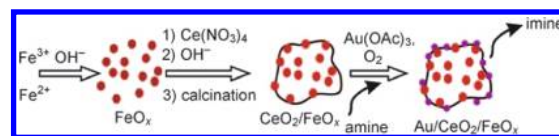


Figure 26. Schematic representation of the catalyst preparation. Brown dots indicate the iron oxide nanoparticles which are embedded in the CeO₂ matrix (white). Gold nanoparticles (purple) are deposited on the CeO₂/FeO_x matrix. Reprinted with permission from ref 301. Copyright 2009 Wiley-VCH.

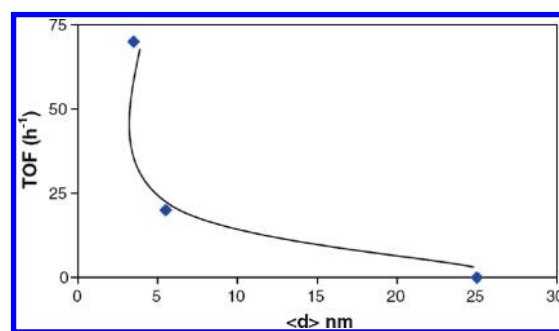


Figure 27. Plot of the turnover frequency (TOF determined from the initial reaction rate divided by the number of gold atoms) for benzylamine oxidation vs the average size of the gold nanoparticles for the Au/TiO₂ series. Reaction conditions: benzylamine, 1 mmol; toluene, 2 mL; oxygen pressure, 5 bar; temperature, 373 K; and Au/substrate mol ratio, 1%. Reprinted with permission from ref 303. Copyright 2009 Elsevier.

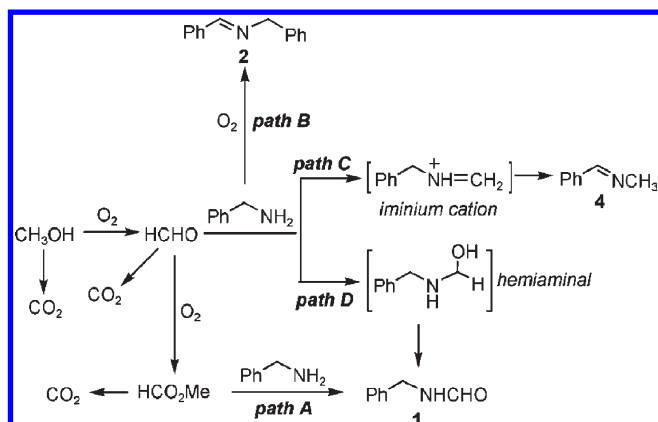
intermediate for generation of formamide, Scheme 15. Otherwise, imine should be observed.

Friend et al. explored the acylation of dimethylamine mediated by oxygen atom on metallic gold surface Au(111).³⁰⁹ After careful characterization and temperature-programmed reaction study it was found that the cross-coupling between dimethylamine and formaldehyde occurs with selectivity approaching 100% at low coverage of adsorbed “O” on Au(111) to form *N*, *N*-dimethylformamide. Different from the mechanism given above,³⁰⁸ the coupling reaction occurs through attack of nucleophilic (CH₃)₂N_(a) on the carbonyl carbon of the aldehyde to form (CH₃)₂NCH₂O_(a), and the desired product was obtained via further oxidation of (CH₃)₂NCH₂O_(a). A proposed reaction pathway was given in Scheme 16.

This reaction was realized with poly(*N*-vinyl-2-pyrrolidone)-stabilized nano-gold cluster as the catalyst with LiOH as the cocatalyst.³¹⁰ The oxidative N-formylation of *N*-phenyl-*N*-alkyl amines with different structures in methanol was realized with up to 99% isolated yields. However, no desired product was observed using *p*-nitro-*N*-phenyl-*N*-methyl amine as starting material. Noteworthy, similar to what was shown in Scheme 16, addition of amine to formaldehyde to generate hemiaminal was suggested to be the key step and the desired formamide was produced through further oxidation of hemiaminal.

Amide synthesis via amine and alcohol oxidation is interesting. Christensen et al. presented the selective oxidation of amines to amides catalyzed by Au/TiO₂.³¹¹ If cyclohexylamine or 1,6-hexamethyldiamine was used as starting material, ϵ -caprolactam was produced. However, conversion was still very low and only poor to moderate selectivity was obtained. Gold species was added into M1 phase MoVNbTeO catalyst in propane ammoxidation to acrylonitrile but resulted in lower activity.³¹²

Scheme 15. Possible Reaction Pathways for N-Formylation of Benzylamine in MeOH^a



^a Reprinted with permission from ref 308. Copyright 2009 Wiley-VCH.

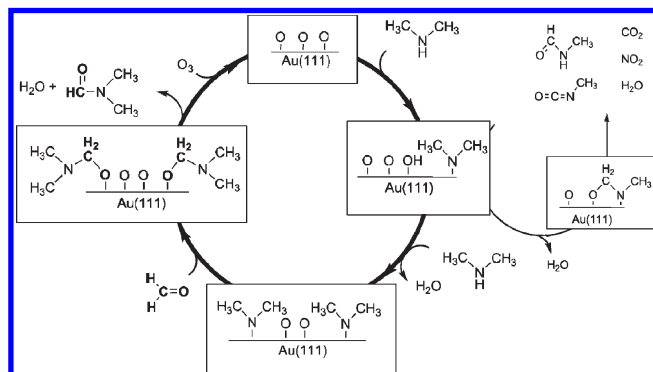
3.6.3. To Other Compounds. Che et al. reported that graphite-supported nano-gold, i.e., AuNPs/C, was a good catalyst for oxidation of cyclic tertiary amines to the corresponding lactams (I) with up to 93% yield, Scheme 17a.³⁰² When using 2-phenyl-1,2,3,4-tetrahydroisoquinoline and 1-ethynyl-4-(trifluoromethyl)benzene as starting materials, addition of nucleophile 1-ethynyl-4-(trifluoromethyl)benzene to cationic iminium intermediate could occur and the yield of the desired product was 80%, Scheme 17b. Moreover, by applying the same AuNPs/C catalyst, benzimidazoles were synthesized from oxidative coupling of benzaldehyde derivatives and benzene-1,2-diamine (90–99% yields), Scheme 17c. Oxidation of cyclic tertiary amines to the corresponding lactams was realized with up to 99% yields at 27–90 °C using Au:PVP catalyst.³¹³

Woo et al. reported that bulk gold powder (~50 μm) and Au/Al₂O₃ were effective catalysts for selective oxidation of 5,6,7-membered cyclic amines to amidines.³¹⁴ Subsequently, lactams in 42–73% yields and amines in 36–63% yields were produced after treating the amidines with Aerosil 200 (fumed silica gel) and water.

Aromatic azo compounds are widely used in industry as dyes, pigments, food additives, and drugs. Normally azobenzenes are produced by reduction of nitrobenzenes with iron, which rendered low-quality product and a vigorous environmental problem.³¹⁵ Catalytic reduction of nitrobenzenes or catalytic oxidation of anilines to produce azobenzene has been the goal for researchers for a long time. By applying the Au/TiO₂ catalyst, Corma et al. developed an effective and clean process for azobenzene synthesis via selective oxidation of anilines.³¹⁶ For example, in 22 h, azobenzene was synthesized with 98% yield. The azobenzene was synthesized via a one-pot/two-step reaction. A mixture of nitrobenzene and Au/TiO₂ catalyst was treated with hydrogen to give aniline with >95% conversion and selectivity. Then the reaction mixture was exposed to molecular oxygen; azobenzene was obtained with 92% yield. This nano-gold catalyst has good generality for selective oxidation of anilines in high yield, Scheme 18.

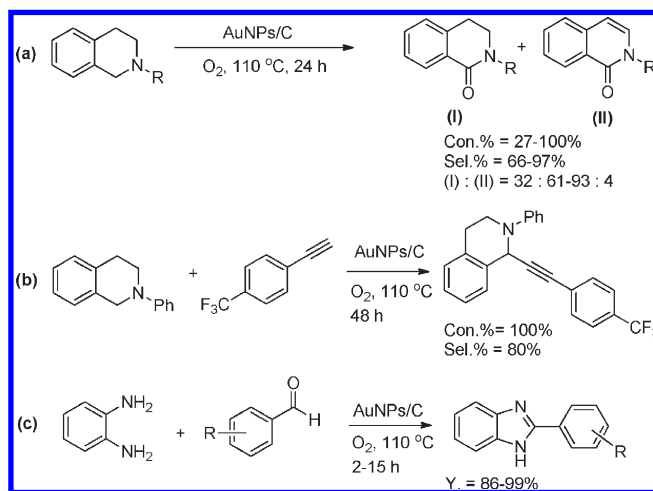
Enamines were synthesized by reacting diazoalkane with amine in the presence of O₂ and Au power, Scheme 19.³¹⁷ Aliphatic amines with different structures including piperidine, morpholine, pyrrolidine, cyclohexylamine, and *n*-butyl amine can react with diazoalkane to give enamines with 58–94% yields.

Scheme 16. Proposed Mechanisms for the Coupling of Dimethylamine with Formaldehyde and the Secondary Oxidation of Dimethylamine Promoted on O/Au(111)^a



^a Reprinted with permission from ref 309. Copyright 2009 Wiley-VCH.

Scheme 17. Graphite-Supported Nano-Gold Catalyzed Amine Oxidation reactions



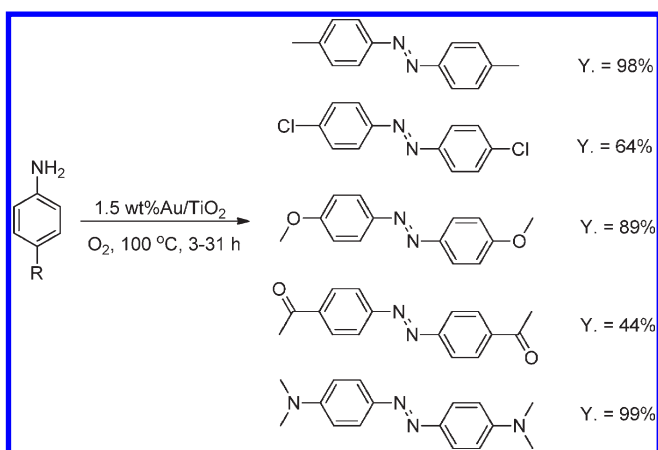
By applying Au/TiO₂ catalyst, quinaldines were photocatalytically synthesized in high yields using ethanol as solvent irradiated by a 365 nm medium-pressure mercury lamp, Scheme 20. Nitrobenzenes with different structures were transformed into the corresponding quinaldines with moderate to excellent yields.³¹⁸

Carbonylic compounds were synthesized through oxidative deoxygenation reaction with nano-gold catalysts.³¹⁹ This is a reverse reaction of an industrially important reaction, i.e., ketone oximation. Typical oxime such as cyclohexanone oxime was oxidized into cyclohexanone quantitatively using Au/CeO₂ as the catalyst.

3.7. Silanes Oxidation and Hydrosilylation Reactions

Silanol are valuable building blocks for silicon-based polymeric materials and nucleophilic coupling partners in organic synthesis.^{320–322} Catalytic oxidation of silanes using H₂O or molecular oxygen as oxidant is an attractive route for clean and economic synthesis of silanols. Recently, it was found that Au/hydroxyapatite (HAP) was an effective catalyst for oxidation of silanes to silanols under mild conditions.³²³ Silanes with different structures were converted into the corresponding silanols with high yield except triphenylsilane. The yield to triphenylsilanol was only 28% even when the reaction was prolonged 24 h due to

Scheme 18. Aromatic Azo Compound Synthesis through Aniline Oxidation



the strong steric hindrance. Moreover, silyl ether was synthesized in high yield using Au/Al₂O₃ as catalyst, and moderate to excellent yields were obtained.³²⁴ Under the same reaction conditions the hydrosilylation reaction to benzaldehyde and acetophenone was realized with >95% conversion.

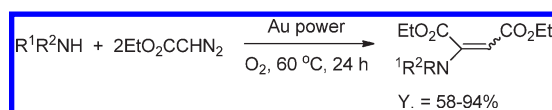
A novel nano-gold catalyst was prepared and used in the hydrosilylation of 1-hexyne.³²⁵ First, three different Au/acetone solutions, whose concentrations were 0.16, 0.43, and 1.42 mg Au/mL, were obtained by the metal vapor synthesis (MVS) technique. Then, the Au nanocluster in acetone was directly deposited on a wide series of different supports including Al₂O₃, Fe₂O₃, CeO₂, TiO₂, and ZrO₂. The supported gold nanoclusters were the catalysts for hydrosilylation of 1-hexyne, Scheme 21. Under optimized reaction conditions the regioselectivity to the *E* isomer is >90%. After extensive study it was found that the size of the gold particles and their interaction with the support play a key role in obtaining high activity and selectivity. Normally catalysts prepared from diluted MVS solutions resulted in highly dispersed small gold particles and good catalytic activity. Moreover, a strong interfacial contact between Au and the metal oxide could reduce the number of active sites of the catalysts.

3.8. Biomass Transformation to Fine Chemicals

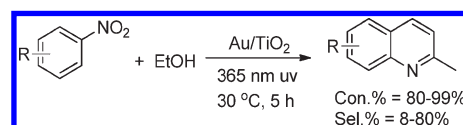
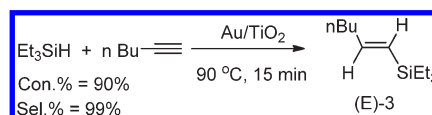
3.8.1. Glucose Oxidation. Gluconic acid and its salts are important chemical intermediates and extensively used as a food and beverage additive and water-soluble cleaning agents. Currently, production of gluconic acid and its salts is based on biochemical transformation,^{326,327} which is complicated by the large amounts of waste produced. Synthesis of gluconic acid with catalytic oxidation methods is a good choice in industry but is severely restricted due to the low catalyst efficiency and stability, Scheme 22.

Au/C exhibited excellent performance in the selective oxidation of D-glucose.^{328,329} The reaction was remarkably promoted under basic conditions. In a solution at pH 9.5 full conversion was obtained in 0.5 h, but it needed more than 1 h in a solution at pH = 8. A much longer reaction time was necessary if other catalysts such as 1%Pt–4%Pd–5%B/C, 5%Pd–5%B/C, and 5%Pt/C were used, and the reaction could not be finished in solutions at pH 7 or 8.5.

The effect of nano-gold particle size on the catalytic oxidation of D-glucose was explored.³³⁰ A series of Au/C catalysts was prepared by the gold sol method with different reducing agents

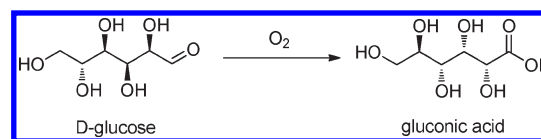
Scheme 19. Reaction of Diazoalkane with Amine in the Presence of O₂

Scheme 20. Quinaldine Synthesis from Nitrobenzenes and Ethanol

Scheme 21. Hydrosilylation of 1-Hexyne with Et₃SiH Catalyzed by Supported Gold Nanoparticles^a

^a Reprinted with permission from ref 325. Copyright 2009 Elsevier.

Scheme 22. Selective Oxidation of D-Glucose to D-Gluconic Acid



and different kinds of carbon support providing Au mean particle diameters in the range 3–6 nm. In order to exclude the difference in Au loading, the specific surface area (*A*_{spec}) of the active component of each catalyst was calculated based on the results of ICP-OES and TEM analysis by assuming closed-shell gold particles of nearly spherical shape. The results showed that nano-gold catalyst with a smaller particle size exhibited higher catalytic activity.

Baatz et al. reported that Au/Al₂O₃ catalysts with <2 nm Au particle size were prepared with the incipient wetness impregnation method, and their catalytic activity in D-glucose oxidation was tested.³³¹ TEM characterization showed that nano-gold catalysts with <2 nm gold particle were produced with excellent reproducibility. By applying these catalysts the selectivity to desired sodium gluconate was ~100%. The number was ~50% higher than that prepared by the DP method. Moreover, no deactivation occurred on the catalyst after it was reused for 20 runs.

0.45% Au/TiO₂ was shown to be a nice nano-gold catalyst in the selective oxidation of glucose to gluconic acid.³³² Under optimized reaction conditions the conversion and selectivity all reached ~100% in an aqueous solution at pH 9. Noteworthy, this 0.45% Au/TiO₂ exhibited excellent long-term stability. No deactivation occurred even if it was reused at the 17th run. Au/TiO₂, Au/SiO₂, and Au/CeO₂ prepared by colloidal gold deposition were used in glucose oxidation.³³³ CO total oxidation

with the same catalysts and some interesting results were obtained. A smaller gold particle size and the reducible oxide supports favored the activity of the CO total oxidation reaction. On the contrary, in the glucose oxidation reaction SiO₂-supported larger size gold is more active.

Haruta et al. prepared a series of ion-exchange resin-supported nano-gold catalysts and used them in glucose oxidation reactions.³³⁴ By applying a strongly basic anion-exchange resin, such as quaternary ammonium salt ($-N^+Me_3$), as support the best catalyst performance was obtained with a TOF of 27 000 h⁻¹ at 60 °C and pH 9.5. Then, they prepared several Au/C catalysts through direct deposition of gold from a solution of bis-(ethylenediamine)Au(III) trichloride (0.1 mM) using NaBH₄ as reducing agent.³³⁵ The nano-Au particles possessed a mean diameter as small as 1.9 nm, and high catalytic activity was obtained. Later, an interesting catalyst was prepared for the glucose oxidation reaction, i.e., the nano-gold particle with a mean diameter of ~2 nm was deposited directly onto cellulose by the solid grinding method with dimethyl Au(III) acetylacetonate followed by hydrogen reduction.³³⁶ At 60 °C and pH 9.5 this Au/cellulose catalyst showed appreciably high catalytic activity with a turnover frequency of 11 s⁻¹.

The Au–Pd/C catalyst showed superior activity in the glucose oxidation reaction in comparison with the monometallic Pd/C analogues.³³⁷ Under improved reaction conditions the yield to gluconic acid was >90% applying Au–Pd/C catalyst, but <20% yield was obtained using Pd/C. Recently, Toshima et al. developed a poly(*n*-vinyl-2-pyrrolidone)-stabilized Au/Pt/Ag trimetallic nanocluster catalyst for aerobic oxidation of glucose.³³⁸ Au/Pt/Ag trimetallic nanoclusters were prepared by reduction of the corresponding precursors with rapid injection of NaBH₄, and their average particle size was ~1.5 nm. The results suggested a suitable nanocluster composed with a Au:Pt:Ag ratio of 7:2:1. By applying this novel catalyst to glucose oxidation, the TOF value reached 13 970 h⁻¹.

Rossi et al. reported an interesting result about “naked” nano-gold-catalyzed selective oxidation of D-glucose.³³⁹ Under controlled conditions water-dispersed gold sol exhibits high activity in the absence of common protectors. “Naked” gold particles having a mean diameter of 3.6 nm behave as an active catalyst, allowing 21% glucose conversion in the first 200 s, Figure 28. If “naked” nano-Pd, -Ag, -Cu, or -Pt with a particle size 3–5 nm was used as the catalyst, conversion of D-glucose was less than 5%. Moreover, if comparing this result with that of the Au/C catalyst it was seen that they exhibited similar initial activity. However, no catalytic activity was observed after 300 s if “naked” nano-gold was used, but stable activity was maintained in the presence of Au/C until full conversion. According to TEM characterization, it was revealed that the nano-gold particle aggregated during the reaction. The particle size was close to 10 nm after 300 s; deactivation occurred with “naked” nano-gold catalyst.

Furthermore, the catalytic activity of “naked” Au–Pt nanocluster and immobilized Au–Pt/C catalysts was compared.³⁴⁰ The Au–Pt (Au:Pt = 2:1; w/w) bimetallic catalyst offered a more stable “naked” nanocluster, which can result in >80% D-glucose conversion. This result is similar to the supported bimetallic catalyst and 5-fold higher than the monometallic systems. Moreover, by applying Au–Pt/C catalyst the TOF could reach 924 h⁻¹ with 77% conversion, whereas the TOF was only 51–60 h⁻¹ if Au or Pt was used solely. Then, comparison of Au/C catalysis with current industrially enzymatic catalysis suggested that nano-gold catalyst is a potential alternative.³⁴¹ Similar indications

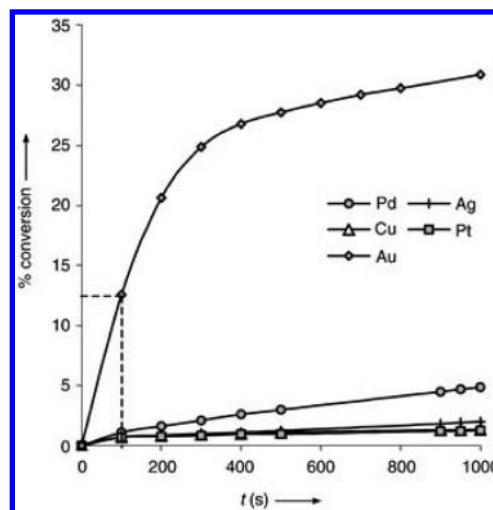


Figure 28. Activity of different metal particles in glucose oxidation. [Metal] = 10⁻⁴ M, [glucose] = 0.4 M, T = 303 K. Reprinted with permission from ref 339. Copyright 2004 Wiley-VCH.

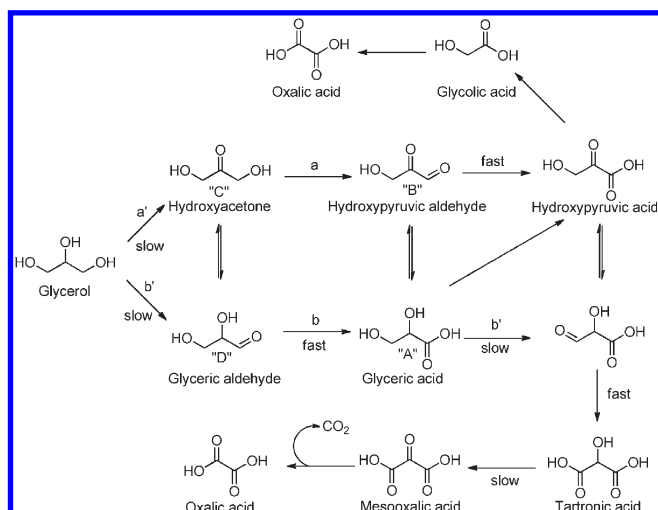
resulted by comparing the activity of colloidal gold with homogeneous enzymatic catalyst *Hyderase* under similar reaction conditions.³⁴²

The catalytic activity of colloidal gold in the presence of different polymers, such as poly(diallyldimethyl ammonium chloride), chitosan, poly-2,2-trimethyl ammonium methylmethachloride, polyvinyl alcohol, ethylene imine, and poly(*N*-vinyl-2-pyrrolidone), was studied,³⁴³ but it was lower than 0.45% Au/TiO₂.³³²

The catalytic activity of support-free nanoporous gold, which was prepared by dealloying the Ag from Ag–Au alloy, in D-glucose selective oxidation was tested.³⁴⁴ The catalytic activity of this nanoporous gold was determined by the ligament size. For example, in 7 h conversion of D-glucose was ~80% with 100% selectivity to gluconic acid when the ligament size is ~6 nm. Conversion dramatically dropped to ~25% if nanoporous gold with ~30 nm ligament size was employed. The amount of residue Ag has a significant effect on the catalytic activity. Lower Ag residue resulted in higher catalytic activity.

3.8.2. Glycerol Oxidation. Selective oxidation of glycerol and other alcohols was further tested with Au/C catalysts.^{345–348} Fine chemical synthesis using glycerol as a starting material has attracted extensive attention because it is a byproduct of biodiesel production. In order to understand this complicated reaction better, the general reaction pathways concerned are shown in Scheme 23. After catalyst screening and reaction condition optimization, the yield of glycerate acid/sodium glycerate was 92%.

The catalytic behavior of Au/Al₂O₃ and Au/Nb₂O₅ in selective oxidation of glycerol with oxygen in water was investigated, but only a moderate result was obtained.³⁴⁹ Recently, the effect of the surface structure of activated carbon on the activity of Au/C catalyst in glycerol oxidation was studied extensively.³⁵⁰ Activated carbons with different levels of oxygenated functional groups on the surface were prepared by treating the same activated carbon with nitric acid and calcining them at different temperatures. Thus, the resulted samples possessed the same textural structure. The total amount of oxygenated surface groups (carboxylic acids, carboxylic anhydrides, lactones, phenols, and carbonyls or quinones) on carbon materials was evaluated by CO/CO₂ TPD characterization, Figure 29. Nano-gold catalysts with similar average particle sizes were prepared

Scheme 23. General Reaction Pathways^a

^a Reprinted with permission from ref 345. Copyright 2004 Elsevier.

with these carbons and used in glycerol oxidation reactions. Indeed, these catalysts exhibited quite different catalytic performances depending on the amount of oxygenated groups on the surface of the support. Basic oxygen-free supports led to an enhancement activity because of the capability of oxygen-free supports to promote electron mobility. With the improved catalyst and reaction conditions, the yield to acid/sodium glycerate was ~60%.

In order to check the effect of preparation method on the catalytic activity of Au/TiO₂ in the selective oxidation of glycerol, a series of Au/TiO₂ catalysts were prepared by varying the deposition and reduction methods, i.e., deposition–precipitation versus sol immobilization and calcination versus chemical reduction.³⁵¹ The results showed that the best catalytic performance was obtained by reducing gold species at low temperature through chemical reduction and immobilizing it by the DP method, which resulted in metallic Au⁰ species with a 2–5 nm particle size. By applying this catalyst the yield to glyceric acid was >60%.

If the oxidation reaction of glycerol was performed in methanol using Au/TiO₂ or Au/Fe₂O₃ as the catalyst and NaOCH₃ as the cocatalyst, dimethyl mesoxalate was the major product with 89% selectivity, Scheme 24.³⁵² If 1,2-propanediol and 1,3-propanediol were used as starting materials the corresponding products were methyl lactate and methyl-3-hydroxyl propionate with 72% and 90% selectivities.

As a nice catalyst for selective oxidation of alcohol, Au–Pd bimetallic catalyst supported on carbon or graphite was tried in the aerobic selective oxidation of glycerol by Prati et al.^{353,354} The results showed that bimetallic catalysts are more active than monometallic catalysts, indicating that a synergetic effect exists between Au and Pd. According to the TOF values, catalytic activity was enhanced 50–100% but the yields were all ~60%. Later, it was reported that incorporation of Pd did not enhance the catalytic activity significantly when compared to monometallic Au if the rates have been properly normalized to the surface metal concentration.³⁵⁵ However, the selectivity to glyceric acid was improved slightly because the presence of Pd can reduce production of hydrogen peroxide during reaction, which is correlated to the C–C bond cleavage products. After

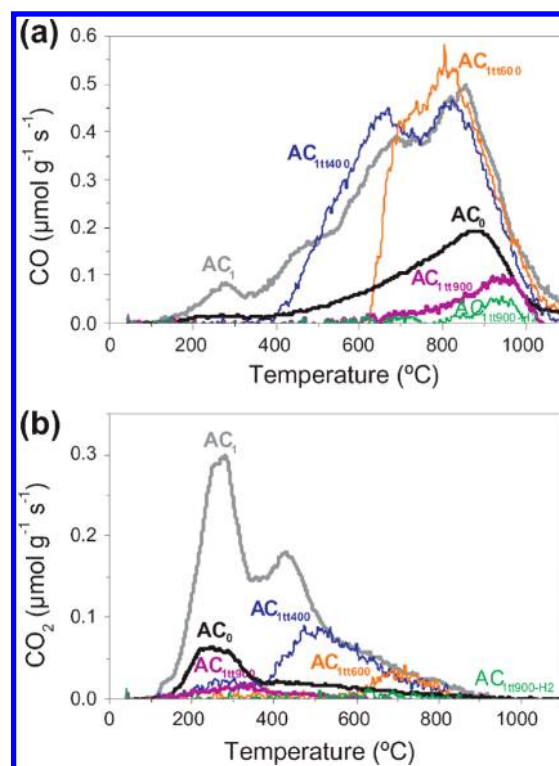
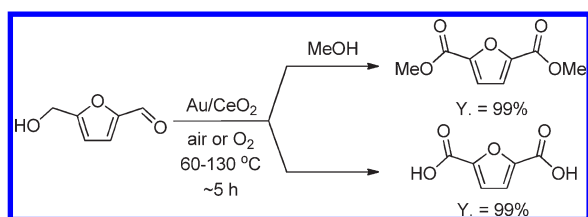


Figure 29. TPD spectra of the different activated carbons: (a) CO; (b) CO₂. AC₀: Commercial NORIT ROX 0.8 activated carbon; AC₁: AC₀ was treated with 6 M HNO₃ and dried at 110 °C for 24 h; AC_{1t400}, AC_{1t600}, AC_{1t900}: AC₁ was treated under nitrogen flow for 30 min at different temperatures (400, 600, or 900 °C) followed by a treatment under dry air flow at room temperature for 1 h; AC_{1t900-H2}: AC₁ was treated under nitrogen flow for 30 min at 900 °C followed by a treatment under dry air flow at room temperature for 1 h. Reprinted with permission from ref 350. Copyright 2011 Elsevier.

improvement with different preparation methods, ~60% yield to glyceric acid/sodium glycerate was obtained. Recently, Hutchings et al. investigated the employment of TiO₂ or carbon-immobilized nano-Au–Pd bimetallic catalyst in glycerol oxidation.^{356,357} It was found that the combination of gold and palladium as supported alloy nanocrystals resulted in a significant enhancement in the catalyst activity, i.e., ~2000 h^{−1} turnover frequency values to the desired product was obtained.³⁵⁶ Au–Pt bimetallic catalyst was prepared and used in the glycerol oxidation reaction.³⁴⁷ The yield to glyceric acid/sodium glycerate was ~60% after optimization. Using an improved Au–Pd/TiO₂ catalyst for selective oxidation of 1,2-propanediol in methanol, 94% conversion and 95.9% selectivity to the methyl lactate were achieved.³⁵⁸

Recently, Prati et al. reported the base-free oxidation of glycerol to glyceric acid with good conversion and selectivity.³⁵⁹ The best catalyst was 1% AuPt(6:4)/H-mordenite, which was prepared by modifying the Au/H-mordenite with a K₂PtCl₄ solution. This Au–Pt/H-mordenite catalyst has an average particle size of 4.8 ± 1.80 nm. Energy-dispersive spectroscopy (EDS) analysis of 20 randomly selected clusters indicated that all of the clusters contained a mixture of Pt and Au but the Au/Pt ratio was inhomogeneous from cluster to cluster. By applying this Au–Pt/H-mordenite in the selective oxidation of glycerol, conversion of glycerol was 70% with 83% selectivity to glyceric acid. The selectivity decreased to 81% at full conversion of

Scheme 24. Selective Oxidation of Glycerol, 1,2-Propanediol and 1,3-Propanediol

glycerol. One reason for the high efficiency of this catalyst is the inhibition of hydrogen peroxide formation during reaction, which has been proved to be a possible oxidant for C–C bond cleavage, as found in the Au–Pd/C catalyst system. These results introduced a new standpoint to understand the glycerol oxidation reaction and design of catalysts.

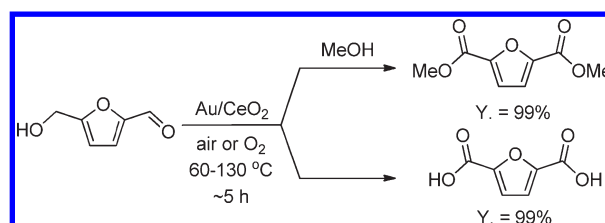
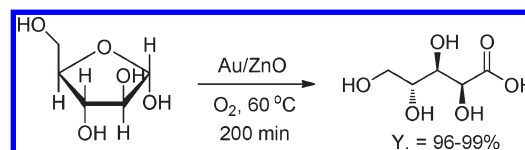
3.8.3. Cellobiose Oxidation. Han et al. developed an Au/Cs₂HPW₁₂O₄₀ catalyst for one-step formation of gluconic acid from cellobiose.³⁶⁰ This novel bifunctional catalyst possessed acid sites for hydrolysis of β -1,4-glycosidic bond and redox sites for oxygen activation to oxidize the aldehyde group to the carboxyl group. The phosphotungstate support was essential to gain high catalytic activity, i.e., providing solid acid sites for hydrolysis and improving Au redox sites for selective oxidation. The bifunctional catalyst exhibited excellent performance in the one-pot transformation of cellobiose into gluconic acid. The yield of gluconic acid reached 96.4%, which was better than those systems combining nano-gold catalyst with different inorganic acids. DFT calculations indicated that the strong metal–support interfacial interaction accounts for the catalytic activity modulation.

Selective oxidation of D-glucose with hydrogen peroxide was performed using polymer-immobilized nano-gold catalysts, and moderate to good results were obtained.³⁶¹

3.8.4. 5-Hydroxymethyl-2-furfural Oxidation. Selective oxidation of 5-hydroxymethyl-2-furfural was studied with supported nano-Au as catalyst, Scheme 25. Corma et al. reported that Au/CeO₂ was a good catalyst for oxidative esterification of 5-hydroxymethyl-2-furfural into 2,5-dimethyl, 2,5-diethyl, or 2,5-dibutyl furate in different alcohols.³⁶² Under optimized reaction conditions the conversion and selectivity were all >99%. If performing the reaction in water using air as oxidant, 5-hydroxymethyl-2-furfural was transferred into 2,5-furandicarboxylic acid with >99% yield.³⁶³ Unfortunately, it required the use of a base to obtain a high yield, and serious catalytic activity degradation occurred when it was reused for the second run. However, deactivation was not caused by metal leaching, as verified by chemical analysis of the solution, and no reaction occurred after removing the catalyst by filtration.

Risager et al. showed that aerobic oxidation of 5-hydroxymethyl-2-furfural was realized using a commercial 1 wt % Au/TiO₂ catalyst (Mintek, Brunauer–Emmett–Teller) at ambient temperature.³⁶⁴ As discussed above, addition of base was indispensable in order to obtain a high yield and with addition of excess base 71% yield of 2,5-furandicarboxylic acid was obtained with full 5-hydroxymethyl-2-furfural conversion.

3.8.5. Arabinose Oxidation. Selective oxidation of arabinose to arabinonic acid by molecular oxygen is an important reaction in sustainable chemistry, Scheme 26. Supported nano-gold catalysts such as Au/C, Au/Al₂O₃, Au/TiO₂, and

Scheme 25. Selective Oxidation of 5-Hydroxymethyl-2-Furfural to Ester and Acid**Scheme 26. Selective Oxidation of Arabinose to Arabinonic Acid**

Au/ZnO were fine catalysts in selective oxidation of arabinose.³⁶⁵ Although the activities were different, at 60 °C and pH 8–9 in aqueous solution, arabinose was quantitatively converted into arabinonic acid no matter which nano-gold catalyst was used as catalyst.

4. OTHER REACTIONS

4.1. Hydrochlorination of Alkynes

Clean and economic synthesis of vinyl chloride with a mercury-free catalyst system is an important topic in catalysis and chemical industry. Continued from early reports about Au³⁺/C-catalyzed alkyne hydrochlorination reactions,^{3,366} the mechanism and reactivity of higher primary and internal alkynes in the hydrochlorination reaction were explored.³⁶⁷ Sequential exposure of the catalysts to C₂H₂ and HCl demonstrated that exposure to HCl before reaction improved the activity, whereas exposure to C₂H₂ lead to deactivation. The activity of higher alkynes was mainly affected by steric hindrance, and it follows the following order for the hydrochlorination reaction, i.e., acetylene (ca. 40% conversion) > hex-1-yne (10%) > phenyl acetylene (7%) > hex-2-yne (2%). A reaction mechanism was obtained according to DFT study, Figure 30. The results suggested that simultaneous coordination of alkyne and HCl to the Au(III) center of AuCl₃ is unlikely. The calculated transition state for HCl addition to the π complex of C₂H₂ with AuCl₃ demonstrated that the stereochemistry of Cl addition is controlled by a hydrogen bond between HCl and a Cl ligand of Au.

Fine results were obtained by Au–M/C bimetallic catalyst.³⁶⁸ It was revealed that the initial activity of metal chlorinated salts on carbon was linearly correlated to their standard electrode potential, Figure 31. In this case the data for the chlorides was used. The enhancement of catalytic activity might be ascribed to the enhanced dispersion of Au after addition of the second metal. As an exception, the initial activity for platinum was much lower than that expected from the correlation. The major reason is possibly due to rapid deactivation during reaction. However, addition of a second metal caused a significant loss in selectivity, and deactivation occurred rapidly in all cases in ~30 min.

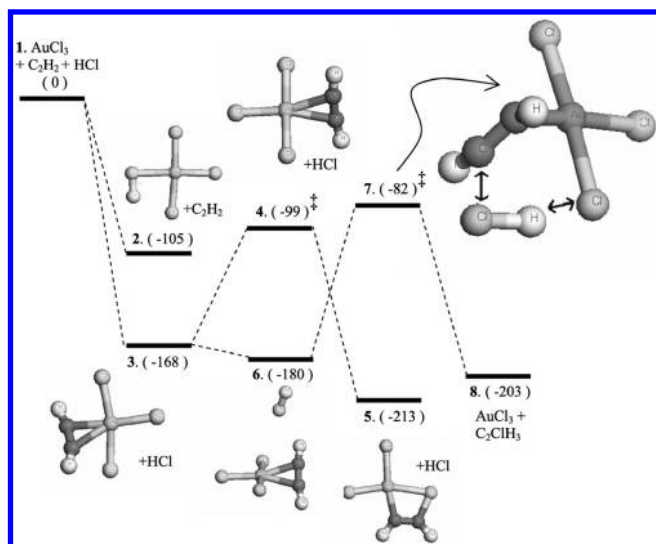


Figure 30. Reaction energy profile for hydrochlorination of acetylene; all energies in kJ mol^{-1} ; transition states marked. Reprinted with permission from ref 367. Copyright 2007 Elsevier.

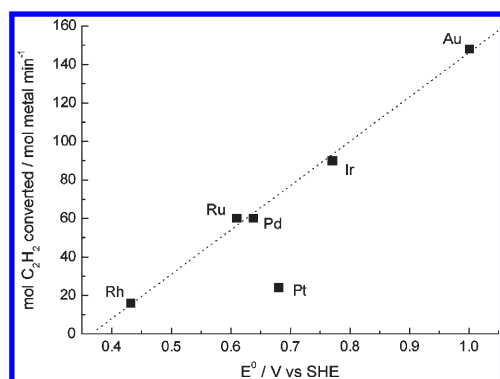


Figure 31. Correlation between initial acetylene conversion versus the standard electrode potential of the various metals used in this study. Potentials are obtained from the reduction potentials of the following chloride salts (RhCl_6^{3-} , $(\text{RuCl}_5)^{2-}$, PdCl_2 , $(\text{PtCl}_6)^{2-}$, $(\text{IrCl}_6)^{3-}$, and $(\text{AuCl}_4)^-$) to the corresponding metals. Reprinted with permission from ref 368. Copyright 2008 Elsevier.

Deactivation might be explained by the high activity of Pd and Pt as dehydrochlorination catalysts, which tended to react with the vinyl chloride and lead to coke deposition on the surface, decreasing the vinyl chloride selectivity.

As the reverse reactions, hydrodechlorination of $\text{CHCl}=\text{CCl}_2$, CCl_2F_2 , and 2,4-dichlorophenol were tested using nano-gold catalysts.^{369–373}

4.2. Carbon–Carbon Bond Formation Reactions

Carbon–carbon (C–C) bond formation reactions are a powerful and versatile tool in synthetic organic chemistry. Traditionally, C–C bond formation was catalyzed by a homogeneous catalyst system,^{374–376} which was complicated and difficult to be isolated and reused. In the past decade, preparation and application of nanopalladium catalyst in C–C bond formation reactions have been studied extensively and great progress has been achieved.^{377,378} Although it is not as general as

palladium catalyst, nano-gold exhibited specific activity in some cases.

4.2.1. Coupling Reactions. Early work on nano-gold-catalyzed homocoupling of phenylboric acid was reported by Tsukuda et al. using PVP-stabilized nano-Au clusters with a 1–2 nm particle size.³⁷⁹ The yield to the homocoupling product was 72%. If *m*-methyl-phenylboric acid was used as starting material, the yield was 72% too. However, the yields were 4% and 49% when *o*- and *p*-methylphenylboric acid were applied. Subsequently, Corma et al. successfully developed the Au/ CeO_2 -catalyzed homocoupling of phenylboric acid with high conversion and selectivity.³⁸⁰ The catalytic activity derived from CeO_2 or leached Au species was excluded carefully. In the blank experiments using ceria, no conversion was observed. Moreover, AAS analysis of the solution showed 0.3 ± 0.1 ppm of gold was detectable, so 3 ppm of gold was added in the form of HAuCl_4 , but only 1.1% conversion was obtained, which suggested the real catalyst in the reaction was Au/ CeO_2 but not CeO_2 and leached Au species. This simple nano-gold catalyst was applied in the homocoupling reaction of phenylboric acid derivatives with 97–99% yield, Scheme 27.

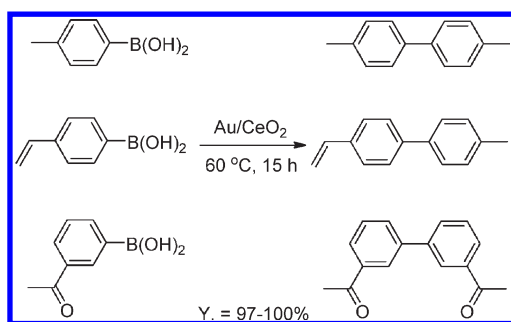
The homocoupling reaction of potassium aryltrifluoroborates was effectively catalyzed by PVP-stabilized nano-gold cluster under aerobic conditions.³⁸¹ Several PVP-stabilized nano-gold clusters with particle sizes of 1.3, 2.3, 3.3, 4.3, 4.7, 5.9, and 9.5 nm were prepared, and their catalytic activity was tested. Clearly, nano-gold cluster with a 1.3 nm particle size exhibited the highest catalytic activity with >99% yield to the homocoupling product, but no activity resulted in the sample with a 9.5 nm particle size. The active site of the nano-gold cluster might be the positively charged surface, which results in Lewis-acid-type behavior in the reaction.

Recently, the Suzuki–Miyaura cross-coupling reaction was realized in water using PAPT (poly(2-aminothiophenol))-stabilized gold nanoparticles.³⁸² This nano-gold catalyst possessed an average particle size of ~ 4 nm and exhibited excellent activity in the coupling reaction of chlorobenzene and phenylboronic acid with >85% yield. This nano-gold catalyst was reused for 6 runs without deactivation and applied in the coupling reaction of bromobenzene/iodobenzene and phenylboronic acid with 82–90% yield.

The Sonogashira coupling of phenylacetylene (PA) with iodobenzene (IB) on an extended Au(111) surface was studied.³⁸³ Temperature-programmed reaction (TPR) and scanning tunneling microscopy (STM) characterization showed the reaction of PA and IB on the Au(111) facet and reconstruction of Au(111) facet after reaction, Figure 32(I). Clearly, on the smooth Au(111), three products, i.e., diphenyldiacetylene (DPDA), biphenyl (BP), and diphenylacetylene (DPA), were formed. However, no reaction occurred on the roughened Au(111) facet, Figure 32(II). Thus, the coupling reactions on gold are very sensitive to the surface structure. The inactivity of the rough Au surface may be due to the unavailability of well-defined crystal facets of sufficient size.

Lambert et al. tried to determine the real catalyst species in the Sonogashira coupling reaction catalyzed by nano-gold.³⁸⁴ After extensive study of the activity of leached gold into solution and supported nano-gold catalyst it was found that the turnover numbers of the nano-Au are orders of magnitude higher than the leached Au. Moreover, by comparing supported nano-gold catalysts with different particle sizes, it was revealed that large nano-gold particles were more active, which was possibly due to

Scheme 27. Results of Homocoupling Reaction of Phenylboric Acid Derivatives



the demands of a big facet for the reaction to progress, Figure 33. Thus, it was concluded that nano-Au but not cationic Au was the active species.

Two types of Pd nanoshells enclosed by high-index {730} and {221} facets were prepared, and their catalytic activity in the Suzuki coupling reaction was measured and compared to those of Pd and Au–Pd core–shell nanocubes that possess {100} facets.³⁸⁵ These high-index-faceted Pd nanoshells have been found to exhibit higher catalytic activities with 94–96% yields and 10.8–11.9 TON (s^{−1}). If Au–Pd core–shell nanocubes were applied, the yield was only 56% with 1.6 TON (s^{−1}). The higher catalytic performance of the Pd nanoshells is attributed to the presence of a large number of Pd atoms at steps on the high-index facets. The Pd atoms at steps are more coordinatively unsaturated than those on flat terraces and thus more efficient in the coupling reaction.

Beton et al. studied the dimerization of tri(4-bromophenyl)benzene (TBPB) by aryl–aryl coupling on Au(111) surface using ambient scanning tunneling microscopy (STM) and time-of-flight secondary-ion mass spectrometry (ToF-SIMS).³⁸⁶ TBPB molecular layers were prepared by allowing sessile drops of solution to dry on a gold substrate, and ordered arrays of TBPB in three distinct packing arrangements were observed clearly. STM and ToF-SIMS characterization showed the surface-induced aryl–aryl coupling to yield dimers and a small number of trimers, Figure 34. Suppression of further coupling reaction is due to the lower mobility of the dimerization product on the surface.

Although many successful examples about homogeneous and nano-Au catalysts in catalytic C–C bond formation reactions have been reported,^{387–390} it is still arguable if the transformation is really catalyzed by nano-Au but not palladium impurities. In 2010 Espinet et al. claimed that the Sonogashira coupling reaction was not catalyzed by gold.³⁹¹ They tested several gold complexes in the coupling reaction in the absence of palladium contamination, and no coupling product was detectable. Moreover, they supposed the mechanism about gold-catalyzed Sonogashira coupling might be wrong. In order to clarify this question, kinetic and theoretical studies were performed by Corma et al.³⁹² The results suggested that the Sonogashira coupling reaction between phenylacetylene and iodobenzene can occur on gold when it is in the form of nanoparticles. Moreover, for homogeneous coupling reactions with gold complex in solution, it might be decomposed to generate nano-Au particle, and the coupling reaction thus can progress. In one word, the Pd contamination problem in gold-catalyzed C–C bond formation reactions remains unsolved to date.

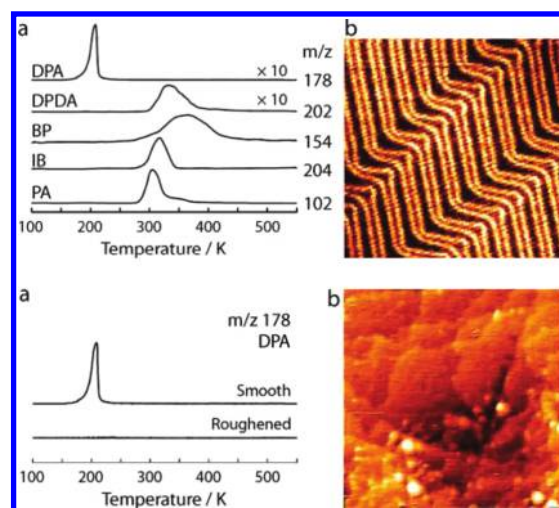


Figure 32. (Top) (a) TPR spectra of the reactants PA and IB and products diphenylacetylene (DPA), diphenyldiacetylene (DPDA), and biphenyl (BP) after adsorption of 0.55 ML of IB + 0.25 ML of PA on Au(111) at 90 K. (b) Typical STM image of a clean Au(111) surface showing the herringbone reconstruction (65 nm × 65 nm, V_{gap} 2.41 V, I 0.21 nA); (Bottom) (a) Diphenylacetylene (DPA, m/z 178) TPR spectra after dosing 0.55 ML of IB + 0.25 ML of PA on smooth and roughened Au(111) surfaces. (b) STM image of the roughened Au(111) surface (65 nm × 65 nm, V_{gap} −1.00 V, I 0.87 nA). Reprinted with permission from ref 383. Copyright 2010 American Chemical Society.

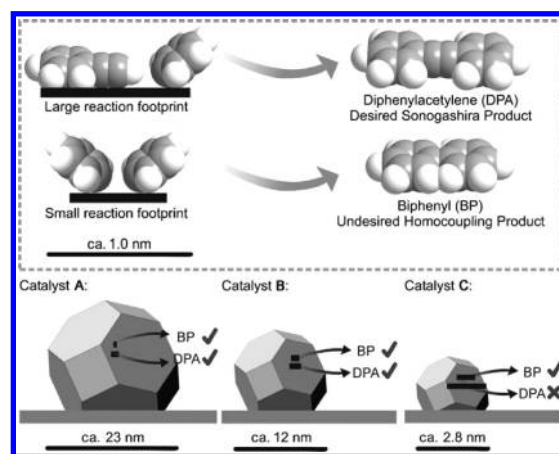


Figure 33. Possible origin of the particle size effect on selectivity due to the steric demands of the reactant adsorption footprint size; DPA formation inhibited on small particles. Reprinted with permission from ref 384. Copyright 2010 Wiley-VCH.

4.2.2. Sequential Oxidation–Addition Reactions.

Nano-gold supported on aluminum oxyhydroxide was active for aerobic oxidation of alcohol and sequential carbon–carbon bond formation with ketone.³⁹³ With addition of 1.5–3 equiv of Cs₂CO₃, various secondary alcohols and benzyl alcohol derivatives with different substituting groups were oxidized into the corresponding ketones or esters with up to 99% yield. During oxidation of benzyl alcohol, carbon–carbon bond formation occurred through sequential addition reactions when ketones were added, Scheme 28. Aromatic α,β -unsaturated ketones were produced in 70–90% yields. However, no desired product was detected when using aliphatic primary alcohols as starting materials.

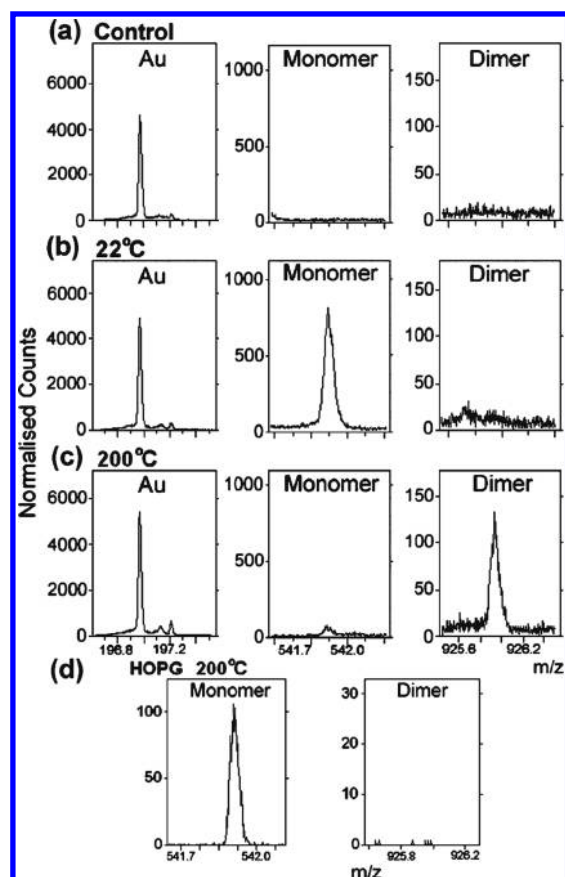
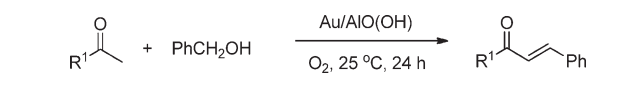


Figure 34. Secondary-ion mass spectrometry of surfaces: (a) control Au sample exposed to ethanol while being heated to 200 °C, (b) Au sample with TBPB deposited at room temperature, (c) Au sample with TBPB deposited at 200 °C, and (d) HOPG sample with TBPB deposited at 200 °C. Columns correspond to spectral data for Au (a–c), TBPB, and TBPQ. Data confirm that TBPQ formation arises from deposition on a heated Au substrate, as discussed in the text. Reprinted with permission from ref 386. Copyright 2011 American Chemical Society.

Recently, a general Au–Pd bimetallic catalyst was developed for the oxidation–addition reaction of 1,3-dicarbonyl compounds and allylic alcohols, Scheme 29.³⁹⁴ The composition of the catalyst was polymer-incarcerated gold–palladium nanocluster with boron on carbon (PI/CB-Au/Pd/B). It was prepared through coreduction of Au(PPh₃)Cl and Pd(OAc)₂ with NaBH₄ in the diglyme solution of styrene-based polymer containing abundant hydroxyl groups. Using PI/CB-Au/Pd/B as catalyst, 1,3-dicarbonyl compounds and allylic alcohols with different structures could smoothly be converted into the corresponding tricarbonyl products with 83–98% yields. This catalyst was recovered and reused for 5 runs without deactivation. The dual role of NaBH₄ as reducing agent for generation of Au–Pd bimetallic nanoclusters and as a precursor for the addition reaction was the key point to obtain high activity.

4.2.3. Benzylation by Benzyl Alcohol. Benzylation of aromatics using benzyl alcohol as the alkylation reagent was catalyzed by Au/SiO₂, Scheme 30.³⁹⁵ The key step to achieve the highly active catalyst was using ionic liquid [C₄mim][NTf₂] as the deposition medium for preparation of nano-gold catalyst. Applying the alkylation of toluene with benzyl alcohol as a model reaction, 84.1% benzyl alcohol conversion and 92.9% selectivity

Scheme 28. Oxidative C–C Bond Formation of Ketone and Benzyl Alcohol



Scheme 29. Aerobic Oxidation–Michael Addition of 1,3-Dicarbonyl Compounds to Allylic Alcohols^a



^a Reprinted with permission from ref 394. Copyright 2011 American Chemical Society.

to benzyl toluene was obtained with 1.5% Au/SiO₂ IL, which was prepared in ionic liquid [C₄mim][NTf₂], as catalyst. However, no any alkylation product was observed if applying 2.0% Au/SiO₂ IMP, which was prepared by the impregnation method in aqueous solution. Further measurement showed that 0.5% Au/SiO₂ IL was effective for alkylation of toluene derivatives, and normally >80% conversion and >90% selectivity were obtained. However, if using benzene and benzene halide as starting materials, conversion of benzyl alcohol was <30%, although >70% selectivity was maintained.

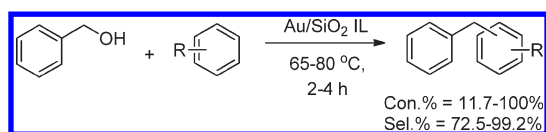
4.2.4. Synthesis of Substituted Phenols. Oxidative C–C coupling reactions of 2,6-di-*tert*-butyl phenol and 2,3,6-trimethyl phenol were successfully realized using Au/TiO₂ as catalyst.³⁹⁶ Commonly, in the presence of Ti-containing silica catalysts, benzoquinone was the major product. After improvement, the yields to DPQ and HMBP were all >90% using Au/TiO₂ as the catalyst and H₂O₂ as the oxidant, Scheme 31.

4.3. C–N Bond Formation

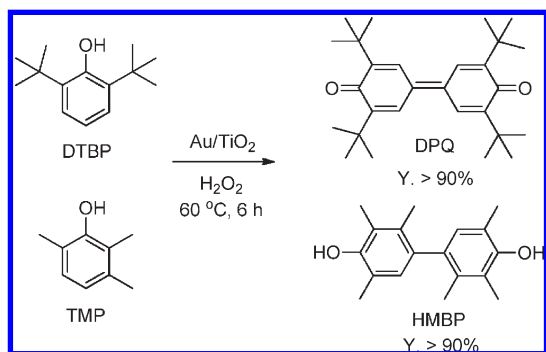
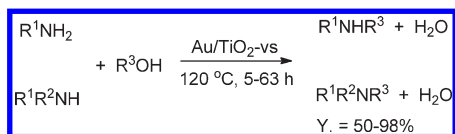
4.3.1. Amination Reactions. Amines and their derivatives are usually prepared by alkylation of amines with halides.^{397,398} An environmentally benign procedure to produce N-substituted amines is catalytic alkylation of amines with alcohols via the borrowing-hydrogen technology.^{399,400} Nano-gold catalysts were employed in this reaction by Ishida et al.⁴⁰¹ After catalyst screening they found that Au/Al-MIL 53([Al(OH)(benzene-1,4-dicarboxylate)]_n) was active for amination of aniline with benzyl alcohol. The yield to N-benzyl aniline was 48% with >70% selectivity. Subsequently, it was reported that Au/TiO₂-vs with very small nano-gold particle size was a good catalyst for N-alkylation of amines with alcohols, Scheme 32.⁴⁰² In the scope evaluation it covers the alkylation of primary and secondary amines with primary alcohols with various structures. With the benzylation of aniline as a model reaction, the yield to N-benzyl aniline was >90% but only 64% yield was obtained using Au/TiO₂–WGC (provided by the World Gold Council, average Au particle ≈ 3.2 nm).

The one-pot reductive amination of nitro compounds with alcohols could progress well using nano-gold catalysts without additional organic ligand and inorganic base, Scheme 33.⁴⁰³ Several metal oxide-supported nano-gold catalysts such as Au/Fe₂O₃, Au/CeO₂, Au/NiO, and Au/Co₃O₄ were used in the

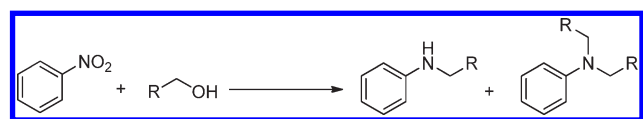
Scheme 30. Friedel–Crafts Alkylation of Aromatics with Benzyl Alcohol



Scheme 31. Oxidative Coupling of Substituted Phenols

Scheme 32. Au/TiO₂-vs-Catalyzed N-Alkylation Reaction with Alcohol

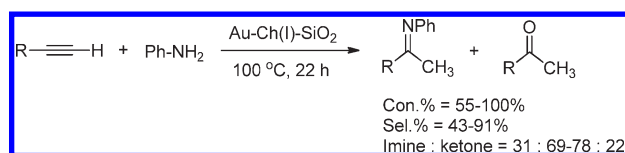
Scheme 33. Catalytic Amination of Nitrobenzene with Alcohol



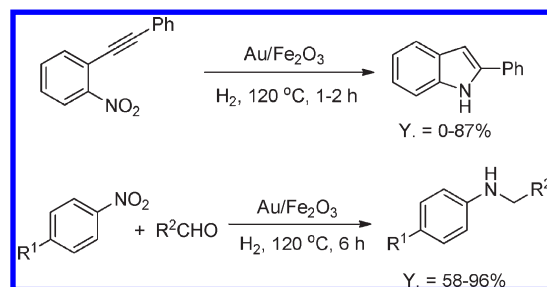
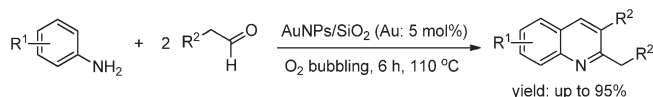
reaction, and Au/Fe₂O₃ or NiO exhibited the best performance. The nano-gold particle size in these samples was in the range of 3–6 nm. After optimization, reductive amination of nitrobenzenes with various substituents was realized in high yields to N-alkylated or N,N-dialkylated amines. The mono- or disubstituted product was obtained by tuning the catalyst and alcohol amounts. On the basis of GC-MS measurement of the reaction using nitrobenzene and *d*₇-benzyl alcohol at the initial stage it was found that the proton on the nitrogen of PhNH₂ was totally derived from the proton of the hydroxyl group of benzyl alcohol and one of the benzylic protons was transferred into water.

Au/TiO₂ was employed as the catalyst for the same reactions.⁴⁰⁴ Al₂O₃, ZnO, Fe₂O₃, CeO₂, and ZrO₂ as supports were tested, but much lower activity was observed in comparison with TiO₂. Au/TiO₂ could act effectively under milder reaction conditions, and secondary and tertiary amines with different structures were efficiently synthesized in high yields.

Scheme 34. Hydroamination of 1-Octyne To Yield Amine and Ketone



Scheme 35. One-Pot Synthesis of Indoles and N-Alkylated Anilines from Nitrobenzenes

Scheme 36. AuNPs/SiO₂-Catalyzed One-Pot, Tandem Aerobic Oxidative Cyclization of Anilines with Aldehydes to Quinolines

4.3.2. Nucleophilic Addition. It was found that nano-gold supported on polysaccharide (chitosan)/SiO₂ (Ch/SiO₂) was an effective catalyst for regioselective hydroamination of alkynes in the absence of acid promoter and under inert atmosphere.⁴⁰⁵ Au-Ch/SiO₂ was prepared through deposition of chitosan onto SiO₂ to gain Ch/SiO₂, and then gold species was deposited onto Ch/SiO₂. This Au-Ch/SiO₂ catalyst was active for hydroamination of alkynes, and amine and ketone were obtained after hydrolysis, Scheme 34. The hydroamination reactions of different anilines on terminal alkynes could achieve 43–91% yields of the imine and the ketone products.

Tokunaga et al. reported the one-pot synthesis of indoles and aniline derivatives catalyzed by Au/Fe₂O₃ under hydrogenation conditions, Scheme 35.⁴⁰⁶ Under optimized reaction conditions the isolated yield of 2-phenyl-1*H*-indole reached 87%. When an intramolecular reductive amination was performed with 2-(2-nitrophenyl)acetaldehyde, indole was formed in 71% yield. This catalyst is active for nitrobenzene reduction–reductive amination reactions, which normally gave ~80–90% yield to the desired N-alkylated aniline.

Recently, Che et al. reported that quinolines were synthesized via the one-pot, tandem aerobic oxidative cyclization of anilines with aldehydes using Au/SiO₂ catalyst, Scheme 36.⁴⁰⁷ A series of quinoline derivatives with different substituent groups was successfully synthesized with up to 95% ¹H NMR yield. The catalyst was recovered and reused for 7 runs without any deactivation.

4.4. Carbonylation Reactions

4.4.1. Carbamates Synthesis. Traditionally, the carbonylation reactions were catalyzed by noble metal catalysts such as Pd, Ru, Rh, etc.^{408–410} About 10 years earlier, the possibility of using gold as carbonylation catalysts was explored but the catalytic efficiency was not good enough.^{411,412} Subsequently, it was found that the catalytic activity was improved dramatically if gold species were deposited onto commercially available resin, which resulted in an active catalyst for oxidative carbonylation of amines.^{413,414} Preparation of this polymer-supported nano-gold catalyst was performed by dipping the NaOH-treated polymer into the acetone solution of HAuCl₄. The gold species thus deposited onto the polymer quickly, cationic gold was reduced by the organics on the polymer surface, and thus nano-gold particle formed on the polymer surface after it was dried at 60 °C. The particle size of the Au/polymer was ~12 nm. It was quite big if comparing with nano-gold catalyst prepared with other methods, but it exhibited good catalytic performance in the oxidative carbonylation of aniline. The conversion was 95% with 99% selectivity to methyl *N*-phenyl carbamate, Scheme 37. Moreover, if methanol was excluded from the reaction mixture, diphenyl urea was produced in ~70% yield. Noteworthy, there is no concern about removing the chlorine on the catalyst. The presence of chlorine seems does not affect formation of the catalytically active position.

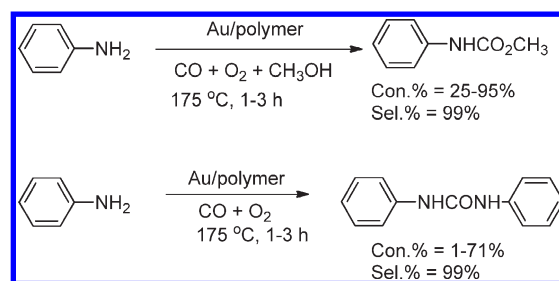
Angelici et al. reported that Au powder possessed catalytic activity in the oxidative carbonylation of amines too.⁴¹⁶ In the presence of 1.0 g of Au powder and 0.5 mmol of amine, a moderate yield, i.e., 0–46%, to the corresponding disubstituted urea was obtained at 45 °C and 1 atm mixture gas of CO and O₂. Although the reaction condition is milder than that shown in Scheme 37, a large excess of Au was employed in this work. An explanation for activation of carbon monoxide and carbonylation reaction was given, Scheme 38.

Carbonylation of 2,4-diaminotoluene (DAT) with dimethyl carbonate (DMC) catalyzed by nano-gold catalyst was reported.⁴¹⁷ Normally, this reaction was catalyzed by Lewis-acid catalysts, which often caused formation of the *N*-methylation product and corrosion to the equipment. After optimization, Au/CeO₂ was shown to be an ideal catalyst for this carbonylation reaction. The dicarbamate product yield reached 96% without deactivation occurring after 3 runs. One-pot synthesis of the dicarbamate product from 2,4-dinitrotoluene (DNT) and DMC was carried out in the presence of molecular hydrogen, Scheme 39. The conversion of DNT was 95.2% with 98.3% selectivity to the desired product.

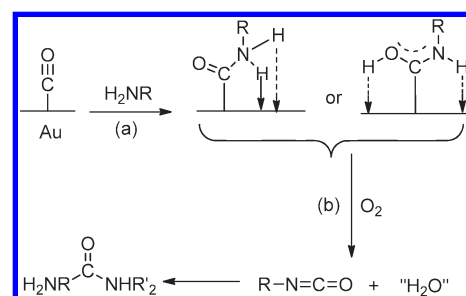
Later, the same group reported the continuous flow carbonylation of aniline by dimethyl carbonate using a microreactor.⁴¹⁸ The nanoparticles of Au/CeO₂ were deposited on a stainless steel plate (5 × 10 cm²) having parallel channels of 10 μm width and activated at 700 °C before reaction. The results showed that the catalyst could remain stable for more than 20 h with ~35% aniline conversion and >90% *N*-phenyl methyl carbamate selectivity at 120 °C and 5 bar pressure.

4.4.2. Carbonates Synthesis. Au/polymer catalyst was very active in carbon dioxide activation. Cyclic carbonates were effectively synthesized from epoxide and carbon dioxide.⁴¹⁵ The results showed that higher Au loading can result in higher conversion of epoxide, but the TOF number decreased if calibrated according to the quantity of gold. For the carbonylation of different epoxides, normally >90% yield was obtained.

Scheme 37. Oxidative Carbonylation of Aniline To Yield Methyl *N*-Phenyl Carbamate and Diphenyl Urea

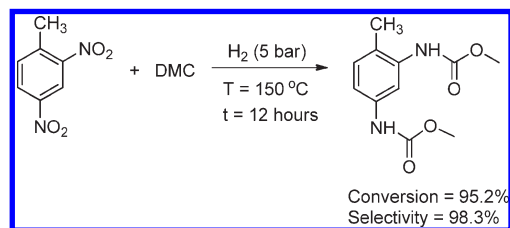


Scheme 38. Reaction Pathway of Au-Catalyzed Oxidative Carbonylation of Amines^a



^a Reprinted with permission from ref 416. Copyright 2006 American Chemical Society.

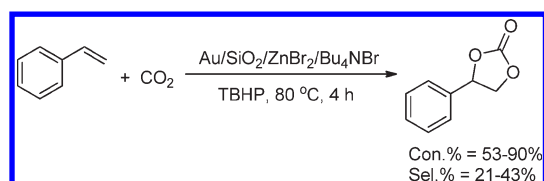
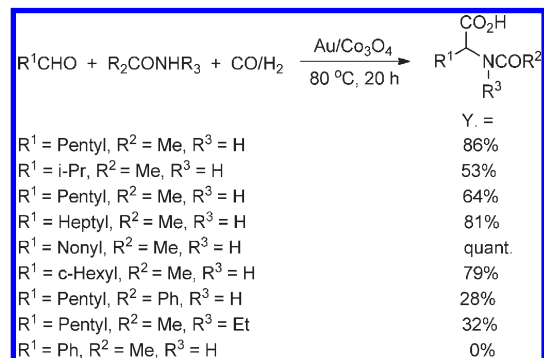
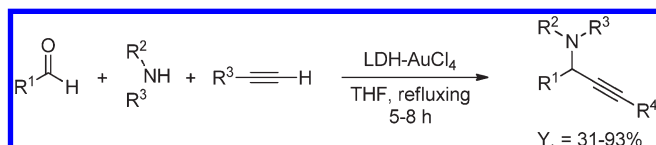
Scheme 39. One-Pot Reaction of 2,4-Dinitrotoluene with DMC over Au/CeO₂^a



^a Reprinted with permission from ref 417. Copyright 2010 Wiley-VCH.

Synthesis of dimethyl carbonate via transalkylation of propylene carbonate (PC) with methanol was realized using Au/CeO₂ as the catalyst with 63% conversion and 55% selectivity to dimethyl carbonate.⁴¹⁹ Styrene carbonate (SC) was one-pot synthesized from styrene, oxygen, and carbon dioxide catalyzed by the Au/SiO₂–ZnBr₂/Bu₄NBr catalytic system, but only poor to moderate selectivity, i.e., <50%, to SC was obtained, Scheme 40.⁴²⁰

The selectivity to SC was improved slightly using *tert*-butyl hydroperoxide as the oxidant.^{421,422} Under optimized reaction conditions, 0.01% Au/R201 (Amberlite IRA-400) exhibited the best performance and 98.1% conversion of styrene with 50.6% selectivity to SC was achieved without additional Lewis-acid catalyst. If Au/Fe(OH)₃–ZnBr₂/Bu₄NBr was used as the catalyst, the yield to SC reached 53%. Although the results are still not good enough, it helps to understand these reactions well.

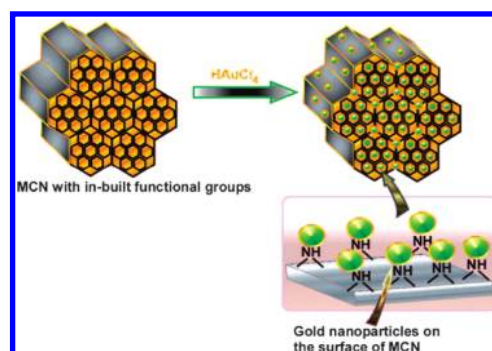
Scheme 40. One-Pot Synthesis of Styrene Carbonate from Styrene**Scheme 41. Amidocarbonylation of Aldehydes Catalyzed by Cobalt Oxide-Supported Nano-Au****Scheme 42. Three-Component Coupling of Benzaldehyde, Piperidine, and Phenylacetylene**

4.4.3. Hydroformylation. Tokunaga et al. reported that Au/Co₃O₄ was active in the hydroformylation reaction.⁴²³ In the model reaction using 1-hexene as the starting material the conversion was 99.5% with 83.9% selectivity to aldehydes and the linear to branching ratio was 1.2. The combination of nano-Au with Co₃O₄ should be the crucial point to realize this transformation. If applying Au/C or Co₃O₄ as the hydroformylation catalyst, the selectivities to the desired aldehydes were 3.1% and 0%, respectively. Subsequently, hydroformylation of olefins with different structures including *cis*-2-hexene, *cis*-3-hexene, cyclohexene, methyl enecyclohexane, and 3,3-dimethyl-1-butene was performed.⁴²⁴ Excellent selectivities (84.3–91.6%) to aldehydes were obtained no matter which kind of olefins was used. However, only poor to moderate conversions (<50%) were obtained except when using 3,3-dimethyl-1-butene as starting material (95.4%).

Au/Co₃O₄ was active in the amidocarbonylation of aldehydes, Scheme 41.⁴²⁵ The reaction could progress well when using aliphatic aldehydes and primary aliphatic amides as starting materials. The yields to *N*-acyl- α -amino acid derivatives were 53–86%.

4.5. Three-Component Coupling Reactions

Propargyl amines are versatile precursors for the synthesis of nitrogen-containing biologically active compounds.⁴²⁶ Traditionally they were synthesized by nucleophilic addition of

**Figure 35.** Encapsulation of gold nanoparticles over MCN with in-built functional groups without any external stabilizing agent. Reprinted with permission from ref 432. Copyright 2010 Wiley-VCH.

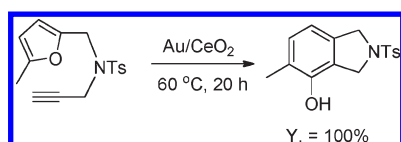
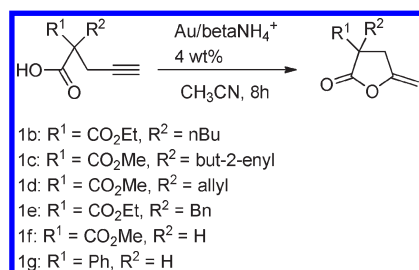
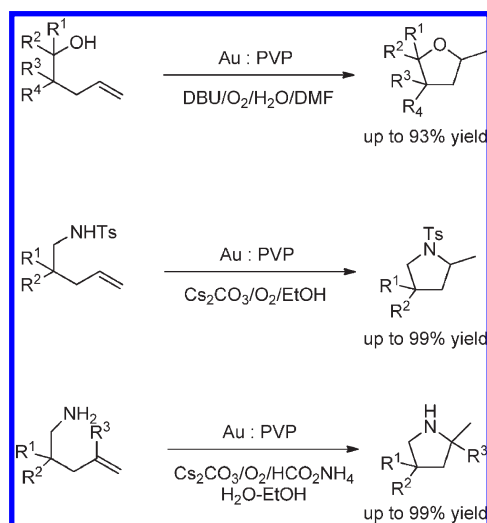
an alkynyl-Li or -Mg reagent to imine or other similar C=N electrophiles.^{427,428} Kantam et al. developed a layered double-hydroxides (LDHs) supported gold catalyst (LDH-AuCl₄) by the ion-exchange method for three-component coupling reactions from amine, aldehyde, and alkyne, Scheme 42.⁴²⁹ Coupling reactions of amines, aldehydes, and alkynes with different structures were realized over LDH-AuCl₄ with up to 93% yields. The catalytically active species of this catalyst were Au³⁺ and Au⁰. Formation of Au⁰ during reaction resulted in deactivation. Corma et al. reported that CeO₂-immobilized nano-gold catalyst was highly efficient for this coupling reaction too.⁴³⁰ Benzaldehydes, secondary amines, and alkynes with different structures were transformed into propargyl amines with up to 99% yields. They suggested cationic Au³⁺ might be the active species while CeO₂ can stabilize the alkyne-Au-H intermediate during the reaction. Subsequently, it was reported that sulfide-gold, i.e., CdS-Au, CdSe-Au, and PbS-Au, was a fine catalyst for three-component coupling of benzaldehyde, piperidine, and phenylacetylene; PbS-Au exhibited better performance.⁴³¹ PbS-Au was immobilized onto activated carbon and used in the coupling reaction in water after optimization of the desired product in >85% isolated yield.

Recently, Vinu et al. prepared a nano-gold catalyst for the coupling reaction again.⁴³² In this catalyst the nano-gold particle was embedded in the mesoporous carbon nitride; thus, it was effectively supported. The preparation procedure of this catalyst is shown in Figure 35. According to BET analysis and TEM characterization the mesoporous structure was confirmed and the nano-gold particles were clearly observed along the nano-channels of the support. This nano-gold catalyst exhibited good activity in the coupling reaction with benzaldehyde, *p*-nitrobenzaldehyde, and *p*-chlorobenzaldehyde as starting materials, and 36–96% conversion with 60–77% selectivity were obtained.

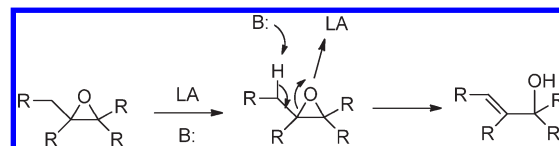
4.6. Cyclization Reactions

Au/CeO₂ was an active catalyst for isomerization of ω -alkynylfurans to phenols,⁴³³ which was first realized with homogeneous gold catalyst,⁴³⁴ Scheme 43. After improvement, 100% conversion was obtained but the reusability was not fine. Around 35% conversion was maintained at the third run.

Functionalized lactones were synthesized with high efficiency using zeolite beta-NH₄⁺-supported nano-gold as the catalyst, Scheme 44.⁴³⁵ Carboxylic acid with terminal alkyne and other functional groups was cyclized to yield the corresponding lactones with 25–88% yields. The catalyst was reused for 5 runs without deactivation.

Scheme 43. Reaction Scheme of Au/CeO₂-Catalyzed Phenol Synthesis**Scheme 44. Au-Catalyzed Cyclization of Functionalized Carboxylic Acids^a**^a Reprinted with permission from ref 435. Copyright 2008 Wiley-VCH.**Scheme 45. Heterocyclization of γ -Hydroxyalekenes and γ -Toluenesulfonylaminoalkenes**

Intramolecular heterocyclization reactions were developed with Au:PVP catalysts by Sakurai et al., Scheme 45.⁴³⁶ Using 1.3 nm Au nanoclusters as catalysts, heterocyclization of γ -hydroxyalekenes, γ -toluenesulfonylaminoalkenes, and γ -aminoalekenes was realized under aerobic oxidation conditions. Tetrahydrofuran and pyrrolidine derivatives with up to 99% yields were obtained. Although it was not involved in the final product, molecular oxygen played a crucial role in the cyclization reactions, which was similar to former reports.^{49,272} As an example, in the heterocyclization of γ -hydroxyalekenes, the activated oxygen on nano-Au cluster promoted the cyclization reaction on the catalyst surface and the involvement of *N,N*-dimethylformamide resulted in the final product. In the end, molecular oxygen and *N,N*-dimethylformamide were transformed into HNMe₂, CO₂, and H₂O₂.

Scheme 46. Schematic Representation of the Isomerization of an Epoxide into an Allylic Alcohol Using a Bifunctional Acid/Base Catalyst^a^a LA = Lewis acid, B = Lewis base. Reprinted with permission from ref 437. Copyright 2009 Wiley-VCH.

4.7. Epoxide Isomerization to Allylic Alcohol

The last reaction discussed here is the TiO₂-supported nano-gold-catalyzed epoxide isomerization to allylic alcohol, Scheme 46.⁴³⁷ Epoxides with various functional groups were effectively transformed into the corresponding allylic alcohols with 82–98% yields. Stereoisotopic study and mechanism exploration were reported.

5. CONCLUSIONS AND OUTLOOK

Since the beginning of nano-gold catalysis in fine chemicals synthesis at the end of the 1980s, more than 20 years have passed and many excellent studies have been done. Now we summarize the results and give insights into what should be done in the future. Thus, the first question is what has nano-gold catalysis contributed to fine chemical synthesis? From our personal perspective, we think the following points are important.

- (1) A unique catalyst was discovered for elimination of environmentally harmful compounds such as carbon monoxide, nitrogen oxides, ozone, halocarbons, sulfur dioxide, dioxins, and volatile organic compounds (VOC). Although it is not in the field of fine chemical synthesis, it must be mentioned when nano-gold catalysis is discussed. This is the starting point of nano-gold catalysis, which has attracted more and more researchers to join this field and remain a hot topic in catalysis.
- (2) Several important reactions that could not proceed well with traditional noble metal catalysts such as Pd, Ru, and Rh, etc., were realized by gold catalysis. The first one is the hydrochlorination of alkynes. This is the starting point of nano-gold catalysis in fine chemical synthesis. The second one is the epoxidation of terminal olefins, especially propylene. It offered a new choice for catalysis researchers to develop a clean and an economic route for propylene oxide production.
- (3) Another achievement in nano-gold catalysis is establishment of a Au–Pd bimetallic alloy catalytic system. This catalytic system possesses specific activity in selective oxidation reactions such as biomass oxidation, alcohol oxidation, and toluene oxidation, etc. During development of nano-gold catalysis in fine chemical synthesis, hydrogen peroxide was produced from hydrogen and oxygen using the Au–Pd alloy catalyst efficiently. This should be a breakthrough in catalysis and chemical industry.

Moreover, the more important point is what we are doing and what we should do in the future in the field of nano-gold catalysis. Similar to the great achievements listed above, we think the following points should be concentrated on.

- (1) Controllable preparation of nano-gold catalysts. Although a variety of nano-gold catalysts have been prepared and numerous reactions have been performed, we are often confused by the reproducibility of nano-gold catalysts. There is no unified

theory in the design and preparation of nano-gold catalyst for specific reaction. This should be the first objective in the future for catalysis researchers, i.e., trying to establish a theory for controllable preparation of nano-gold catalysts.

- (2) Utilization of nano-gold catalyst in pure organic reactions in large-scale processes. Although has been rare to date, as an area studied much less in the past, it offers new possibility for catalytic researchers/organic chemists to discover unknown properties of nano-gold as catalyst.
- (3) Increase the range of application to industrially interesting chemical reactions. Nano-gold catalysis can play a significant role in the development of green chemistry and green technology. It offers new opportunities in developing sustainable chemical industry.

AUTHOR INFORMATION

Corresponding Author

*E-mail: fshi@licp.cas.cn.

BIOGRAPHIES



Yan Zhang was born in 1980 in Inner Mongolia, China. She received her Ph.D. degree in Physical Chemistry from the Lanzhou Institute of Chemical Physics in 2009. She then worked at the Centre for Green Chemistry and Catalysis in Lanzhou Institute of Chemical Physics (CAS) as a research assistant. She has authored or coauthored more than 10 journal papers. Her current research focuses on heterogeneous catalysis, including catalyst preparation, characterization, catalytic activity measurement, and mechanism study, etc.



Xinjiang Cui received his B.S. degree in 2007 from Shangdong University of Science and Technology. In 2007, he started his career in the Graduate University of Chinese Academy of Sciences

for 1 year. Since 2009 he has been studying for his Ph.D. degree at the Lanzhou Institute of Chemical Physics, Chinese Academy of Sciences. His doctoral research is concerned with development of novel catalysts for clean synthesis of N-substituted amines.



Feng Shi received his B.S. degree in Chemistry from ShanDong Normal University in 1998. In 2004, he completed his Ph.D. studies in physical chemistry under the guidance of Professor Youquan Deng at the Lanzhou Institute of Chemical Physics, Chinese Academy of Sciences. He was a postdoctoral fellow with Professor Matthias Beller at the Leibniz Institute for Catalysis as an Alexander von Humboldt Research Fellowship (2005–2007) and Research Fellowship of the Leibniz Institute for Catalysis (2007–2008). At the end of 2008 he joined the faculty of the Lanzhou Institute of Chemical Physics, Chinese Academy of Sciences. His research interests are focused on nanocatalysis and green chemistry.



Youquan Deng received his B.S. degree at Lanzhou University and his Ph.D. degree at the University of Portsmouth (United Kingdom). He is a Research Professor of Physics Chemistry in the Centre for Green Chemistry and Catalysis, Lanzhou Institute of Chemical Physics, Chinese Academy of Sciences. He is also Professor of Graduate School of the Chinese Academy of Sciences, Head of the Centre for Green Chemistry and Catalysis. He has been engaging in catalytic scientific and technology for many years. He has authored 40 patents and more than 110 scientific papers in international journals. He is a member of the Chinese Catalysis Society and the Chinese Green Chemistry Society.

ACKNOWLEDGMENT

We are grateful to the National Natural Science Foundation of China (21073208) and the Chinese Academy of Sciences for financial support of this work.

REFERENCES

- (1) Haruta, M.; Kobayashi, T.; Sano, H.; Yamada, N. *Chem. Lett.* **1987**, 405.
- (2) Haruta, M.; Kageyama, H.; Kamijo, N.; Kobayashi, T.; Delannay, F. *Stud. Surf. Sci. Catal.* **1989**, 44, 33.
- (3) Hutchings, G. J. *J. Catal.* **1985**, 96, 292.
- (4) Bond, G. C.; Sermon, P. A.; Webb, G.; Buchanan, D. A.; Wells, P. B. *J. Chem. Soc., Chem. Commun.* **1973**, 444.
- (5) Bond, G. C.; Sermon, P. A. *Gold Bull.* **1973**, 6, 102.
- (6) Sermon, P. A.; Bond, G. C.; Wells, P. B. *J. Chem. Soc., Faraday Trans.* **1979**, 175, 385.
- (7) Hutchings, G. J. *Catal. Today* **2005**, 100, 55.
- (8) Roduner, E. *Chem. Soc. Rev.* **2006**, 35, 583.
- (9) Hu, M.; Chen, J.; Li, Z.-Y.; Au, L.; Hartland, G. V.; Li, X.; Marquez, M.; Xia, Y. *Chem. Soc. Rev.* **2006**, 35, 1084.
- (10) Hashmi, A. S. K.; Rudolph, M. *Chem. Soc. Rev.* **2008**, 37, 1766.
- (11) Ofir, Y.; Samanta, B.; Rotello, V. M. *Chem. Soc. Rev.* **2008**, 37, 1814.
- (12) Chen, M.; Goodman, D. W. *Chem. Soc. Rev.* **2008**, 37, 1860.
- (13) Sperling, R. A.; Rivera Gil, P.; Zhang, F.; Zanella, M.; Parak, W. J. *Chem. Soc. Rev.* **2008**, 37, 1896.
- (14) Wilson, R. *Chem. Soc. Rev.* **2008**, 37, 2028.
- (15) Della Pina, C.; Falletta, E.; Prati, L.; Rossi, M. *Chem. Soc. Rev.* **2008**, 37, 2077.
- (16) Corma, A.; Garcia, H. *Chem. Soc. Rev.* **2008**, 37, 2096.
- (17) Fierro-Gonzalez, J. C.; Gates, B. C. *Chem. Soc. Rev.* **2008**, 37, 2127.
- (18) Boisselier, E.; Astruc, D. *Chem. Soc. Rev.* **2009**, 38, 1759.
- (19) Bracey, C. L.; Ellis, P. R.; Hutchings, G. J. *Chem. Soc. Rev.* **2009**, 38, 2231.
- (20) Marion, N.; Nolan, S. P. *Chem. Soc. Rev.* **2008**, 37, 1776.
- (21) Häkkinen, H. *Chem. Soc. Rev.* **2008**, 37, 1847.
- (22) Hashmi, A. S. K.; Hutchings, G. J. *Angew. Chem., Int. Ed.* **2006**, 45, 7896.
- (23) Gimeno, M. C.; Laguna, A. *Chem. Rev.* **1997**, 97, 511.
- (24) Shaw, C. F. *Chem. Rev.* **1999**, 99, 2589.
- (25) Daniel, M. C.; Astruc, D. *Chem. Rev.* **2004**, 104, 293.
- (26) Min, B. K.; Friend, C. M. *Chem. Rev.* **2007**, 107, 2709.
- (27) Hashmi, A. S. K. *Chem. Rev.* **2007**, 107, 3180.
- (28) Ghosh, S. K.; Pal, T. *Chem. Rev.* **2007**, 107, 4797.
- (29) Li, Z.; Brouwer, C.; He, C. *Chem. Rev.* **2008**, 108, 3239.
- (30) Arcadi, A. *Chem. Rev.* **2008**, 108, 3266.
- (31) Jiménez-Núñez, E. s.; Echavarren, A. M. *Chem. Rev.* **2008**, 108, 3326.
- (32) Puddephatt, R. J. *Chem. Soc. Rev.* **2008**, 37, 2012.
- (33) Grzelczak, M.; Pérez-Juste, J.; Mulvaney, P.; Liz-Marzán, L. M. *Chem. Soc. Rev.* **2008**, 37, 1783.
- (34) Tykot, R. H. *Acc. Chem. Res.* **2002**, 35, 618.
- (35) Chen, M.; Goodman, D. W. *Acc. Chem. Res.* **2006**, 39, 739.
- (36) Murphy, C. J.; Gole, A. M.; Stone, J. W.; Sisco, P. N.; Alkilany, A. M.; Goldsmith, E. C.; Baxter, S. C. *Acc. Chem. Res.* **2008**, 41, 1721.
- (37) Risse, T.; Shaikhutdinov, S.; Nilius, N.; Sterrer, M.; Freund, H. J. *Acc. Chem. Res.* **2008**, 41, 949.
- (38) Schwerdtfeger, P. *Angew. Chem., Int. Ed.* **2003**, 42, 1892.
- (39) Shan, J.; Tenhu, H. *Chem. Commun.* **2007**, 4580.
- (40) Hutchings, G. J. *Chem. Commun.* **2008**, 1148.
- (41) Hutchings, G. J. *Dalton Trans.* **2008**, 5523.
- (42) Michelet, V.; Toullec, P. Y.; Genet, J. P. *Angew. Chem., Int. Ed.* **2008**, 47, 4268.
- (43) Furstner, A. *Chem. Soc. Rev.* **2009**, 38, 3208.
- (44) Toste, F. D.; Gorin, D. J. *Nature* **2007**, 446, 395.
- (45) Toste, F. D.; Shapiro, N. D. *Synlett* **2010**, 675.
- (46) Díez-González, S.; Nolan, S. P. *Acc. Chem. Res.* **2008**, 41, 349.
- (47) Gorin, D. J.; Sherry, B. D.; Toste, F. D. *Chem. Rev.* **2008**, 108, 3351.
- (48) Claus, P. *Appl. Catal., A: Chem.* **2005**, 291, 222.
- (49) Tsukuda, T.; Tsunoyama, H.; Sakurai, H. *Chem. Asian J.* **2011**, 6, 736.
- (50) Corma, A.; Leyva-Perez, A.; Sabater, M. J. *Chem. Rev.* **2011**, 111, 1657.
- (51) Qi, S. T.; Cheney, B. A.; Zheng, R. Y.; Lonergan, W. W.; Yu, W. T.; Chen, J. G. *Appl. Catal., A: Chem.* **2011**, 393, 44.
- (52) Pattamakomsan, K.; Ehret, E.; Morfin, F.; Gelin, P.; Jugnet, Y.; Prakash, S.; Bertolini, J. C.; Panpranot, J.; Aires, F. J. C. *S. Catal. Today* **2011**, 164, 28.
- (53) Primo, A.; Concepcion, P.; Corma, A. *Chem. Commun.* **2011**, 47, 3613.
- (54) Fu, J.; Lu, X. Y.; Savage, P. E. *ChemSusChem* **2011**, 4, 481.
- (55) Bond, G. C.; Sermon, P. A.; Webb, G.; Buchanan, D. A.; Wells, P. B. *J. Chem. Soc., Chem. Commun.* **1973**, 444.
- (56) Krauth, A. C.; Bernstein, G. H.; Wolf, E. E. *Catal. Lett.* **1997**, 45, 177.
- (57) Buchanan, D. A.; Webb, G. J. *Chem. Soc., Faraday Trans. 1* **1975**, 71, 134.
- (58) Okumura, M.; Akita, T.; Haruta, M. *Catal. Today* **2002**, 74, 265.
- (59) Piccolo, L.; Piednoir, A.; Bertolini, J. C. *Surf. Sci.* **2005**, 592, 169.
- (60) Hugon, A.; Delannoy, L.; Louis, C. *Gold Bull.* **2008**, 41, 127.
- (61) Hugon, A.; Delannoy, L.; Krafft, J.-M.; Louis, C. *J. Phys. Chem. C* **2010**, 114, 10823.
- (62) Zhang, X.; Shi, H.; Xu, B. Q. *Angew. Chem., Int. Ed.* **2005**, 44, 7132.
- (63) Zhang, X.; Shi, H.; Xu, B. Q. *Catal. Today* **2007**, 122, 330.
- (64) Zhang, X.; Shi, H.; Xu, B.-Q. *J. Catal.* **2011**, 279, 75.
- (65) Liu, Z. P.; Wang, C. M.; Fan, K. N. *Angew. Chem., Int. Ed.* **2006**, 45, 6865.
- (66) Gallezot, P.; Richard, D. *Cat. Rev.-Sci. Eng.* **1998**, 40, 81.
- (67) Ando, C.; Kurokawa, H.; Miura, H. *Appl. Catal., A: Chem.* **1999**, 185, L181.
- (68) Bailie, J. E.; Hutchings, G. J. *Chem. Commun.* **1999**, 2151.
- (69) Okumura, M.; Akita, T.; Haruta, M. *Catal. Today* **2002**, 74, 265.
- (70) Bailie, J. E.; Abdullah, H. A.; Anderson, J. A.; Rochester, C. H.; Richardson, N. V.; Hodge, N.; Zhang, J.-G.; Burrows, A.; Kiely, C. J.; Hutchings, G. J. *Phys. Chem. Chem. Phys.* **2001**, 3, 4113.
- (71) Zanella, R. J. *Catal.* **2004**, 223, 328.
- (72) Campo, B.; Volpe, M.; Ivanova, S.; Touroude, R. J. *Catal.* **2006**, 242, 162.
- (73) Campo, B.; Petit, C.; Volpe, M. J. *Catal.* **2008**, 254, 71.
- (74) Campo, B.; Santori, G.; Petit, C.; Volpe, M. *Appl. Catal., A: Chem.* **2009**, 359, 79.
- (75) Chen, H.-Y.; Chang, C.-T.; Chiang, S.-J.; Liaw, B.-J.; Chen, Y.-Z. *Appl. Catal., A: Chem.* **2010**, 381, 209.
- (76) Yang, Q.-Y.; Zhu, Y.; Tian, L.; Xie, S.-H.; Pei, Y.; Li, H.; Li, H.-X.; Qiao, M.-H.; Fan, K.-N. *Appl. Catal., A: Chem.* **2009**, 369, 67.
- (77) Zhu, Y.; Tian, L.; Jiang, Z.; Pei, Y.; Xie, S.; Qiao, M.; Fan, K. J. *Catal.* **2011**, 281, 106.
- (78) Lenz, J.; Campo, B. C.; Alvarez, M.; Volpe, M. A. J. *Catal.* **2009**, 267, 50.
- (79) Claus, P.; Bruckner, A.; Mohr, C.; Hofmeister, H. *J. Am. Chem. Soc.* **2000**, 122, 11430.
- (80) Mohr, C.; Hofmeister, H.; Claus, P. *J. Catal.* **2003**, 213, 86.
- (81) Mohr, C.; Hofmeister, H.; Radnik, J.; Claus, P. *J. Am. Chem. Soc.* **2003**, 125, 1905.
- (82) Wang, C. M.; Fan, K. N.; Liu, Z. P. *J. Catal.* **2009**, 266, 343.
- (83) Milone, C.; Tropeano, M. L.; Gulino, G.; Neri, G.; Ingoglia, R.; Galvagno, S. *Chem. Commun.* **2002**, 868.
- (84) Protasova, L. N.; Rebrov, E. V.; Skelton, H. E.; Wheatley, A. E. H.; Schouten, J. C. *Appl. Catal., A: Chem.* **2011**, 399, 12.
- (85) Shi, H.; Xu, N.; Zhao, D.; Xu, B. Q. *Catal. Commun.* **2008**, 9, 1949.
- (86) You, K.-J.; Chang, C.-T.; Liaw, B.-J.; Huang, C.-T.; Chen, Y.-Z. *Appl. Catal., A: Chem.* **2009**, 361, 65.
- (87) Milone, C.; Trapani, M. C.; Galvagno, S. *Appl. Catal., A: Chem.* **2008**, 337, 163.
- (88) Milone, C. J. *Catal.* **2004**, 222, 348.
- (89) Milone, C.; Ingoglia, R.; Schipilliti, L.; Crisafulli, C.; Neri, G.; Galvagno, S. *J. Catal.* **2005**, 236, 80.

- (90) Mertens, P.; Vandezande, P.; Ye, X.; Poelman, H.; Vankelecom, I.; Devos, D. *Appl. Catal., A: Chem.* **2009**, *355*, 176.
- (91) Zhu, Y.; Qian, H.; Drake, B. A.; Jin, R. *Angew. Chem., Int. Ed.* **2010**, *49*, 1295.
- (92) Lawrence, S. A. *Amines: Synthesis, Properties and Applications*; Cambridge University Press: New York, 2004.
- (93) Coq, B.; Tijani, A.; Dutartre, R.; Figueras, F. *J. Mol. Catal.* **1993**, *79*, 253.
- (94) Yu, Z. K.; Liao, S. J.; Xu, Y.; Yang, B.; Yu, D. R. *J. Chem. Soc., Chem. Commun.* **1995**, 1155.
- (95) Zuo, B. J.; Wang, Y.; Wang, Q. L.; Zhang, J. L.; Wu, N. Z.; Peng, L. D.; Gui, L. L.; Wang, X. D.; Wang, R. M.; Yu, D. P. *J. Catal.* **2004**, *222*, 493.
- (96) Chen, Y. Y.; Qiu, J. S.; Wang, X. K.; Xiu, J. H. *J. Catal.* **2006**, *242*, 227.
- (97) He, D. P.; Shi, H.; Wu, Y.; Xu, B. Q. *Green Chem.* **2007**, *9*, 849.
- (98) Cardenas-Lizana, F.; Gomez-Quero, S.; Keane, M. A. *Catal. Commun.* **2008**, *9*, 475.
- (99) Cardenas-Lizana, F.; Gomez-Quero, S.; Keane, M. A. *ChemSusChem* **2008**, *1*, 215.
- (100) Corma, A.; Serna, P. *Science* **2006**, *313*, 332.
- (101) Yang, P.; Zhang, W.; Li, L.; Du, Y. K.; Wang, X. M. *Catal. Lett.* **2009**, *127*, 429.
- (102) Valden, M.; Lai, X.; Goodman, D. W. *Science* **1998**, *281*, 1647.
- (103) Zhu, Y.; Qian, H.; Jin, R. *J. Mater. Chem.* **2011**, *21*, 6793.
- (104) Liu, L. Q.; Qiao, B. T.; Ma, Y. B.; Zhang, J.; Deng, Y. Q. *Dalton Trans.* **2008**, 2542.
- (105) Liu, L. Q.; Qiao, B. T.; Chen, Z. J.; Zhang, J.; Deng, Y. Q. *Chem. Commun.* **2009**, 653.
- (106) He, L.; Wang, L. C.; Sun, H.; Ni, J.; Cao, Y.; He, H. Y.; Ean, K. N. *Angew. Chem., Int. Ed.* **2009**, *48*, 9538.
- (107) Liu, Y. C.; Chen, Y. W. *Ind. Eng. Chem. Res.* **2006**, *45*, 2973.
- (108) Kratky, V.; Kralik, M.; Mearova, M.; Stolicova, M.; Zalibera, L.; Hronec, M. *Appl. Catal., A: Chem.* **2002**, *235*, 225.
- (109) Coq, B.; Tijani, A.; Figueras, F. *J. Mol. Catal.* **1991**, *68*, 331.
- (110) Cardenas-Lizana, F.; Gomez-Quero, S.; Hugon, A.; Delannoy, L.; Louis, C.; Keane, M. A. *J. Catal.* **2009**, *262*, 235.
- (111) Boronat, M.; Concepcion, P.; Corma, A.; Gonzalez, S.; Illas, F.; Serna, P. *J. Am. Chem. Soc.* **2007**, *129*, 16230.
- (112) Serna, P.; Concepcion, P.; Corma, A. *J. Catal.* **2009**, *265*, 19.
- (113) Boronat, M.; Corma, A. *Langmuir* **2010**, *26*, 16607.
- (114) Zhu, H. Y.; Ke, X. B.; Yang, X. Z.; Sarina, S.; Liu, H. W. *Angew. Chem., Int. Ed.* **2010**, *49*, 9657.
- (115) Cardenas-Lizana, F.; Gómez-Quero, S.; Idriss, H.; Keane, M. A. *J. Catal.* **2009**, *268*, 223.
- (116) Cardenas-Lizana, F.; Gómez-Quero, S.; Baddeley, C. J.; Keane, M. A. *Appl. Catal., A: Chem.* **2010**, *387*, 155.
- (117) Kuroda, K.; Ishida, T.; Haruta, M. *J. Mol. Catal. A: Chem.* **2009**, *298*, 7.
- (118) Yan, N.; Zhang, J. G.; Yuan, Y.; Chen, G. T.; Dyson, P. J.; Li, Z. C.; Kou, Y. *Chem. Commun.* **2010**, *46*, 1631.
- (119) Lou, X. B.; He, L.; Qian, Y.; Liu, Y. M.; Cao, Y.; Fan, K. N. *Adv. Synth. Catal.* **2011**, *353*, 281.
- (120) Budroni, G.; Corma, A. *J. Catal.* **2008**, *257*, 403.
- (121) Liu, Y.; Xing, T.; Wei, Z.; Li, X.; Yan, W. *Catal. Commun.* **2009**, *10*, 2023.
- (122) Navarro, R. M.; Pawelec, B.; Trejo, J. M.; Mariscal, R.; Fierro, J. L. G. *J. Catal.* **2000**, *189*, 184.
- (123) Nomura, K.; Ishino, M.; Hazama, M. *Bull. Chem. Soc. Jpn.* **1991**, *64*, 2624.
- (124) Yasuda, H.; Sato, T.; Yoshimura, Y. *Catal. Today* **1999**, *50*, 63.
- (125) Dekkers, M. A. P.; Lippits, M. J.; Nieuwenhuys, B. E. *Catal. Today* **1999**, *54*, 381.
- (126) Bonarowska, M.; Malinowski, A.; Juszczak, W.; Karpinski, Z. *Appl. Catal., B: Environ.* **2001**, *30*, 187.
- (127) Rodriguez, J. A.; Liu, G.; Jirsak, T.; Hrbek, J.; Chang, Z. P.; Dvorak, J.; Maiti, A. *J. Am. Chem. Soc.* **2002**, *124*, 5242.
- (128) Venezia, A. M.; La Parola, V.; Deganello, G.; Pawelec, B.; Fierro, J. L. G. *J. Catal.* **2003**, *215*, 317.
- (129) Venezia, A. M.; La Parola, V.; Nicoli, V.; Deganello, G. *J. Catal.* **2002**, *212*, 56.
- (130) Pawelec, B.; Venezia, A. M.; La Parola, V.; Cano-Serrano, E.; Campos-Martin, J. M.; Fierro, J. L. G. *Appl. Surf. Sci.* **2005**, *242*, 380.
- (131) Pawelec, B.; La Parola, V.; Thomas, S.; Fierro, J. L. G. *J. Mol. Catal. A: Chem.* **2006**, *253*, 30.
- (132) Castano, P.; Zepeda, T. A.; Pawelec, B.; Makkee, M.; Fierro, J. L. G. *J. Catal.* **2009**, *267*, 30.
- (133) Mitsudome, T.; Noudjima, A.; Mikami, Y.; Mizugaki, T.; Jitsukawa, K.; Kaneda, K. *Angew. Chem., Int. Ed.* **2010**, *49*, 5545.
- (134) Noudjima, A.; Mitsudome, T.; Mizugaki, T.; Jitsukawa, K.; Kaneda, K. *Angew. Chem., Int. Ed.* **2011**, *50*, 2986.
- (135) Ni, J.; He, L.; Liu, Y. M.; Cao, Y.; He, H. Y.; Fan, K. N. *Chem. Commun.* **2011**, 47, 812.
- (136) Su, F. Z.; He, L.; Ni, J.; Cao, Y.; He, H. Y.; Fan, K. N. *Chem. Commun.* **2008**, 3531.
- (137) He, L.; Ni, J.; Wang, L. C.; Yu, F. J.; Cao, Y.; He, H. Y.; Fan, K. N. *Chem.—Eur. J.* **2009**, *15*, 11833.
- (138) Rodriguez-Rivera, G. J.; Kim, W. B.; Evans, S. T.; Voigt, T.; Dumesic, J. A. *J. Am. Chem. Soc.* **2005**, *127*, 10790.
- (139) In *Modern Oxidation Methods*; Bäckvall, J.-E., Ed.; Wiley-VCH: New York, 2004.
- (140) In *Catalysts for Fine Chemical Synthesis*; Roberts, S. M.; Poignant, G., Eds.; Wiley-VCH: New York, 2007; Vol. 1.
- (141) Hughes, M. D.; Xu, Y. J.; Jenkins, P.; McMorn, P.; Landon, P.; Enache, D. I.; Carley, A. F.; Attard, G. A.; Hutchings, G. J.; King, F.; Stitt, E. H.; Johnston, P.; Griffin, K.; Kiely, C. J. *Nature* **2005**, *437*, 1132.
- (142) Wang, L.; Wang, H.; Hapala, P.; Zhu, L.; Ren, L.; Meng, X.; Lewis, J. P.; Xiao, F.-S. *J. Catal.* **2011**, *281*, 30.
- (143) Cai, Z.-Y.; Zhu, M.-Q.; Chen, J.; Shen, Y.-Y.; Zhao, J.; Tang, Y.; Chen, X.-Z. *Catal. Commun.* **2010**, *12*, 197.
- (144) Sakurai, H.; Kamiya, I.; Kitahara, H.; Tsunoyama, H.; Tsukuda, T. *Synlett* **2009**, 245.
- (145) Moreau, F.; Bond, G. C. *Catal. Commun.* **2007**, *8*, 1403.
- (146) Xu, J.; Huang, J.; Liu, Y. M.; Cao, Y.; Li, Y. X.; Fan, K. N. *Catal. Lett.* **2011**, *141*, 198.
- (147) Bravo-Suarez, J. J.; Bando, K. K.; Lu, J. Q.; Fujitani, T.; Oyama, S. T. *J. Catal.* **2008**, *255*, 114.
- (148) Dapurkar, S. E.; Shervani, Z.; Yokoyama, T.; Ikushima, Y.; Kawanami, H. *Catal. Lett.* **2009**, *130*, 42.
- (149) Kesavan, L.; Tiruvalam, R.; Ab Rahim, M. H.; bin Saiman, M. I.; Enache, D. I.; Jenkins, R. L.; Dimitratos, N.; Lopez-Sanchez, J. A.; Taylor, S. H.; Knight, D. W.; Kiely, C. J.; Hutchings, G. J. *Science* **2011**, *331*, 195.
- (150) Schuchardt, U.; Cardoso, D.; Sercheli, R.; Pereira, R.; de Cruz, R. S.; Guerreiro, M. C.; Mandelli, D.; Spinace, E. V.; Fires, E. L. *Appl. Catal., A: Chem.* **2001**, *211*, 1.
- (151) Zhao, R.; Ji, D.; Lv, G.; Qian, G.; Yan, L.; Wang, X.; Suo, J. *Chem. Commun.* **2004**, 904.
- (152) Lv, G.; Zhao, R.; Qian, G.; Qi, Y.; Wang, X.; Suo, J. *Catal. Lett.* **2004**, *97*, 115.
- (153) Lu, G.; Ji, D.; Qian, G.; Qi, Y.; Wang, X.; Suo, J. *Appl. Catal., A: Chem.* **2005**, *280*, 175.
- (154) Zhu, K.; Hu, J.; Richards, R. *Catal. Lett.* **2005**, *100*, 195.
- (155) Hutchings, G. J.; Carrettin, S.; Landon, P.; Edwards, J. K.; Enache, D.; Knight, D. W.; Xu, Y.-J.; Carley, A. F. *Top. Catal.* **2006**, *38*, 223.
- (156) Xu, L.-X.; He, C.-H.; Zhu, M.-Q.; Fang, S. *Catal. Lett.* **2007**, *114*, 202.
- (157) Xu, L.-X.; He, C.-H.; Zhu, M.-Q.; Wu, K.-J.; Lai, Y.-L. *Catal. Lett.* **2007**, *118*, 248.
- (158) Xu, L.-X.; He, C.-H.; Zhu, M.-Q.; Wu, K.-J.; Lai, Y.-L. *Catal. Commun.* **2008**, *9*, 816.
- (159) Li, L.; Jin, C.; Wang, X.; Ji, W.; Pan, Y.; Knaap, T.; Stoel, R.; Au, C. T. *Catal. Lett.* **2009**, *129*, 303.
- (160) Xie, J.; Wang, Y.; Wei, Y. *Catal. Commun.* **2009**, *11*, 110.

- (161) Hereijgers, B. P. C.; Weckhuysen, B. M. *J. Catal.* **2010**, *270*, 16.
- (162) Liu, Y.; Tsunoyama, H.; Akita, T.; Xie, S.; Tsukuda, T. *ACS Catal.* **2011**, *1*, 2.
- (163) Carneiro, J. T.; Yang, C.-C.; Moma, J. A.; Moulijn, J. A.; Mul, G. *Catal. Lett.* **2009**, *129*, 12.
- (164) Min, B. K.; Deng, X.; Liu, X.; Friend, C. M.; Alemozafar, A. R. *ChemCatChem* **2009**, *1*, 116.
- (165) Ajaikumar, S.; Ahlqvist, J.; Larsson, W.; Shchukarev, A.; Leino, A. R.; Kordas, K.; Mikkola, J. P. *Appl. Catal., A: Chem.* **2011**, *392*, 11.
- (166) In *Kirk–Othmer Encyclopedia of Chemical Technology*, 3rd ed; Lutz, J. T., Grayson, M., Eckroth, D., Bushey, G. J., Eastman, C. L., Klingsberg, A., Eds.; Wiley: New York, 1994; Vol. 9.
- (167) Hayashi, T.; Tanaka, K.; Haruta, M. *J. Catal.* **1998**, *178*, 566.
- (168) Qi, C.; Akita, T.; Okumura, M.; Haruta, M. *Appl. Catal., A: Chem.* **2001**, *218*, 81.
- (169) Sinha, A. K.; Seelan, S.; Akita, T.; Tsubota, S.; Haruta, M. *Appl. Catal., A: Chem.* **2003**, *240*, 243.
- (170) Qi, C. *Appl. Catal., A: Chem.* **2004**, *263*, 19.
- (171) Nijhuis, T. A.; Huizinga, B. J.; Makkee, M.; Moulijn, J. A. *Ind. Eng. Chem. Res.* **1999**, *38*, 884.
- (172) Kapoor, M. P.; Sinha, A. K.; Seelan, S.; Inagaki, S.; Tsubota, S.; Yoshida, H.; Haruta, M. *Chem. Commun.* **2002**, 2902.
- (173) Uphade, B. S.; Akita, T.; Nakamura, T.; Haruta, M. *J. Catal.* **2002**, *209*, 331.
- (174) Wang, F.; Qi, C.; Ma, J. *Catal. Commun.* **2007**, *8*, 1947.
- (175) Cumaratanunge, L.; Delgass, W. N. *J. Catal.* **2005**, *232*, 38.
- (176) Zhan, G.; Du, M.; Huang, J.; Li, Q. *Catal. Commun.* **2011**, *12*, 830.
- (177) Qi, C.; Huang, J.; Bao, S.; Su, H.; Akita, T.; Haruta, M. *J. Catal.* **2011**, *281*, 12.
- (178) Zwijnenburg, A.; Saleh, M.; Makkee, M.; Moulijn, J. A. *Catal. Today* **2002**, *72*, 59.
- (179) Llorca, J.; Dominguez, M.; Ledesma, C.; Chimentao, R. J.; Medina, F.; Sueiras, J.; Angurell, I.; Seco, M.; Rossell, O. *J. Catal.* **2008**, *258*, 187.
- (180) Liu, T.; Hacırlıoğlu, P.; Oyama, S. T.; Luo, M. F.; Pan, X. R.; Lu, J. Q. *J. Catal.* **2009**, *267*, 202.
- (181) Claus, P.; Mennemann, C. *Catal. Lett.* **2010**, *134*, 31.
- (182) Yuan, Y.; Zhou, X.; Wu, W.; Zhang, Y.; Yuan, W.; Luo, L. *Catal. Today* **2005**, *105*, 544.
- (183) Oyama, S. T.; Zhang, X. M.; Lu, J. Q.; Gu, Y. F.; Fujitani, T. *J. Catal.* **2008**, *257*, 1.
- (184) Huang, J. H.; Akita, T.; Faye, J.; Fujitani, T.; Takei, T.; Haruta, M. *Angew. Chem., Int. Ed.* **2009**, *48*, 7862.
- (185) Lee, S.; Molina, L. M.; Lopez, M. J.; Alonso, J. A.; Hammer, B.; Lee, B.; Seifert, S.; Winans, R. E.; Elam, J. W.; Pellin, M. J.; Vajda, S. *Angew. Chem., Int. Ed.* **2009**, *48*, 1467.
- (186) Mul, G.; Zwijnenburg, A.; van der Linden, B.; Makkee, M.; Moulijn, J. A. *J. Catal.* **2001**, *201*, 128.
- (187) Ruiz, A.; van der Linden, B.; Makkee, M.; Mul, G. *J. Catal.* **2009**, *266*, 286.
- (188) Nijhuis, T. A. R.; Visser, T.; Weckhuysen, B. M. *Angew. Chem., Int. Ed.* **2005**, *44*, 1115.
- (189) Nijhuis, T. A.; Visser, T.; Weckhuysen, B. M. *J. Phys. Chem. B* **2005**, *109*, 19309.
- (190) Nijhuis, T.; Weckhuysen, B. *Catal. Today* **2006**, *117*, 84.
- (191) Nijhuis, T. A.; Gardner, T. Q.; Weckhuysen, B. M. *J. Catal.* **2005**, *236*, 153.
- (192) Nijhuis, T. A.; Sacaliuc, E.; Beale, A. M.; van der Eerden, A. M. J.; Schouten, J. C.; Weckhuysen, B. M. *J. Catal.* **2008**, *258*, 256.
- (193) Nijhuis, T. A.; Sacaliuc-Parvulescu, E.; Govender, N. S.; Schouten, J. C.; Weckhuysen, B. M. *J. Catal.* **2009**, *265*, 161.
- (194) Sacaliuc, E.; Beale, A. M.; Weckhuysen, B. M.; Nijhuis, T. A. *J. Catal.* **2007**, *248*, 235.
- (195) Roldan, A.; Torres, D.; Ricart, J. M.; Illas, F. *J. Mol. Catal. A: Chem.* **2009**, *306*, 6.
- (196) Stangland, E. E.; Stavens, K. B.; Andres, R. P.; Delgass, W. N. *J. Catal.* **2000**, *191*, 332.
- (197) Taylor, B.; Lauterbach, J.; Blau, G. E.; Delgass, W. N. *J. Catal.* **2006**, *242*, 142.
- (198) Yap, N.; Andres, R. P.; Delgass, W. N. *J. Catal.* **2004**, *226*, 156.
- (199) Bravo-Suarez, J. J.; Lu, J. Q.; Dallos, C. G.; Fujitani, T.; Oyama, S. T. *J. Phys. Chem. C* **2007**, *111*, 17427.
- (200) Gaudet, J.; Bando, K. K.; Song, Z.; Fujitani, T.; Zhang, W.; Su, D. S.; Oyama, S. T. *J. Catal.* **2011**, *280*, 40.
- (201) Friend, C. M.; Quiller, R. G.; Liu, X. Y. *Chem. Asian J.* **2010**, *5*, 78.
- (202) Patil, N.; Uphade, B.; McCulloh, D.; Bhargava, S.; Choudhary, V. *Catal. Commun.* **2004**, *5*, 681.
- (203) Boualleg, M.; Guillois, K.; Istria, B.; Burel, L.; Veyre, L.; Basset, J. M.; Thieuleux, C.; Caps, V. *Chem. Commun.* **2010**, *46*, 5361.
- (204) Bawaked, S.; Dummer, N. F.; Dimitratos, N.; Bethell, D.; He, Q.; Kiely, C. J.; Hutchings, G. J. *Green Chem.* **2009**, *11*, 1037.
- (205) Yin, D. H.; Qin, L. S.; Liu, H. F.; Li, C. Y.; Jin, Y. *J. Mol. Catal. A: Chem.* **2005**, *240*, 40.
- (206) Chimentao, R. J.; Medina, F.; Fierro, J. L. G.; Llorca, J.; Sueiras, J. E.; Cesteros, Y.; Salagre, P. *J. Mol. Catal. A: Chem.* **2007**, *274*, 159.
- (207) Zhang, F.; Zhao, X.; Feng, C.; Li, B.; Chen, T.; Lu, W.; Lei, X.; Xu, S. *ACS Catal.* **2011**, *1*, 232.
- (208) Nur, H.; Misnon, I. I.; Hamdan, H. *Catal. Lett.* **2009**, *130*, 161.
- (209) Li, B.; He, P.; Yi, G.; Lin, H.; Yuan, Y. *Catal. Lett.* **2009**, *133*, 33.
- (210) Luo, L.; Yu, N.; Tan, R.; Jin, Y.; Yin, D.; Yin, D. *Catal. Lett.* **2009**, *130*, 489.
- (211) Liu, J. H.; Wang, F.; Xu, T.; Gu, Z. G. *Catal. Lett.* **2010**, *134*, 51.
- (212) Rojluechai, S.; Chavadej, S.; Schwank, J. W.; Meeyoo, V. *Catal. Commun.* **2007**, *8*, 57.
- (213) Smith, M. B.; March, J. *March's Advanced Organic Chemistry: Reactions, Mechanism and Structures*. 6th Edition. John Wiley & Sons, Ltd.: Hoboken, New Jersey, 2007.
- (214) Milone, C.; Ingoglia, R.; Neri, G.; Pistone, A.; Galvagno, S. *Appl. Catal., A: Chem.* **2001**, *211*, 251.
- (215) Abad, A.; Almela, C.; Corma, A.; Garcia, H. *Chem. Commun.* **2006**, 3178.
- (216) Abad, A.; Almela, C.; Corma, A.; Garcia, H. *Tetrahedron* **2006**, *62*, 6666.
- (217) Choudhary, V. R.; Dhar, A.; Jana, P.; Jha, R.; Uphade, B. S. *Green Chem.* **2005**, *7*, 768.
- (218) Choudhary, V. R.; Jha, R.; Jana, P. *Green Chem.* **2007**, *9*, 267.
- (219) Wang, L. C.; Liu, Y. M.; Chen, M.; Cao, Y.; He, H. Y.; Fan, K. N. *J. Phys. Chem. C* **2008**, *112*, 6981.
- (220) Sun, H.; Tang, Q. H.; Du, Y.; Liu, X. B.; Chen, Y.; Yang, Y. H. *J. Colloid Interface Sci.* **2009**, *333*, 317.
- (221) Wang, L.-C.; He, L.; Liu, Q.; Liu, Y.-M.; Chen, M.; Cao, Y.; He, H.-Y.; Fan, K.-N. *Appl. Catal., A: Chem.* **2008**, *344*, 150.
- (222) Su, F. Z.; Chen, M.; Wang, L. C.; Huang, X. L.; Liu, Y. M.; Cao, Y.; He, H. Y.; Fan, K. N. *Catal. Commun.* **2008**, *9*, 1027.
- (223) Haider, P.; Kimmerle, B.; Krumeich, F.; Kleist, W.; Grunwaldt, J.-D.; Baiker, A. *Catal. Lett.* **2008**, *125*, 169.
- (224) Zhu, J.; Figueiredo, J. L.; Faria, J. L. *Catal. Commun.* **2008**, *9*, 2395.
- (225) Yang, J.; Guan, Y. J.; Verhoeven, T.; van Santen, R.; Li, C.; Hensen, E. J. M. *Green Chem.* **2009**, *11*, 322.
- (226) Yang, X.; Wang, X.; Liang, C.; Su, W.; Wang, C.; Feng, Z.; Li, C.; Qiu, J. *Catal. Commun.* **2008**, *9*, 2278.
- (227) Mitsudome, T.; Noudjima, A.; Mizugaki, T.; Jitsukawa, K.; Kaneda, K. *Adv. Synth. Catal.* **2009**, *351*, 1890.
- (228) Oliveira, R. L.; Kiyohara, P. K.; Rossi, L. M. *Green Chem.* **2010**, *12*, 144.
- (229) Wang, X.; Kawanami, H.; Dapurkar, S. E.; Venkataramanan, N. S.; Chatterjee, M.; Yokoyama, T.; Ikushima, Y. *Appl. Catal., A: Chem.* **2008**, *349*, 86.
- (230) Karimi, B.; Kabiri Esfahani, F. *Chem. Commun.* **2009**, 5555.
- (231) Han, D. Q.; Xu, T. T.; Su, J. X.; Xu, X. H.; Ding, Y. *ChemCatChem* **2010**, *2*, 383.

- (232) Jørgensen, B.; Egholmchristiansen, S.; Dahlthomsen, M.; Christensen, C. *J. Catal.* **2007**, *251*, 332.
- (233) Sun, K.-Q.; Luo, S.-W.; Xu, N.; Xu, B.-Q. *Catal. Lett.* **2008**, *124*, 238.
- (234) Nielsen, I. S.; Taarning, E.; Egeblad, K.; Madsen, R.; Christensen, C. H. *Catal. Lett.* **2007**, *116*, 35.
- (235) Zheng, N.; Stucky, G. D. *Chem. Commun.* **2007**, 3862.
- (236) Klitgaard, S. K.; Riva, A. T.; Helveg, S.; Werchmeister, R. M.; Christensen, C. H. *Catal. Lett.* **2008**, *126*, 213.
- (237) Liu, G.; Li, G.; Song, H. *Catal. Lett.* **2009**, *128*, 493.
- (238) Oliveira, R. L.; Kiyohara, P. K.; Rossi, L. M. *Green Chem.* **2009**, *11*, 1366.
- (239) Parreira, L. A.; Bogdanchikova, N.; Pestryakov, A.; Zepeda, T. A.; Tuzovskaya, I.; Farias, M. H.; Gusevskaya, E. V. *Appl. Catal., A: Chem.* **2011**, *397*, 145.
- (240) Choudhary, V. R.; Dumbre, D. K.; Bhargava, S. K. *Ind. Eng. Chem. Res.* **2009**, *48*, 9471.
- (241) Ni, J.; Yu, W. J.; He, L.; Sun, H.; Cao, Y.; He, H. Y.; Fan, K. N. *Green Chem.* **2009**, *11*, 756.
- (242) Patil, N. S.; Uphade, B. S.; Jana, P.; Bharagava, S. K.; Choudhary, V. R. *J. Catal.* **2004**, *223*, 236.
- (243) Choudhary, V. R.; Dumbre, D. K. *Appl. Catal., A: Chem.* **2010**, *375*, 252.
- (244) Liu, Y.; Tsunoyama, H.; Akita, T.; Tsukuda, T. *Chem. Lett.* **2010**, *39*, 159.
- (245) Kidwai, M.; Bhardwaj, S. *Appl. Catal., A: Chem.* **2010**, *387*, 1.
- (246) Choudhary, V. R.; Dumbre, D. K. *Catal. Commun.* **2009**, *10*, 1738.
- (247) Burato, C.; Centomo, P.; Pace, G.; Favaro, M.; Prati, L.; Corain, B. *J. Mol. Catal. A: Chem.* **2005**, *238*, 26.
- (248) Tsunoyama, H.; Tsukuda, T.; Sakurai, H. *Chem. Lett.* **2007**, *36*, 212.
- (249) Tsunoyama, H.; Sakurai, H.; Negishi, Y.; Tsukuda, T. *J. Am. Chem. Soc.* **2005**, *127*, 9374.
- (250) Lucchesi, C.; Inasaki, T.; Miyamura, H.; Matsubara, R.; Kobayashi, S. *Adv. Synth. Catal.* **2008**, *350*, 1996.
- (251) Ishida, T.; Nagaoka, M.; Akita, T.; Haruta, M. *Chem.—Eur. J.* **2008**, *14*, 8456.
- (252) Enache, D. I.; Edwards, J. K.; Landon, P.; Solsona-Espriu, B.; Carley, A. F.; Herzing, A. A.; Watanabe, M.; Kiely, C. J.; Knight, D. W.; Hutchings, G. J. *Science* **2006**, *311*, 362.
- (253) Lopez-Sanchez, J. A.; Dimitratos, N.; Miedziak, P.; Ntainjua, E.; Edwards, J. K.; Morgan, D.; Carley, A. F.; Tiruvalam, R.; Kiely, C. J.; Hutchings, G. J. *Phys. Chem. Chem. Phys.* **2008**, *10*, 1921.
- (254) Dimitratos, N.; Villa, A.; Wang, D.; Porta, F.; Su, D.; Prati, L. *J. Catal.* **2006**, *244*, 113.
- (255) Villa, A.; Janjic, N.; Spontoni, P.; Wang, D.; Su, D. S.; Prati, L. *Appl. Catal., A: Chem.* **2009**, *364*, 221.
- (256) Chen, Y.; Lim, H.; Tang, Q.; Gao, Y.; Sun, T.; Yan, Q.; Yang, Y. *Appl. Catal., A: Chem.* **2010**, *380*, 55.
- (257) Miyamura, H.; Matsubara, R.; Kobayashi, S. *Chem. Commun.* **2008**, 2031.
- (258) Mertens, P. G. N.; Corthals, S. L. F.; Ye, X.; Poelman, H.; Jacobs, P. A.; Sels, B. F.; Vankelecom, I. F. J.; De Vos, D. E. *J. Mol. Catal. A: Chem.* **2009**, *313*, 14.
- (259) Della Pina, C.; Falletta, E.; Rossi, M. J. *Catal.* **2008**, *260*, 384.
- (260) Zhao, G.; Hu, H.; Deng, M.; Ling, M.; Lu, Y. *Green Chem.* **2011**, *13*, 55.
- (261) Wang, Y.; Zheng, J.-M.; Fan, K.; Dai, W.-L. *Green Chem.* **2011**, *13*, 1644.
- (262) Balcha, T.; Strobl, J. R.; Fowler, C.; Dash, P.; Scott, R. W. J. *ACS Catal.* **2011**, 425.
- (263) Wang, N.; Matsumoto, T.; Ueno, M.; Miyamura, H.; Kobayashi, S. *Angew. Chem., Int. Ed.* **2009**, *48*, 4744.
- (264) Zhu, Y.; Qian, H. F.; Zhu, M. Z.; Jin, R. C. *Adv. Mater.* **2010**, *22*, 1915.
- (265) Turner, M.; Vaughan, O. P. H.; Lambert, R. M. *Chem. Commun.* **2008**, 2316.
- (266) Gong, J.; Mullins, C. B. *J. Am. Chem. Soc.* **2008**, *130*, 16458.
- (267) Xu, B. J.; Liu, X. Y.; Haubrich, J.; Madix, R. J.; Friend, C. M. *Angew. Chem., Int. Ed.* **2009**, *48*, 4206.
- (268) Haider, P.; Urakawa, A.; Schmidt, E.; Baiker, A. *J. Mol. Catal. A: Chem.* **2009**, *305*, 161.
- (269) Boronat, M.; Corma, A.; Illas, F.; Radilla, J.; Ródenas, T.; Sabater, M. *J. Catal.* **2011**, *278*, 50.
- (270) Shang, C.; Liu, Z.-P. *J. Am. Chem. Soc.* **2011**, *133*, 9938.
- (271) Kwon, Y.; Lai, S. C. S.; Rodriguez, P.; Koper, M. T. M. *J. Am. Chem. Soc.* **2011**, *133*, 6914.
- (272) Tsunoyama, H.; Ichikuni, N.; Sakurai, H.; Tsukuda, T. *J. Am. Chem. Soc.* **2009**, *131*, 7086.
- (273) Conte, M.; Miyamura, H.; Kobayashi, S.; Chechik, V. *J. Am. Chem. Soc.* **2009**, *131*, 7189.
- (274) Porta, F.; Rossi, M. *J. Mol. Catal. A: Chem.* **2003**, *204*, 553.
- (275) Berndt, H. *Appl. Catal., A: Chem.* **2003**, *244*, 169.
- (276) Villa, A.; Wang, D.; Su, D. S.; Prati, L. *ChemCatChem* **2009**, *1*, 510.
- (277) Hayashi, T.; Inagaki, T.; Itayama, N.; Baba, H. *Catal. Today* **2006**, *117*, 210.
- (278) Biella, S.; Prati, L.; Rossi, M. *Inorg. Chim. Acta* **2003**, *349*, 253.
- (279) Leite, L.; Stonkus, V.; Ilieva, L.; Plyasova, L.; Tabakova, T.; Andreeva, D.; Lukevics, E. *Catal. Commun.* **2002**, *3*, 341.
- (280) Huang, J.; Dai, W. L.; Li, H. X.; Fan, K. J. *Catal.* **2007**, *252*, 69.
- (281) Huang, J.; Dai, W. L.; Fan, K. N. *J. Phys. Chem. C* **2008**, *112*, 16110.
- (282) Huang, J.; Dai, W. L.; Fan, K. N. *J. Catal.* **2009**, *266*, 228.
- (283) Mitsudome, T.; Noujima, A.; Mizugaki, T.; Jitsukawa, K.; Kaneda, K. *Green Chem.* **2009**, *11*, 793.
- (284) Venturello, C.; Gambaro, M. *J. Org. Chem.* **1991**, *56*, 5924.
- (285) Anelli, P. L.; Biffi, C.; Montanari, F.; Quici, S. *J. Org. Chem.* **1987**, *52*, 2559.
- (286) Besson, M.; Gallezot, P. *Catal. Today* **2000**, *57*, 127.
- (287) Girgis, M. J.; Shekhar, R.; NOVARTIS A. G. WO Patent 03/008367A2, 2003.
- (288) Biella, S.; Prati, L.; Rossi, M. *J. Mol. Catal. A: Chem.* **2003**, *197*, 207.
- (289) Corma, A.; Domine, M. E. *Chem. Commun.* **2005**, 4042.
- (290) Marsden, C.; Taarning, E.; Hansen, D.; Johansen, L.; Klitgaard, S. K.; Egeblad, K.; Christensen, C. H. *Green Chem.* **2008**, *10*, 168.
- (291) Fristrup, P.; Johansen, L. B.; Christensen, C. H. *Chem. Commun.* **2008**, 2750.
- (292) Laursen, A. B.; Højholt, K. T.; Lundegaard, L. F.; Simonsen, S. B.; Helveg, S.; Schuth, F.; Paul, M.; Grunwaldt, J. D.; Kegnoes, S.; Christensen, C. H.; Egeblad, K. *Angew. Chem., Int. Ed.* **2010**, *49*, 3504.
- (293) Xu, B.; Liu, X.; Haubrich, J.; Friend, C. M. *Nat. Chem.* **2011**, *2*, 61.
- (294) Krieger, R. M.; Jagodzinski, P. W. *J. Mol. Struct.* **2008**, *876*, 56.
- (295) Barbaro, G.; Battaglia, A.; Giorgianni, P. *J. Org. Chem.* **1988**, *53*, 5501.
- (296) Mennen, S. M.; Gipson, J. D.; Kim, Y. R.; Miller, S. J. *J. Am. Chem. Soc.* **2005**, *127*, 1654.
- (297) Zhu, B. L.; Angelici, R. J. *Chem. Commun.* **2007**, 2157.
- (298) Zhu, B. L.; Lazar, M.; Trewyn, B. G.; Angelici, R. J. *J. Catal.* **2008**, *260*, 1.
- (299) Aschwanden, L.; Mallat, T.; Grunwaldt, J. D.; Krumeich, F.; Baiker, A. *J. Mol. Catal. A: Chem.* **2009**, *300*, 111.
- (300) Aschwanden, L.; Mallat, T.; Maciejewski, M.; Krumeich, F.; Baiker, A. *ChemCatChem* **2010**, *2*, 666.
- (301) Aschwanden, L.; Panella, B.; Rossbach, P.; Keller, B.; Baiker, A. *ChemCatChem* **2009**, *1*, 111.
- (302) Che, C. M.; So, M. H.; Liu, Y. G.; Ho, C. M. *Chem. Asian J.* **2009**, *4*, 1551.
- (303) Grirrane, A.; Corma, A.; Garcia, H. J. *Catal.* **2009**, *264*, 138.
- (304) Miyamura, H.; Morita, M.; Inasaki, T.; Kobayashi, S. *Bull. Chem. Soc. Jpn.* **2011**, *84*, 588.
- (305) Sun, H.; Su, F. Z.; Ni, J.; Cao, Y.; He, H. Y.; Fan, K. N. *Angew. Chem., Int. Ed.* **2009**, *48*, 4390.
- (306) Guo, H.; Kemell, M.; Al-Hunaiti, A.; Rautiainen, S.; Leskelä, M.; Repo, T. *Catal. Commun.* **2011**, *12*, 1260.

- (307) Kegnaes, S.; Mielby, J.; Mentzel, U. V.; Christensen, C. H.; Riisager, A. *Green Chem.* **2010**, *12*, 1437.
- (308) Ishida, T.; Haruta, M. *ChemSusChem* **2009**, *2*, 538.
- (309) Xu, B.; Zhou, L.; Madix, R. J.; Friend, C. M. *Angew. Chem., Int. Ed.* **2009**, *48*, 1.
- (310) Preedasuriyachai, P.; Kitahara, H.; Chavasiri, W.; Sakurai, H. *Chem. Lett.* **2010**, *39*, 1174.
- (311) Klitgaard, S. K.; Egeblad, K.; Mentzel, U. V.; Popov, A. G.; Jensen, T.; Taarning, E.; Nielsen, I. S.; Christensen, C. H. *Green Chem.* **2008**, *10*, 419.
- (312) Biswas, P.; Woo, J.; Gulians, V. V. *Catal. Commun.* **2010**, *12*, 58.
- (313) Sakurai, H.; Preedasuriyachai, P.; Chavasiri, W. *Synlett* **2011**, *2011*, 1121.
- (314) Klobukowski, E. R.; Mueller, M. L.; Angelici, R. J.; Woo, L. K. *ACS Catal.* **2011**, 703.
- (315) Patai, S. *The Chemistry of the Hydrazo, Azo and Azoxy Groups*. John Wiley & Sons, Ltd.: Baffins Lane, Chichester, 1997, Vol 2.
- (316) Grirrane, A.; Corma, A.; Garcia, H. *Science* **2008**, *322*, 1661.
- (317) Zhou, Y.; Angelici, R. J.; Keith Woo, L. *Catal. Lett.* **2010**, *137*, 8.
- (318) Selvam, K.; Swaminathan, M. *Catal. Commun.* **2011**, *12*, 389.
- (319) Grirrane, A.; Corma, A.; Garcia, H. *J. Catal.* **2009**, *268*, 350.
- (320) Corriu, R. J. P.; Guerin, C.; Moreau, J. J. E. *Top. Stereochem.* **1984**, *15*, 43.
- (321) Hirabayashi, K.; Kawashima, J.; Nishihara, Y.; Mori, A.; Hiyama, T. *Org. Lett.* **1999**, *1*, 299.
- (322) Hirabayashi, K.; Ando, J.; Kawashima, J.; Nishihara, Y.; Mori, A.; Hiyama, T. *Bull. Chem. Soc. Jpn.* **2000**, *73*, 1409.
- (323) Mitsudome, T.; Noujima, A.; Mizugaki, T.; Jitsukawa, K.; Kaneda, K. *Chem. Commun.* **2009**, 5302.
- (324) Raffa, P.; Evangelisti, C.; Vitulli, G.; Salvadori, P. *Tetrahedron Lett.* **2008**, *49*, 3221.
- (325) Aronica, L. A.; Schiavi, E.; Evangelisti, C.; Caporusso, A. M.; Salvadori, P.; Vitulli, G.; Bertinetti, L.; Martra, G. *J. Catal.* **2009**, *266*, 250.
- (326) Pohland, H. D.; Schierz, V.; Schumann, R. *Acta Biotechnol.* **1993**, *13*, 257.
- (327) Ramachandran, S.; Fontanille, P.; Pandey, A.; Larroche, C. *Food Technol. Biotechnol.* **2006**, *44*, 185.
- (328) Biella, S.; Prati, L.; Rossi, M. *J. Catal.* **2002**, *206*, 242.
- (329) Comotti, M.; Pina, C.; Matarrese, R.; Rossi, M.; Siani, A. *Appl. Catal., A: Chem.* **2005**, *291*, 204.
- (330) Onal, Y.; Schimpf, S.; Claus, P. *J. Catal.* **2004**, *223*, 122.
- (331) Baatz, C.; Prusse, U. *J. Catal.* **2007**, *249*, 34.
- (332) Prusse, U.; Mirescu, A.; Berndt, H.; Martin, A. *Appl. Catal., A: Chem.* **2007**, *317*, 204.
- (333) Benkő, T.; Beck, A.; Geszti, O.; Katona, R.; Tungler, A.; Frey, K.; Gucci, L.; Schay, Z. *Appl. Catal., A: Chem.* **2010**, *388*, 31.
- (334) Ishida, T.; Okamoto, S.; Makiyama, R.; Haruta, M. *Appl. Catal., A: Chem.* **2009**, *353*, 243.
- (335) Okatsu, H.; Kinoshita, N.; Akita, T.; Ishida, T.; Haruta, M. *Appl. Catal., A: Chem.* **2009**, *369*, 8.
- (336) Ishida, T.; Watanabe, H.; Bebeko, T.; Akita, T.; Haruta, M. *Appl. Catal., A: Chem.* **2010**, *377*, 42.
- (337) Hermans, S.; Deffernez, A.; Devillers, M. *Appl. Catal., A: Chem.* **2011**, *395*, 19.
- (338) Zhang, H.; Toshima, N. *Appl. Catal., A: Chem.* **2011**, *400*, 9.
- (339) Comotti, M.; Della Pina, C.; Matarrese, R.; Rossi, M. *Angew. Chem., Int. Ed.* **2004**, *43*, 5812.
- (340) Comotti, M.; Della Pina, C.; Rossi, M. *J. Mol. Catal. A: Chem.* **2006**, *251*, 89.
- (341) Comotti, M.; Della Pina, C.; Falletta, E.; Rossi, M. *J. Catal.* **2006**, *244*, 122.
- (342) Beltrame, P.; Comotti, M.; Dellapina, C.; Rossi, M. *Appl. Catal., A: Chem.* **2006**, *297*, 1.
- (343) Mirescu, A.; Pruse, U. *Catal. Commun.* **2006**, *7*, 11.
- (344) Yin, H. M.; Zhou, C. Q.; Xu, C. X.; Liu, P. P.; Xu, X. H.; Ding, Y. *J. Phys. Chem. C* **2008**, *112*, 9673.
- (345) Porta, F.; Prati, L. *J. Catal.* **2004**, *224*, 397.
- (346) Prati, L.; Porta, F. *Appl. Catal., A: Chem.* **2005**, *291*, 199.
- (347) Dimitratos, N.; Messi, C.; Porta, F.; Prati, L.; Villa, A. *J. Mol. Catal. A: Chem.* **2006**, *256*, 21.
- (348) Demirelgulen, S.; Lucas, M.; Claus, P. *Catal. Today* **2005**, *102–103*, 166.
- (349) Musialska, K.; Finocchio, E.; Sobczak, I.; Busca, G.; Wojcieszak, R.; Gaigneaux, E.; Ziolk, M. *Appl. Catal., A: Chem.* **2010**, *384*, 70.
- (350) Rodrigues, E. G.; Pereira, M. F. R.; Chen, X.; Delgado, J. J.; Órfão, J. J. M. *J. Catal.* **2011**, *281*, 119.
- (351) Dimitratos, N.; Villa, A.; Bianchi, C.; Prati, L.; Makkee, M. *Appl. Catal., A: Chem.* **2006**, *311*, 185.
- (352) Taarning, E.; Madsen, A. T.; Marchetti, J. M.; Egeblad, K.; Christensen, C. H. *Green Chem.* **2008**, *10*, 408.
- (353) Dimitratos, N.; Porta, F.; Prati, L. *Appl. Catal., A: Chem.* **2005**, *291*, 210.
- (354) Bianchi, C.; Canton, P.; Dimitratos, N.; Porta, F.; Prati, L. *Catal. Today* **2005**, *102–103*, 203.
- (355) Ketchie, W. C.; Murayama, M.; Davis, R. J. *J. Catal.* **2007**, *250*, 264.
- (356) Dimitratos, N.; Lopez-Sanchez, J. A.; Anthonykutty, J. M.; Brett, G.; Carley, A. F.; Tiruvalam, R. C.; Herzing, A. A.; Kiely, C. J.; Knight, D. W.; Hutchings, G. J. *J. Phys. Chem. Phys.* **2009**, *11*, 4952.
- (357) Sankar, M.; Dimitratos, N.; Knight, D. W.; Carley, A. F.; Tiruvalam, R.; Kiely, C. J.; Thomas, D.; Hutchings, G. J. *ChemSusChem* **2009**, *2*, 1145.
- (358) Dimitratos, N.; Lopez-Sanchez, J. A.; Meenakshisundaram, S.; Anthonykutty, J. M.; Brett, G.; Carley, A. F.; Taylor, S. H.; Knight, D. W.; Hutchings, G. J. *Green Chem.* **2009**, *11*, 1209.
- (359) Villa, A.; Veith, G. M.; Prati, L. *Angew. Chem., Int. Ed.* **2010**, *49*, 4499.
- (360) Zhang, J.; Liu, X.; Hedhili, M. N.; Zhu, Y.; Han, Y. *ChemCatChem* **2011**, *3*, 1.
- (361) Ishida, T.; Kuroda, K.; Kinoshita, N.; Minagawa, W.; Haruta, M. *J. Colloid Interface Sci.* **2008**, *323*, 105.
- (362) Casanova, O.; Iborra, S.; Corma, A. *J. Catal.* **2009**, *265*, 109.
- (363) Casanova, O.; Iborra, S.; Corma, A. *ChemSusChem* **2009**, *2*, 1138.
- (364) Gorbaney, Y. Y.; Klitgaard, S. K.; Woodley, J. M.; Christensen, C. H.; Riisager, A. *ChemSusChem* **2009**, *2*, 672.
- (365) Kusema, B. T.; Campo, B. C.; Mäki-Arvela, P.; Salmi, T.; Murzin, D. Y. *Appl. Catal., A: Chem.* **2010**, *386*, 101.
- (366) Conte, M.; Carley, A. F.; Hutchings, G. J. *Catal. Lett.* **2008**, *124*, 165.
- (367) Conte, M.; Carley, A. F.; Heirene, C.; Willock, D. J.; Johnston, P.; Herzing, A. A.; Kiely, C. J.; Hutchings, G. J. *J. Catal.* **2007**, *250*, 231.
- (368) Conte, M.; Carley, A. F.; Attard, G.; Herzing, A. A.; Kiely, C. J.; Hutchings, G. J. *J. Catal.* **2008**, *257*, 190.
- (369) Bonarowska, M.; Burda, B.; Juszczak, W.; Pielaszek, J.; Kowalczyk, Z.; Karpinski, Z. *Appl. Catal., B: Environ.* **2001**, *35*, 13.
- (370) Heck, K. N.; Nutt, M. O.; Alvarez, P.; Wong, M. S. *J. Catal.* **2009**, *267*, 97.
- (371) Keane, M. A.; Gómez-Quero, S.; Cárdenas-Lizana, F.; Shen, W. *ChemCatChem* **2009**, *1*, 270.
- (372) Fang, Y.-L.; Heck, K. N.; Alvarez, P. J. J.; Wong, M. S. *ACS Catal.* **2011**, *1*, 128.
- (373) Nutt, M. O.; Heck, K. N.; Alvarez, P.; Wong, M. S. *Appl. Catal., B: Environ.* **2006**, *69*, 115.
- (374) In *Metal-Catalyzed Cross-Coupling Reactions*; Meijere, A. d., Diederich, F., Eds.; Wiley-VCH: New York, 2004.
- (375) Tamao, K.; Miyauchi, N. *Top. Curr. Chem.* **2002**, *219*, 1.
- (376) Hassan, J.; Seignion, M.; Gozzi, C.; Schulz, E.; Lemaire, M. *Chem. Rev.* **2002**, *102*, 1359.
- (377) In *Metal-Catalyzed Cross-Coupling Reactions*; de Meijere, A., Diederich, F., Eds.; Wiley-VCH: Weinheim, 2004; Vols. 1–2.
- (378) Littke, A. F.; Fu, G. C. *Angew. Chem., Int. Ed.* **2002**, *41*, 4176.

- (379) Tsunoyama, H.; Sakurai, H.; Ichikuni, N.; Negishi, Y.; Tsukuda, T. *Langmuir* **2004**, *20*, 11293.
- (380) Carrettin, S.; Guzman, J.; Corma, A. *Angew. Chem., Int. Ed.* **2005**, *44*, 2242.
- (381) Sakurai, H.; Tsunoyama, H.; Tsukuda, T. *J. Organomet. Chem.* **2007**, *692*, 368.
- (382) Han, J.; Liu, Y.; Guo, R. *J. Am. Chem. Soc.* **2009**, *131*, 2060.
- (383) Kanuru, V. K.; Kyriakou, G.; Beaumont, S. K.; Papageorgiou, A. C.; Watson, D. J.; Lambert, R. M. *J. Am. Chem. Soc.* **2010**, *132*, 8081.
- (384) Kyriakou, G.; Beaumont, S. K.; Humphrey, S. M.; Antonetti, C.; Lambert, R. M. *ChemCatChem* **2010**, *2*, 1444.
- (385) Wang, F.; Li, C. H.; Sun, L. D.; Wu, H. S.; Ming, T. A.; Wang, J. F.; Yu, J. C.; Yan, C. H. *J. Am. Chem. Soc.* **2011**, *133*, 1106.
- (386) Russell, J. C.; Blunt, M. O.; Garfitt, J. M.; Scurr, D. J.; Alexander, M.; Champness, N. R.; H., B. P. *J. Am. Chem. Soc.* **2011**, *133*, 4220.
- (387) González-Arellano, C.; Cormab, A.; Iglesias, M.; Sánchez, F. *J. Catal.* **2006**, *238*, 497.
- (388) Corma, A.; Gutiérrez-Puebl, E.; Iglesias, M.; Monge, A.; Pérez-Ferreras, S.; Sánchez, F. *Adv. Synth. Catal.* **2006**, *348*, 1899.
- (389) Carrettin, S.; Corma, A.; Iglesias, M.; Sánchez, F. *Appl. Catal., A: Chem.* **2005**, *291*, 247.
- (390) Debono, N.; Iglesias, M.; Sanchez, F. *Adv. Synth. Catal.* **2007**, *349*, 2470.
- (391) Lauterbach, T.; Livendahl, M.; Rosellón, A.; Espinet, P.; Echavarren, A. M. *Org. Lett.* **2010**, *12*, 3006.
- (392) Corma, A.; Juárez, R.; Boronat, M.; Sánchez, F.; Iglesias, M.; García, H. *Chem. Commun.* **2011**, *47*, 1446.
- (393) Kim, S.; Bae, S.; Lee, J.; Park, J. *Tetrahedron* **2009**, *65*, 1461.
- (394) Yoo, W.-J.; Miyamura, H.; Kobayashi, S. *J. Am. Chem. Soc.* **2011**, *133*, 3095.
- (395) Taylor, S. F. R.; Sa, J.; Hardacre, C. *ChemCatChem* **2011**, *3*, 119.
- (396) Chenevierre, Y.; Caps, V.; Tuel, A. *Appl. Catal., A: Chem.* **2010**, *387*, 129.
- (397) Salvatore, R. N.; Yoon, C. H.; Jung, K. W. *Tetrahedron* **2001**, *57*, 7785.
- (398) In *March's Advanced Organic Chemistry: Reactions, Mechanisms, and Structure*; Smith, M. B., March, J., Eds.; Wiley: Hoboken, 2007.
- (399) Hamid, M. H. S. A.; Slatford, P. A.; Williams, J. M. J. *Adv. Synth. Catal.* **2007**, *349*, 1555.
- (400) Guillena, G.; Ramon, D. J.; Yus, M. *Chem. Rev.* **2010**, *110*, 1611.
- (401) Ishida, T.; Kawakita, N.; Akita, T.; Haruta, M. *Gold Bull.* **2009**, *42*, 267.
- (402) He, L.; Lou, X.-B.; Ni, J.; Liu, Y.-M.; Cao, Y.; He, H.-Y.; Fan, K.-N. *Chem.—Eur. J.* **2010**, *16*, 13965.
- (403) Shi, F.; Peng, Q. L.; Zhang, Y.; Deng, Y. Q. *Chem. Commun.* **2011**, *47*, 6476.
- (404) Tang, C.; He, L.; Liu, Y.; Cao, Y.; He, H.; Fan, K. *Chem.—Eur. J.* **2011**, *17*, 7172.
- (405) Corma, A.; Concepción, P.; Domínguez, I.; Fornés, V.; Sabater, M. J. *J. Catal.* **2007**, *251*, 39.
- (406) Yamane, Y.; Liu, X. H.; Hamasaki, A.; Ishida, T.; Haruta, M.; Yokoyama, T.; Tokunaga, M. *Org. Lett.* **2009**, *11*, 5162.
- (407) So, M.-H.; Liu, Y.; Ho, C.-M.; Lam, K.-Y.; Che, C.-M. *ChemCatChem* **2011**, *3*, 386.
- (408) Brennfürer, A.; Neumann, H.; Beller, M. *ChemCatChem* **2009**, *1*, 28.
- (409) Porta, F.; Tollari, S.; Bianchi, C.; Recchia, S. *Inorg. Chim. Acta* **1996**, *249*, 79.
- (410) Protzmann, G.; Luft, G. *Appl. Catal., A: Chem.* **1998**, *172*, 159.
- (411) Shi, F.; Deng, Y. Q. *Chem. Commun.* **2001**, 443.
- (412) Shi, F.; Deng, Y. Q.; Yang, H. Z.; SiMa, T. L. *Chem. Commun.* **2001**, 345.
- (413) Shi, F.; Deng, Y. Q. *J. Catal.* **2002**, *211*, 548.
- (414) Shi, F.; Deng, Y. *Stud. Surf. Sci. Catal.* **2003**, *145*, 193.
- (415) Shi, F.; Zhang, Q. H.; Ma, Y. B.; He, Y. D.; Deng, Y. Q. *J. Am. Chem. Soc.* **2005**, *127*, 4182.
- (416) Zhu, B. L.; Angelici, R. J. *J. Am. Chem. Soc.* **2006**, *128*, 14460.
- (417) Juárez, R.; Concepción, P.; Corma, A.; Fornés, V.; García, H. *Angew. Chem., Int. Ed.* **2010**, *49*, 1286.
- (418) Garcia, H.; Juarez, R.; Pennemann, H. *Catal. Today* **2011**, *159*, 25.
- (419) Juárez, R.; Corma, A.; García, H. *Green Chem.* **2009**, *11*, 949.
- (420) Sun, J. M.; Fujita, S. I.; Zhao, F. Y.; Hasegawa, M.; Arai, M. *J. Catal.* **2005**, *230*, 398.
- (421) Xiang, D.; Liu, X.; Sun, J.; Xiao, F.-S.; Sun, J. *Catal. Today* **2009**, *148*, 383.
- (422) Wang, Y.; Sun, J.; Xiang, D.; Wang, L.; Sun, J.; Xiao, F.-S. *Catal. Lett.* **2009**, *129*, 437.
- (423) Liu, X.; Haruta, M.; Tokunaga, M. *Chem. Lett.* **2008**, *37*, 1290.
- (424) Liu, X.; Hu, B.; Fujimoto, K.; Haruta, M.; Tokunaga, M. *Appl. Catal., B: Environ.* **2009**, *92*, 411.
- (425) Hamasaki, A.; Liu, X.; Tokunaga, M. *Chem. Lett.* **2008**, *37*, 1292.
- (426) Naota, T.; Takaya, H.; Murahashi, S. I. *Chem. Rev.* **1998**, *98*, 2599.
- (427) Zani, L.; Bolm, C. *Chem. Commun.* **2006**, 4263.
- (428) Huffman, M. A.; Yasuda, N.; Decamp, A. E.; Grabowski, E. J. J. *J. Org. Chem.* **1995**, *60*, 1590.
- (429) Kantam, M. L.; Prakash, B. V.; Reddy, C. R.; Sreedhar, B. *Synlett* **2005**, 2329.
- (430) Zhang, X.; Corma, A. *Angew. Chem., Int. Ed.* **2008**, *47*, 4358.
- (431) Chng, L. L.; Yang, J.; Wei, Y. F.; Ying, J. Y. *Adv. Synth. Catal.* **2009**, *351*, 2887.
- (432) Datta, K. K. R.; Reddy, B. V. S.; Ariga, K.; Vinu, A. *Angew. Chem., Int. Ed.* **2010**, *49*, 5961.
- (433) Carrettin, S.; Blanco, M. C.; Corma, A.; Hashmi, A. S. K. *Adv. Synth. Catal.* **2006**, *348*, 1283.
- (434) Hashmi, A. S. K.; Frost, T. M.; Bats, J. W. *J. Am. Chem. Soc.* **2001**, *122*, 11553.
- (435) Neațu, F.; Li, Z.; Richards, R.; Toullec, P. Y.; Genêt, J. P.; Dumbuya, K.; Gottfried, J. M.; Steinrück, H. P.; Pârvescu, V. I.; Michelet, V. *Chem.—Eur. J.* **2008**, *14*, 9412.
- (436) Sakurai, H.; Kamiya, I.; Kitahara, H. *Pure Appl. Chem.* **2010**, *82*, 2005.
- (437) Raptis, C.; Garcia, H.; Stratakis, M. *Angew. Chem., Int. Ed.* **2009**, *121*, 3179.